



Valentina Barcherini

Licenciatura em Química Aplicada

Hit-to-lead optimization of pharmaceutical interesting tryptophanol-derived scaffolds

Dissertação para obtenção do Grau de Mestre em Química
Bioorgânica

Orientador: Prof. Doutora Maria M. M. Santos, FF-UL

Co-orientador: Prof. Doutora Alexandra M. M. Antunes, IST-CQE

Presidente: Prof. Doutor Antonio Jorge Dias Parola, FCT-UNL

Arguente: Prof. Doutora Paula Sérgio Branco, FCT-UNL

Vogal: Prof. Doutora Maria M. M. Santos, FF-UL



Valentina Barcherini

Licenciatura em Química Aplicada

Hit-to-lead optimization of pharmaceutical interesting tryptophanol-derived scaffolds

Dissertação para obtenção do Grau de Mestre em Química
Bioorgânica

Orientador: Prof. Doutora Maria M. M. Santos, FF-UL

Co-orientador: Prof. Doutora Alexandra M. M. Antunes, IST-CQE

Presidente: Prof. Doutor Antonio Jorge Dias Parola, FCT-UNL

Arguente: Prof. Doutora Paula Sérgio Branco, FCT-UNL

Vogal: Prof. Doutora Maria M. M. Santos, FF-UL



Outubro 2016

Hit-to-lead optimization of pharmaceutical interesting tryptophanol-derived scaffolds

Valentina Barcherini, *Copyright*

A Faculdade de Ciência e Tecnologia e a Universidade Nova de Lisboa têm o direito, perpétuo e sem limite geográficos, de arquivar e publicar esta dissertação através de exemplares impressos reproduzidos em papel ou forma digital, ou por outro qualquer meio conhecido ou que venha a ser inventado e de divulgar através de repositórios científicos e de admitir a sua cópia e distribuição com objectivos educacionais ou de investigação, não comerciais, desde seja dado crédito ao autor e editor.

Acknowledgments

Firstly, I would like to thank professor Dr. Maria M.M. Santos to welcomed me kindly in her research group and to have been my supervisor in this research project. Along this year she did not just transmitted me precious scientific knowledge that let me reach this important phase of my life, but even she rose me up passion for chemistry applied to medicine.

I am grateful to professor Dr. Alexandra Antunes for her availability in terms of personal time, laboratory space and strumentation that permitted me to performed the stability studies in microsomes and plasma. To have followed me during the stability studies, performed in Instituto Superior Tecnico this last spring. I felt her complete didattic support and patience in transmitting me scientific knowledge.

My personal acknowledgments go to professor Dr. Lucilia Saraiva for the screening assays in yeast-colonies, performed in the faculty of pharmacy of University of Porto. I cannot exclude from these acknowledgments Sara Moreira and Joana Soares, as well all the PhD students of the microbiology laboratory of FFUP for the support given during the period I spent in Saraiva's lab (December 2015).

Moreover, I thank to Dr. Miguel Prudêncio, Marta Machado and Diana Fontinha, from Instituto de Medicina Molecular, for performing the activity assays against hepatic phase of *Plasmodium* infection.

I would like also to thank Diogo Magalhães Silva for the synthesis of (*R*)-tryptophanol oxazoloisoindolinones **38b'**, **38c'**, **38d'** and **38f'**, mentioned in this master thesis.

This work was supported by FCT (Fundação para a Ciência e a Tecnologia) through iMed.Ulisboa (UID/DTP/04138/2013), the IF Program (IF/00732/2013) and also by the European Union (FEDER funds POCI/01/0145/FEDER/007728 through Programa Operacional Factores de Competitividade – COMPETE) and National Funds (FCT/MEC, Fundação para a Ciência e Tecnologia and Ministério da Educação e Ciência) under the Partnership Agreement PT2020 UID/MULTI/04378/2013 and the project PTDC/DTP-FTO/1981/2014.

Also, I would like to thank who, since I moved my life in Lisbon, substained me continuously. Firslly professor Dr. Paula Branco for the availability since the first day. She guided me in my first year of master course, giving me always good advices for my professional future. I would thank you the professors and colleagues of the master course for the transmitted knowledge and to have created a welcoming environment during lessons, laboratories and free time.

I would like to thank Margarida Espadinha for her support along this year of practice and work in lab. All the great big group of people of lab 108 of the faculty of pharmacy of the University of Lisbon deserves my warm acknowledgements; for the daily routine and friendship we shared since more than one year and for the great support I received since the beginning.

I would like to thank my friends, met here in Lisbon. Sara, Guilherme, Andre', Miguel, Fulya, Andrea, Valter, Konrad, Sofia, Doina, Ignacio, Julie and Catarina, for the support in the hard times I got in these two years as well as for the adventurous happy time spent together, that made this study experience unforgettable.

My lovely acknowledgements are even for my friends of Padova. Firstly, to Carlotta Battaglin to have been part of this experience every day from two years and to my best friend Riccardo Perlasca, which he was always present, even though the distance. I thank Andrea Frasson for his friendship.

At last I thank my family, which this thesis is dedicated. To my mother Mariana, which she always supported me in the challenges I decided to run for. To my step-father Oscar, which always supported me. To my sisters Manuela and Ramona: my passion for science started with you. To my grandmother Ioana, which I hope one day to be able to share the contents of this research.

Thank you to Edgar for his love and support.

Abstract

The indole nucleus is the core structure of many natural and synthetic molecules. In fact, indole-based compounds have been described with different biological activities, ranging from antitumor to antimalarials.

Recent studies made by our research group led to the discovery of one enantiopure tryptophanol-derived oxazoloisoindolinone as novel activator of wild-type p53 and reactivator of mutant-type p53. The first objective of this thesis was centered on the hit-to-lead optimization of this specific derivative. Several alkyl substituents with increasing size and electron withdrawing/donating groups were selected for the protection of the indole nitrogen to assemble a library of new analogues for biological screening. A study of the activity based on chirality revealed one compound to be more active than the hit compound **34**. Particularly, compound **34d** restores the wt-like growth inhibitory effect to mut p53R280K in a percentage of 86.8%. Finally, the stability-profile of this chemical family was evaluated using compounds **34** and **34e** as models.

The second main goal of this thesis was the investigation of new leads as promising antimalarials, based on the recent report that a library of enantiopure indolizinoindolones exhibits *in vitro* activity against erythrocytic and liver-stages of malaria parasite. Structural derivatization of the hit-compounds was carried out using an enantioselective two-step route, involving an intramolecular cyclization to assemble the final polycyclic indolizinoindolones derivatives. *In vitro* screening of these tryptophanol-derived tricyclic compounds permitted the identification of two indolizinoindolone small molecules as the most active compounds.

Keywords: indole, p53, hit-to-lead optimization, tryptophanol, stability-profile, liver-stage malaria.

Resumo

O núcleo indole possui diferentes atividades biológicas, tais como anti-cancerígenas e anti-maláricas. Estudos recentes feitos pelo nosso grupo de investigação conduziram à descoberta de uma oxazoloisindolinona derivada de triptofanol enantiopura que activa a p53 *wild-type* e a p53 mutant. O primeiro objetivo desta tese consistiu na optimização deste composto *hit*. Em particular, de forma a obter-se uma biblioteca de novos compostos para avaliação biológica, foram seleccionados para a protecção do azoto do indole vários substituintes alquílicos de diferentes volumes, grupos dadores de electrões e grupos eletroatratores. Um estudo da atividade baseado na quiralidade revelou um composto mais ativo que o composto *hit*, que levou a um restabelecimento do efeito inibitório do crescimento wt a mut p53R280K numa percentagem de 86.8%. Finalmente, foi realizado um estudo de estabilidade em plasma, microsomas e PBS desta família química utilizando como modelos os compostos **34** e **34e**.

O Segundo objetivo desta tese foi o desenvolvimento de novos potenciais anti-maláricos, tendo como base uma família de indolizinoindolonas enantiopuras que reportadas recentemente como tendo actividade *in vitro* contra as fases sanguíneas e hepáticas dos parasitas da malária. Os compostos a ser testados foram obtidos enantioselectivamente através de dois passos sintéticos, envolvendo uma ciclização intramolecular para obtenção dos derivados policíclicos de indolizinoindolonas. *In vitro* screening dos compostos tricíclicos derivados de triptofanol sintetizados permitiu a identificação de duas indolizinoindolonas mais ativas.

Palavras-chaves: indole, p53, optimização, triptofanol, estudo de estabilidade, fase hepática da malária.

Contents

List of Figures	ix
List of Tables	xi
List of Schemes	xiii
List of Abbreviations and symbols	xv
1. Introduction	1
1.1. The importance of chirality	3
1.2. Enantioselective Synthesis	4
1.2.1. Separation of enantiomers: resolution of racemates	4
1.2.2. Synthesis of enantiomerically pure compounds: Asymmetric synthesis.....	5
1.2.3. The chiral pool.....	7
1.3. Importance of enantiopure synthesis	10
1.4. The World-wide problem of cancer.....	12
1.4.1. Key role of p53	12
1.4.2. Targeting the p53-MDM2 interaction.....	14
1.4.3. Targeting MDMX	15
1.4.4. Blocking both MDM2 and MDMX	15
1.5. The World-wide problem of malaria: how does it work?.....	17
1.6. The common net of cancer and malaria.....	18
1.7. Biomedical importance of Indole-based small molecules	20
2. Results and Discussion	25
2.1. Synthesis of a library of enantiopure tryptophanol-derived oxazoloisindolinones	27
2.1.1. Biological evaluation of a library of enantiopure tryptophanol-derived oxazoloisindolinones.....	37
2.2. Stability studies in human and rat microsomes, in human plasma and in pH 7.4 phosphate buffer of oxazoloisindolinones 34 and 34e	39
2.2.1. Determination of the metabolic stability of compounds 34 and 34e . Characterization of Phase I metabolites by LC-ESI-MS upon microsomes incubation	39
2.2.2. Determination of the stability of compounds 34 and 34e in human plasma	47
2.3. Synthesis of a library of indolizinoindolones	49
2.3.1. Biological evaluation and SAR study of a library of indolizinoindolones.....	57
3. Conclusions and Future Work	63
4. Experimental Procedure	67
4.1. General Methods.....	69
4.2. Experimental procedure chapter 2.1 Oxazoloisindolinones scaffold	69
4.2.1. General procedure for cyclocondensation reactions	69
4.2.2. General procedure for indole protection reactions	71

4.3. Experimental procedure chapter 2.3 indolizinoindolones scaffold	85
4.3.1. General procedure for cyclocondensation reactions	85
4.3.2. General procedure for <i>N</i> -methylation and <i>N</i> -ethylation.....	88
4.3.3. General procedure for cyclization reactions	91
4.4. Experimental procedure for the <i>in vitro</i> yeast based screening assay of compounds 34 , 34b , 34d , 34e , 38b and 38d	100
4.5. Experimental procedure of the stability studies.....	100
4.5.1. Metabolic stability assay – Identification of Phase I metabolites by LC-ESI-MS upon microsomes incubation of compounds 34 and 34e	100
4.5.2. Determination of stability of compounds 34 and 34e in human plasma by LC-ESI-MS and HPLC/UV-Vis.....	102
4.5.3. Determination of stability of compounds 34 and 34e in phosphate buffer solution by LC-ESI-MS and HPLC/UV-Vis.....	104
5. References	105
6. Annex	115
6.1. Experimental Procedure for the in-vitro screening of indolizinoindoles 49-55a and 49-55b .	117

List of Figures

Figure 1.1. Enantiomeric forms of limonene molecule 1 and 2	3
Figure 1.2. Creativity from the chiral pool in action: Oleandomycin 6 and its carbohydrates of origin 7 and 8 [22]......	8
Figure 1.3. Possible fashions in bicyclic compounds.....	10
Figure 1.4. Outcomes triggered by p53 activation.	13
Figure 1.5. Two examples of small molecules 21 and 22 inhibitors of MDM2 [51] [52].	14
Figure 1.6. Examples of small molecules 23 , inhibitor of MDMX [56], and 24 , inhibitor of both MDM2 and MDMX interactions with p53 [48]......	16
Figure 1.7. Life cycle of Malaria Parasite.....	17
Figure 1.8. Key host signaling pathways in Plasmodium infected hepatocytes. Adapted form [64]...	19
Figure 1.9. Examples of compounds contain the indole frame, important in the biological world.	20
Figure 1.10. General formula for <i>N</i> -hydroxycinnamamide-based HDACIs 30 with an indole-containing cap group [67].	21
Figure 1.11. Indole-based 1,4-disubstituted piperazines 31 as cytotoxic agents [68]......	21
Figure 1.12. Two examples of hybrids of indole and barbituric acids acting as anticancer agents [69].	22
Figure 1.13. Structure of 34	22
Figure 1.14. From left to right: Chemical structure of spiroindolinone 35 , of indoloisoquinolines 36 and enantiopure indolizinoindolones 37 general structures.	23
Figure 2.1. Strategy of hit-to-lead optimization of compound 34	27
Figure 2.2. General structure of the (<i>S</i>)-tryptophanol bicyclic lactams, where the more characteristic protons are reported.	29
Figure 2.3. Expansion of ¹ H-NMR spectrum of compound 34 in CDCl ₃ between 5.0 and 2.6 ppm. ...	30
Figure 2.4. Expansion of ¹ H-NMR spectrum of compound 34c in CDCl ₃ between 5.0 and 2.6 ppm.	34
Figure 2.5. Expansion of ¹ H-NMR spectrum of compound 38c in CDCl ₃ between 5.0 and 2.6 ppm.	34
Figure 2.6. Tandem mass spectrum obtained upon LC-ESI(+)-MS/MS analysis of m/z 319 ion corresponding to the protonated molecule of compound 34	40
Figure 2.7. Proposed ESI(+)-MS/MS fragmentation mechanisms for the protonated molecule (m/z 319) of 34	40
Figure 2.8. A) Tandem mass spectrum obtained by ESI(+) for the mono-hydroxylated metabolite of 34 eluting at 22.90 minutes; B) Proposed fragmentation mechanism for this metabolite.	41
Figure 2.9. A) Total ion chromatogram obtained by LC-ESI(+)-MS of compound 34 under microsomes incubations; B) Extracted ion chromatogram of ion m/z 319 corresponding to the protonated molecule of 34 ; C) Extracted ion chromatogram at m/z 335 corresponding to the protonated molecules of hydroxylated metabolites of 34 ; D) Extracted ion chromatogram at m/z 351 corresponding to the protonated molecules of dihydroxylated metabolites of 34	42

Figure 2.10. B) Proposed fragmentation mechanism for this metabolite.....	43
Figure 2.11. Tandem mass spectrum obtained by ESI(+) of ion at m/z 409, corresponding to the protonated molecule of compound 34e	44
Figure 2.12. Proposed ESI(+)-MS fragmentation mechanism of compound 34e	44
Figure 2.13. A) Total ion chromatogram obtained by ESI(+)-MS for 34e incubations; B) Extracted ion chromatogram at m/z 409, corresponding to the protonated molecule of 34e ; C) Extracted ion chromatogram at m/z 319 corresponding to the debenzilation metabolic product of 34e (corresponding to 34 ; D) Extracted ion chromatogram at m/z 425 corresponding to the protonated molecule of hydroxylated metabolites of 34e	45
Figure 2.14. Fragmentation pattern obtained by LC-ESI-MS/MS of ion at m/z 425 eluting at 30.1 minutes.....	45
Figure 2.15. Proposed ESI(+)-MS/MS fragmentation mechanisms of ion m/z 425, eluting at 30.1 minutes, corresponding to the protonated molecule of the main hydroxylated metabolite of 34e	46
Figure 2.16. Tandem mass spectra obtained by ESI(+) of ion m/z 425 corresponding to the monohydroxylated metabolites of compound 34e eluting at 31.10 min (A) and 32.47 min (B).	46
Figure 2.17. Most characteristic ¹ H-NMR signals for the indolizinoindolones scaffold.	54
Figure 2.18. Expansion of ¹ H-NMR spectrum of compound 52a in DMSO between 5.2 and 2.8 ppm. At 3.33 ppm appears the signal of water of the solvent.	55
Figure 2.19. Expansion of ¹ H-NMR spectrum of compound 52b in DMSO between 5.2 and 2.6 ppm. At 3.33 ppm appears the signal of water of the solvent.	56
Figure 2.20. First in vitro screening of indolizinoindolones 49a , 49b , 50a , 51a , 51b , 52a , 52b , 52a' , 52b' , 53a , 53b , 54a , 54b , 55a , 55a' against liver-stage <i>P. berghei</i> parasites. Activity (infection scale, bars) and toxicity to Huh-7 human hepatoma cells (cell-confluency scale, circles) are reported.....	57
Figure 2.21. SARs (Structure-activity relationships) of (<i>7R</i> , <i>13bR</i>) indolizinoindolone derivatives. (Results reported in percentage of infection).....	59
Figure 2.22. SARs (Structure-activity relationships) of (<i>7S</i> , <i>13bS</i>) indolizinoindolone derivatives. (Results reported in percentage of infection).....	60
Figure 2.23. SARs (Structure-activity relationships) of (<i>7S</i> , <i>13bR</i>) indolizinoindolone derivatives. ...	61

List of Tables

Table 1.1. Bicyclic Lactams 18, 19, 20 via cyclodehydration of several amino alcohols and dicarbonyl compounds [26].	11
Table 2.1. Reaction yields for the <i>N</i> -protected (<i>S</i>)-tryptophanol derivatives 34a-g .	31
Table 2.2. Reactions yields for the <i>N</i> -protected (<i>S</i>)-tryptophanol derivatives 38a-g .	32
Table 2.3. Reaction yields and times for the <i>N</i> -protected (<i>R</i>)-tryptophanol derivatives 38a'-g' .	33
Table 2.4. Comparison between ¹³ C-NMR chemical shifts of the hit-to-lead optimization products, 34a-f and 38a-f .	36
Table 2.5. Percentage of re-establishment of wild-type p53-induced yeast growth inhibition in yeast cells expressing mutant p53R280K; <i>p</i> indicates the result precision. Results correspond to 3-7 independent experiments.	38
Table 2.6. Reaction yields for the diastereoselective intramolecular cyclized indolizinoindolones 49-55a and 49-55b .	52
Table 2.7. Reaction yields for the diastereoselective intramolecular cyclized indolizinoindolones 52a' , 55a' and 52b' and 55b' .	52
Table 2.8. ¹ H-NMR most characteristic signals for compounds 49-55a .	54
Table 2.9. ¹ H-NMR most characteristic signals for compounds 49-54b .	55

List of Schemes

Scheme 1.1. Enzymatic kinetic resolution of racemate 3 [11].	5
Scheme 1.2. (<i>S</i>)-tryptophanol 9 involved in the enantioselective synthesis of indolo[2,3- <i>a</i>]quinolizidines 12 and 13 [23].	8
Scheme 1.3. Rational for the synthesis of enantiomerically pure compounds.	9
Scheme 1.4. Schematic view of the functional domains in p53 [36].	13
Scheme 1.5. MDM2- MDMX -p53 protein-protein interaction.	15
Scheme 2.1. Example of retrosynthetic analysis of compound 34 for the oxazoloisoindolinone library.	28
Scheme 2.2. Mechanism of cyclocondensation reaction.	29
Scheme 2.3. General procedure for the synthesis of (<i>S</i>)-tryptophanol-derived bicyclic lactams 34a-g .	31
Scheme 2.4. General procedure for the synthesis of (<i>S</i>)-tryptophanol derived bicyclic lactams 38a-g .	32
Scheme 2.5. General procedure for the synthesis of (<i>R</i>)-tryptophanol derived bicyclic lactams 38a'-g' .	33
Scheme 2.6. Rational for the synthesis of the benzoindolizinoindolones library.	49
Scheme 2.7. General procedure for the synthesis of indolizinoindolones 49-55a and 49-55b .	51
Scheme 2.8. General procedure for the synthesis of indolizinoindolones 52a' , 55a' and 52b' , 55b' .	51
Scheme 2.9. Mechanism of reaction of cyclization reaction.	53
Scheme 4.1. General procedure for the preparation of (<i>S</i>)- and (<i>R</i>)-tryptophanol bicyclic lactams.	69
Scheme 4.2. (<i>S</i>) and (<i>R</i>)-tryptophanol-derived bicyclic lactams protected on the indole core.	71
Scheme 4.3. (<i>S</i>)-tryptophanol-derived bicyclic lactams cyclocondensation reaction procedure.	85
Scheme 4.4. (<i>S</i>) and (<i>R</i>)-tryptophanol-derived bicyclic lactams protected on the indole moiety.	88
Scheme 4.5. (<i>S</i>)-tryptophanol-derived bicyclic lactams and their cyclized products.	92

List of Abbreviations and symbols

Ac	acetyl
Akt/PKB	protein kinase B
Bad	Bcl-2-associated death promoter
Bcl-2	B-cell lymphoma 2
Bn	benzyl
Boc	tert-butyloxycarbonyl
Bz	benzoyl
C	concentration
°C	Celsius degrees
C-9b	Carbon in position 9b
ca	circa
CALB	Candida Antarctica lipase B
CFU	colony forming units
DCM	dichloromethane
CNS	central nervous system
COSY	correlation spectroscopy
d	doublet or density
dd	double doublet
ddd	double double doublet
DEPT	distorsionless enhancement by polarization transfer
dr	diastereoselectivity ratio
dt	double triplet
DMF	dimethylformamide
DMSO	dimethylsulfoxide
DNA	deoxyribonucleic acid

DNA-PEG	deoxyribonucleic acid-polyethylene glycol
DOPA	3,4-dihydroxyphenylalanine
equiv	equivalent
Et	ethyl
FC	flash chromatography
FCS	fetal calf serum
g	gram
GI₅₀	half minimal growth inhibitory
h	hour
HEPES	<i>N</i> -2-HydroxyEthylPiperazine- <i>N'</i> -2-Ethane sulfonic acid
HMBC	heteronuclear multiple bond correlation
HMQC	heteronuclear multiple-quantum correlation
HPLC-DAD	high performance liquid chromatography with diode-array detection
Hz	hertz
IC₅₀	half maximal inhibitory concentration
IUPAC	International Union of Pure and Applied Chemistry
<i>J</i>	coupling constant
LC-ESI(+)-MS	liquid chromatography electron spray ionization mass spectrometry
LEU	leucine
LiAc/SS carrier	lithium acetate/single stranded carrier
m/z	mass-to-charge ratio
m	multiplet
MDM2	mouse double minute 2 homolog
MDMX	mouse double minute 4 homolog
Me	methyl
min	minute
mL	milli Liter

mmol	milli mole
mp	melting point
mTOR	mechanistic target of rapamycin
nM	nanoMolar
NMR	nuclear magnetic resonance
NRS	NADPH- regenerating system
OD600	optical density at $\lambda = 600$ nm
<i>p</i>	precision
PBS	phosphate buffer solution
pLS76	plasmide 76
ppm	parts per million
Pr	propyl
q	quartet
Rb	retinoblastoma protein
RING	really interesting new gene
RNA	ribonucleic acid
rpm	revolutions per minute
RPMI	roswell park memorial institute
rt	room temperature
s	singlet
SAR	structure activity relationship
SEM	standard error of mean
T	temperature
t	triplet
TLC	thin layer chromatography
Ts	tosyl
WHO	world health organization

wt	wild type
w/w	weight on weight
δ	chemical shift
μM	microMolar
η	yield

1. Introduction

1.1. The importance of chirality

“*L’Univers est dissymétrique*”, Louis Pasteur, ca. 1860

Perhaps even more than Louis Pasteur imagined, this famous conjecture of him turned out to be true, a first brick posed, in the direction of the true knowledge of Nature. At any spatial dimension, from that of elementary particles to the macroscopic scale of mammal morphology and perhaps of galaxies [1], Nature exhibits a curious asymmetry between the left and the right, which is generally called ‘chiral asymmetry’. Nature has a left and a right, and it can tell the difference between them. It is possible that human beings are sadly lacking in this respect, since as children we all had to learn which is which. Anyway, everybody has no doubt in distinguishing for example the smell of oranges from the smell of lemons. The smells of orange and lemon differ in being the left- and right- handed versions of the same molecule, limonene. (*R*)-(+)-limonene **1** smells rounded and orangey; (*S*)-(-)-limonene **2** is sharp and lemony [2] (**Figure 1.1**).

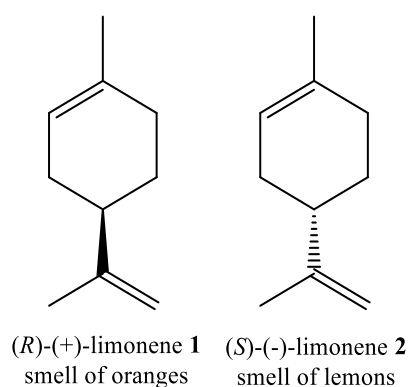


Figure 1.1. Enantiomeric forms of limonene molecule **1** and **2**.

It is already widely stated and defined from IUPAC, International Union of Pure and Applied Chemistry, that an enantiomer is one of a pair of molecular entities, which are mirror images of each other and for this reason they are non-superimposable [3]. The condition, which makes this affirmation verified, consists in the presence in the molecular framework of a structural element which identifies the compound in this way. In organic compounds, it is possible to identify this element with a carbon, which it is attached to four different types of atoms or groups of atoms [4] and for this reason is defined as chiral. Enantiomers are so always present as a couple of two non-superimposable structures and the chiral centre, included in the structure, is a quite powerful tool in the way it is found responsible for the ability of the enantiomers to rotate the plan-polarized light (+/-) by equal amounts but in opposite directions. Moreover, it is important to remark that enantiomers are identical until they are placed in a chiral environment. So, in practise, we take out the lead from Nature: all life is chiral and all living systems are chiral environments. Nature has chosen to make all its living structures starting from chiral

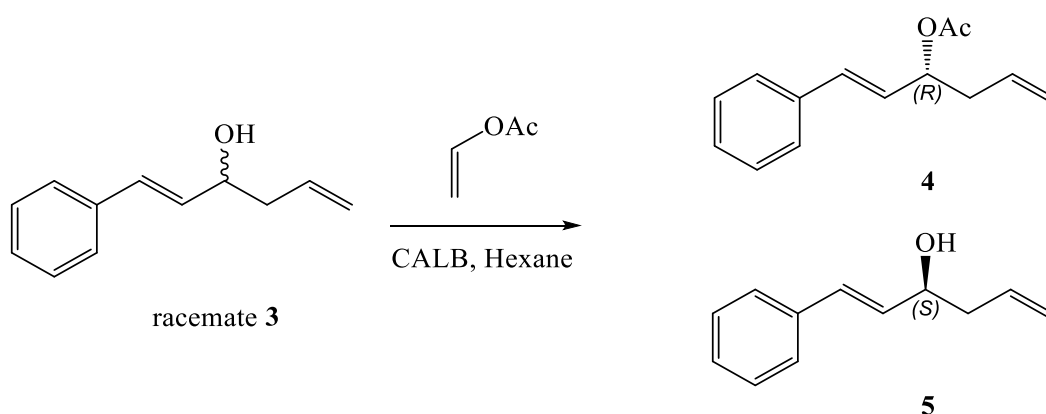
molecules, where fundamental examples are amino acids and sugars. Not a casual example, in the contest of this thesis, it is that every amino acid in our body has the *S* and not the *R* configuration. From another hand, one striking aspect of biological systems is the stereoselectivity associated with many processes [5]. Thus, most chemical substances formed and broken down in metabolic processes are optically active, and usually one particular enantiomer is formed in these processes. Consequently, it has been found in many occasions that the physiological activity of a particular compound resides almost exclusively in one of its optically active forms. The scientific and the practical importance of processes for the preparation of specific optical isomers is therefore quite evident [6]. To resolve this important issue one immediate way to obtain enantiomerically pure compounds is to isolate natural products from the chiral pool of Nature and, if necessary, to derivatize them. Yet, another possibility is a racemic synthesis and the subsequent separation of the enantiomers (resolution of racemates). However, half of this process's result would be undesired side product. As more and more enantiomerically pure active agents are required nowadays, enantioselective synthesis is a widely approached research subject. The selective synthesis of enantiomers is called asymmetric synthesis and it employs chiral agents, which it permits to introduce a chiral centre in a prochiral molecule [7].

1.2. Enantioselective Synthesis

1.2.1. Separation of enantiomers: resolution of racemates

The resolution of racemates consists in the separation of an equimolar mixture of enantiomers, that constitute the racemate. This is carried out by physical or chemical methods [8]. Usually, the separation takes place after a preceding conversion of the enantiomers into diastereoisomers, because, as it is known, pair of enantiomers have identical chemical and physical properties and cannot be separated directly. Certainly, the methods of resolution of racemates can also be applied to non-equimolar mixtures of enantiomers that are usually obtained by asymmetric synthesis, since asymmetric synthesis can never have a stereoselectivity of 100 % [5]. Several are the methods through which the resolution of racemates can occur. *Manual separation of enantiomers* starts when, in the crystallization process of enantiomers, a racemic mixture has the enantiomers crystallizing separately and forms two macroscopically different kinds of crystals. These crystals have the peculiarity to have a mirror-image relationship and they can be separated manually with a pair of tweezers. *Resolution of racemates after conversion into diastereomers* move by formation of a salt with a chiral acid or base. In this way, the enantiomers can be converted into diastereomers, which can then be separated as a result of their different physical and chemical properties. Subsequently, the acid or base is released and the pure enantiomers are recovered. Covalent derivatization of enantiomers with chiral reagents also yields

diastereomers. In this case, the diastereomers are separated by common separation techniques, as they possess different physical and chemical properties. Afterwards, separated derivatives are returned to the initial chiral reagent and the desired pure enantiomers, respectively. In addition, the separation of enantiomers can be carried out by chromatographic methods, such as high-pressure liquid chromatography (HPLC), and thin-layer chromatography (TLC) in association with a chiral stationary phase, which retards one enantiomer relatively more than the other one by stereoselectively constructing of diversely stable, chiral complexes. *Biochemical resolution of racemates* is one more tool used in the field: most enzymes convert their substrate in an enantioselective way. Therefore, microorganisms can be used to metabolize only one of the enantiomers of a racemate. If the microorganism is wisely chosen, the desired enantiomer is the only thing that remains and can then be separated from the mixture by common separation techniques [9]. At last, *kinetic resolution of enantiomers* moves from another starting input [10]. In the reaction with chiral reaction partners or chiral catalysts, enantiomers display different reaction rates. If the difference is large enough, the enantiomers can be separated stereoselectively converting only one of the enantiomers, while the desired enantiomer remains not mutated. Since this is based on different reaction rates, the separation technique is called *kinetic resolution*. An example given in **Scheme 1.1** of kinetic resolution, performed in the first year of master course, is the biochemical resolution of racemic mixture of alcohol **3** by stereoselective enzymatic conversion of one enantiomer, compound **5**, with the use of Lipase CALB, a hydrolase from the yeast species *C. antarctica* [11].



Scheme 1.1. Enzymatic kinetic resolution of racemate **3** [11].

1.2.2. Synthesis of enantiomerically pure compounds: Asymmetric synthesis

Asymmetric synthesis is a reaction or reaction sequence in which one configuration of one or more new stereogenic elements is selectively formed [12]. In an asymmetric synthesis, an achiral molecule is

enantioselectively converted into a chiral molecule or a chiral molecule is diastereoselectively converted into a new chiral molecule that contains at least one more chirality element. In summary: in an asymmetric synthesis, the enantiomers (or diastereomers) of a chiral product are formed in different yields. In effect, a synthesis can be stereoselective if it displays a diastereomeric transition state, because the transition states for the formation of the different stereoisomeric products then usually contain different energies. As a result, the activation energies differ from each other. Consequently, the stereoisomer whose formation requires the lower activation energy is preferably formed. The stereoselectivity increases with growing energy difference of the transition states. An unconditional prerequisite for a diastereomeric transition state is the presence of at least one chiral reactant. This may be either the substrate, a reagent, or a catalyst. In a rationalization of the methods of asymmetric synthesis elaborated it is important to take in account the fact that these methods can be *controlled* either *by reagent* or *controlled by substrate*. In first case, of asymmetric synthesis, if an achiral molecule (substrate) should be stereoselectively converted into a chiral molecule by reaction with an achiral reagent, one of the reactants must previously made chiral [13]. This is achieved by covalently attaching a chiral molecule to a substrate that can be removed and intactly recovered after the asymmetric synthesis. Such a chiral molecule is called chiral auxiliary. The stereoselectivity of the asymmetric synthesis is then controlled by the stereochemistry of the chiral auxiliary [14]. Certainly, to successfully achieve a diastereomeric transition state, a chiral reagent that will not be recovered after the synthesis can also be applied. The stereochemistry of the chiral auxiliary, or the chiral reagent, respectively, controls the stereoselectivity of the asymmetric synthesis. In contrast to a chiral catalyst, the chiral auxiliary, as well as the chiral reagent, must be applied in appropriate amounts, according to the stoichiometry of the reaction. Therefore, that kind of asymmetric synthesis is a stoichiometric, reagent-controlled method. In second case, if the substrate is chiral, the reagent does not necessarily have to be chiral for an asymmetric synthesis [15]. In this case, the stereoselectivity is controlled by the stereochemistry of the substrate. The substrate is obviously applied in stoichiometric amounts. Therefore, the asymmetric synthesis is a stoichiometric, substrate-controlled method. The chiral substrate of such asymmetric syntheses frequently derives from the large pool of chiral natural products. These starting products are often easily available in an enantiomerically (or diastereomerically) pure form and are, therefore, cheaper than chemically synthesized enantiomerically (or diastereomerically) pure starting products. Examples of such chiral natural products are carbohydrates, optically active carbon acids, terpenes, and sesquiterpenes. However, for many asymmetric syntheses, no suitable chiral substrate can be found in the chiral pool of natural products. In such a case, the advantages of reagent- or catalyst-controlled asymmetric syntheses are obvious: they are broadly applicable and contain a high flexibility with respect to the range of starting reagents and products. For asymmetric synthesis, even two main catalytic methods are available. The first methodology is called *synthetic catalysis* [16]. In

industrial asymmetric syntheses, more and more transition-metal catalysts with chiral ligands are applied. Remarkable example of an asymmetric synthesis used in a large-scale production is the Monsanto process for the manufacture of *L*-DOPA (*L*-dihydroxyphenylalanine) [17]. This proved useful in the treatment of Parkinson's disease. In one catalytical step of this asymmetric synthesis, a chiral rhodium catalyst is applied to a stereoselective hydrogenation of a double bond. To conclude, the second catalytic methodology is based on the use of *enzymes*. Enzymes show a high enantioselectivity (or diastereoselectivity) in asymmetric syntheses. However, an enzyme can often be applied only to the conversion of a very small group of substrates and, generally, not to a special process. In addition, they usually need physiologic reaction conditions, which it is a great advantage. Additionally, a common technique of the separation of enantiomers is the chromatography in association with a chiral stationary phase [18]. Such a separation is based on the differently strong interaction of the enantiomers with the chiral stationary phase. In this way, one enantiomer is more retarded than the other, so that they pass through the chromatographic column at different times.

1.2.3. The chiral pool

The chiral pool approach is a highly attractive methodology for the total synthesis of bioactive natural products with diverse and complex architectures ([19], [8]). This strategy is one of the best methods available to synthetic organic chemists for establishing pivotal stereocenters in optically active compounds [20]. The chiral pool is a versatile tool, comprising naturally occurring chiral molecules such as carbohydrates, amino acids, terpenes, alkaloids, and hydroxyacids ([20], [21]). They include enantiomerically enriched species that can be synthetically transformed into the desired target molecules. Chiral pool materials are also inexpensive and commercially available, making them adequate for use in accessing natural products and bioactive compounds [8]. For many decades, the chiral pool method was the only process of synthesis known to obtain a chiral molecule. Carbohydrates, amino acids, alkaloids and terpenes are very important members of the chiral pool (**Figure 1.2**) [8]. For example, Oleandomycin **6** is a medicinally important 14-membered macrolide antibiotic. In 1990, Tatsuta *et al.* reported its total synthesis by the chiral pool approach starting from methyl *L*-rhamnose **7** and *D*-mannose **8** [22].

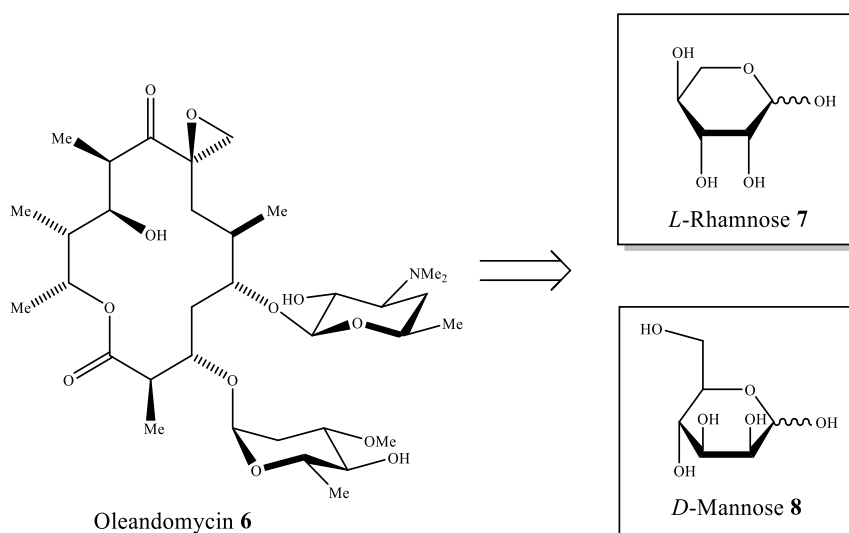
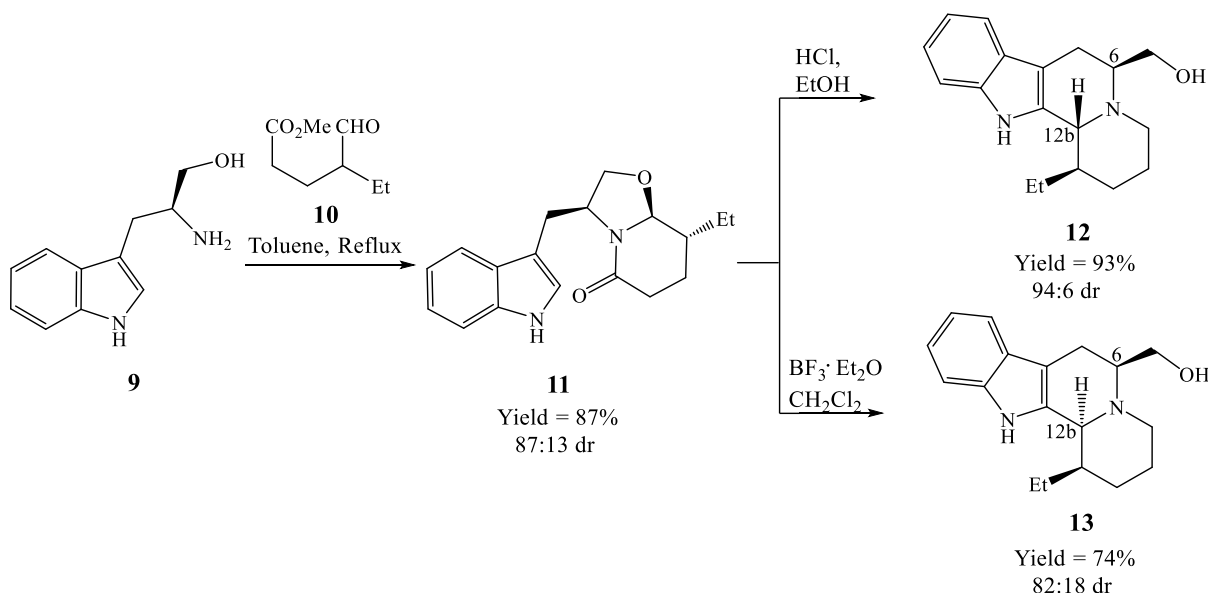


Figure 1.2. Creativity from the chiral pool in action: Oleandomycin **6** and its carbohydrates of origin **7** and **8** [22].

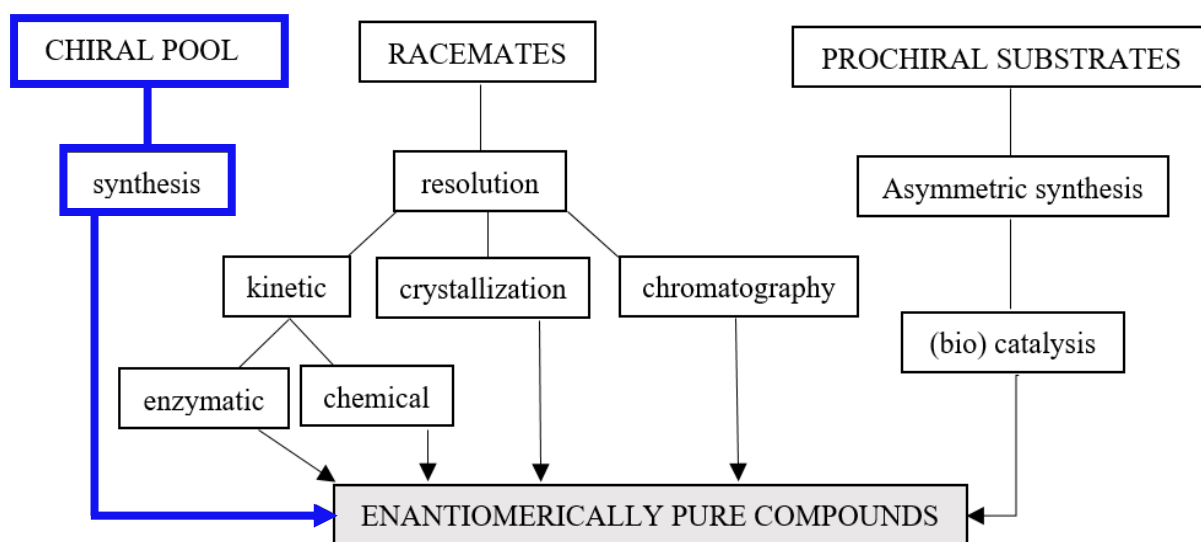
Moreover, it is reported that the amino alcohol (*S*)-tryptophanol **9** was used as starting material and as source of chirality in the enantioselective two-step route that brings to synthesis of indolo[2,3-*a*]quinolizidine scaffold [23]. After the stereoselective cyclocondensation with methyl 4-ethyl-5-oxopentanoate **10**, the resulting indole piperidone **11** underwent intramolecular α -amidoalkylation on the indole 2-position under kinetic control, to give 6,12b-*trans* indoloquinolizidines derivative **12** (**Scheme 1.2**). It is of worth to observe that the use of boron trifluoride etherate, $\text{BF}_3 \cdot \text{OEt}_2$ instead of chloridric acid, HCl changed the stereoselectivity producing the 6,12b-*cis* isomer **13**.



Scheme 1.2. (*S*)-tryptophanol **9** involved in the enantioselective synthesis of indolo[2,3-*a*]quinolizidines **12** and **13** [23].

In the 90s, the chiral pool synthesis was the most used method to synthesize chiral compounds with potential therapeutic use, representing 80% of the asymmetric synthesis methods. Currently, just 25% of the commercial drugs are synthesized from the chiral pool [8].

The methodology of enantioselective synthesis used to obtain most of the compounds synthesized in this thesis was based in chiral pool synthetic approach (**Scheme 1.3**).



Scheme 1.3. Rational for the synthesis of enantiomerically pure compounds.

1.3. Importance of enantiopure synthesis

It is important to promote the chiral separation and analysis of racemic drugs in pharmaceutical industry as well as in clinic since about more than half of the drugs currently in use are chiral compounds and near 90% of the last ones are marketed as racemates, consisting of an equimolar mixture of two enantiomers. Although they have the same chemical structure, most isomers of chiral drugs exhibit marked differences in biological activities such as pharmacology, toxicology, pharmacokinetics, metabolism, etc [17]. In contrast to chiral artificial products, all natural compounds are under single enantiomeric form, for example, all natural amino acids are l-isomer (laevorotatory) as well as all natural sugars (carbohydrates) are d-isomer (dextrorotatory). So, it is important to promote this trend even in organic synthesis [24].

There are mainly three kinds of bicyclic compounds widely studied. With the addition of a new five-membered ring to one already there, it is possible to do it in a bridged, fused or spiro fashion. Bridged bicyclic compounds are just what the name implies: a bridge of atom(s) is thrown across from one side of the ring to the other. Fused bicyclic compounds have one bond common to both rings, while spiro compounds have one atom common to both rings.

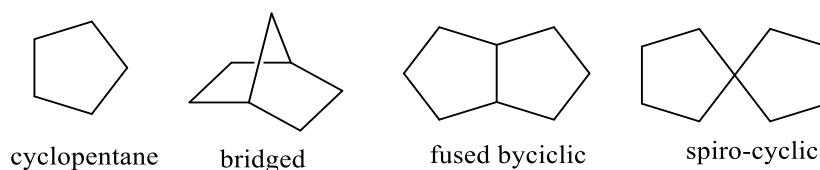
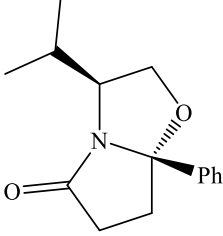
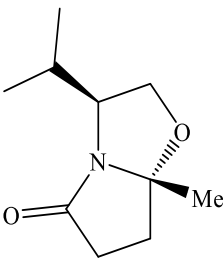
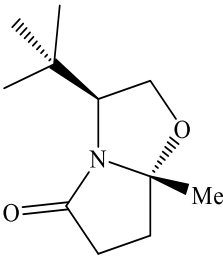


Figure 1.3. Possible fashions in bicyclic compounds.

Bicyclic lactams have proven to be an exceptional chiral template for the construction of a wide variety of optically pure carbocycles and heterocycles. There are diversified methods developed for the synthesis of these functionalized building blocks ([6], [25]). Two general methods have been developed for the construction of the title fused bicyclic systems and involve condensation of two optically pure amino alcohols and dicarbonyl compound [26]. In this case, (*S*)-vaninol **14**, (*S*)-tert-leucinol **15** 3-benzoylpropionic acid **16** and Leuvinilic acid **17** were employed for the synthesis. In the first route a cyclodehydration process was utilized between an optically pure amino alcohol and a γ -ketoacid. This was performed by heating the components at reflux in toluene with azeotropic removal of water. Thus, condensation of a γ -ketoacid and an amino alcohol afforded the bicycle [3,3,0] octanes **18**, **19**, **20** (Table 1.1) as single diastereoisomers.

Table 1.1. Bicyclic Lactams **18**, **19**, **20** via cyclodehydration of several amino alcohols and dicarbonyl compounds [26].

Dicarbonyl compound + Amino alcohol	Bicyclic Lactam formed	η %
(<i>S</i>)-valinol 14 + 3-Benzoylpropionic acid 16	 <p style="text-align: center;">18</p>	85
(<i>S</i>)-valinol 14 + Leuvinilic acid 17	 <p style="text-align: center;">19</p>	85
(<i>S</i>)-tert-leucinol 15 + Leuvinilic acid 17	 <p style="text-align: center;">20</p>	92

This approach is considered quite promising and practical since it involves only one step reaction, with the formation of a new chiral centre. It is quite feasible to get or acquire the starting materials like in this case amino alcohols/acids since they are abundant in nature and nowadays commercially available. They can also be obtained by reduction of the corresponding amino acid with lithium aluminium hydride, as made in this work of thesis [27].

In this thesis, chiral non-racemic bicyclic lactams were synthesized starting from different enantiopure amino alcohols, to be evaluated as potential anti-tumor agents and they have been used in the construction of diversified scaffold of benzoindolizinoindolones small molecules, evaluated as anti-malarials [28].

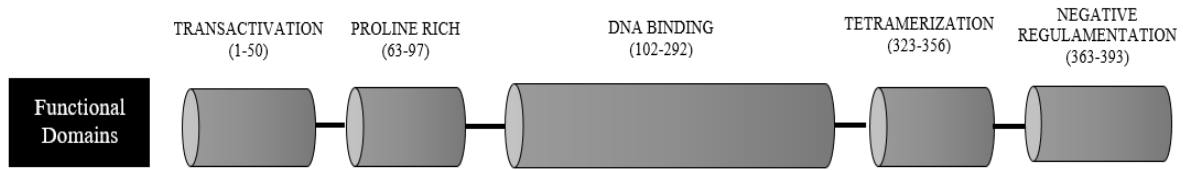
1.4. The World-wide problem of cancer

Cancer is a generic term, with a wide meaning, for a large group of diseases that can affect any part of the body. Other terms commonly used to express this concept are malignant tumours and neoplasms. Characteristic of cancer is the rapid creation of abnormal cells that grow beyond their usual boundaries, and which can then invade adjoining parts of the body and spread to other organs, where the latter process is referred to as metastasizing. Metastases are the major cause of death from cancer [29]. Cancer figures among the leading causes of morbidity and mortality worldwide, with approximately 14 million new cases and 8.2 million cancer related deaths in 2012. The number of new cases is expected to rise by about 70% over the next two decades. The five most common sites of cancer diagnosed in 2012 were lung, prostate, colorectal, stomach and liver in men and in women breast, colorectal, lung, cervix, and stomach, in order of trend. Around one third of cancer deaths are due to high body mass index, low fruit and vegetable intake, lack of physical activity, tobacco use, alcohol use, where tobacco use is the most important risk factor for cancer causing around 20% of global cancer deaths and around 70% of global lung cancer deaths. Cancer arises from one single cell. The transformation from a normal cell into a tumour cell is a multistage process, typically a progression from a pre-cancerous lesion to malignant tumours. These changes are the result of the interaction between a person's genetic factors and three categories of external agents, including physical carcinogens, such as ultraviolet and ionizing radiation, chemical carcinogens such as asbestos, components of tobacco smoke, aflatoxin (a food contaminant) and biological carcinogens such as infections from certain viruses, bacteria or parasites [30]. A correct cancer diagnosis is essential for adequate and effective treatment because every cancer type requires a specific treatment regime which encompasses one or more modalities such as surgery, and/or radiotherapy, and/or chemotherapy. The primary goal is to cure cancer or to considerably prolong life. Improving the patient's quality of life is also an important goal. It can be achieved by supportive or palliative care and psychological support.

1.4.1. Key role of p53

The p53 tumor suppressor is the most frequently inactivated gene in cancer. It was first thought to be an oncogene, but 10 years later, team lead by Bert Vogelstein and Ray White, studying colon cancer showed p53 to be a tumor suppressor gene [31]. Then, several *in vivo* studies using three different approaches to engineer mice with 'switchable' p53, demonstrated that restoration of p53 leads to a substantial regression of already developed tumours-lymphomas, soft tissue sarcomas and hepatocellular carcinomas ([32], [33], [34]). p53 is a potent tumor suppressor and is a subject of

intensive studies for more than 30 years [35]. It is well established that p53 is a transcriptional factor activated by different types of stresses, which regulates the expression of genes involved in the control



Scheme 1.4. Schematic view of the functional domains in p53 [36].

control of cell cycle and cell death [36]. Most of the p53 mutations that can cause cancer are found in the DNA-binding domain (**Scheme 1.4**) [37]. Activated p53 can prevent the propagation of cells carrying oncogenic lesions via a multitude of pathways, i.e.: induction of growth arrest, senescence or apoptosis, modulation of tumor stroma, angiogenesis and metabolism, as well as the block of invasion and metastasis [38]. This explains why loss of p53 function is selected for during tumor development, resulting in the inactivation in the majority of human tumors (**Figure 1.4**). From the other side, reactivation of p53 appears to be feasible, since the p53 protein is usually expressed in tumors, although functionally inert. Other approaches include introduction of wild type p53 into the cells with mutant p53; the use of small molecules to stabilize mutant p53 in wild type, active conformation ([39], [40]) and the introduction of agents to prevent degradation of p53 by proteins that normally targets it is also a promising strategy [36].

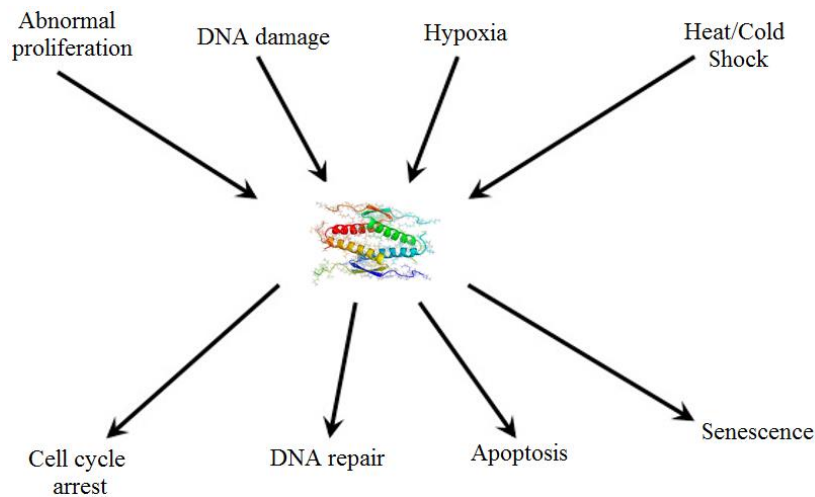


Figure 1.4. Outcomes triggered by p53 activation.

In the absence of Tp53 mutations, the tumor suppressor function of p53 is frequently impaired due to diverse alterations which converge on two p53 inhibitors MDM2 and MDMX. It was proven through mouse models that MDM2 and MDMX are the major negative regulators of p53. Genetically engineered mice lacking either of MDM2 or MDMX die in utero and this fact underscores the

fundamental role of MDM2 and MDMX in p53 regulation ([39]- [41]). MDM2 can inhibit p53 via several mechanisms. The most studied is MDM2 binding to the *N*-terminal transactivation domain of p53 which blocks its transcription function ([42], [43]). MDM2 also is functional as a E3 ubiquitin ligase, which promotes either monoubiquitination of p53 leading to enhanced nuclear export [44], or polyubiquitination of p53 that targets p53 for proteasomal degradation ([45], [46]). While MDMX also binds the p53 *N*-terminus and blocks its transcriptional function, it does not possess any intrinsic E3 ligase activity [47] and it is unable to target p53 for degradation. From the other side, it was found that MDM2 forms oligomers with itself or MDMX through RING-finger domains; hetero-oligomerization of MDM2 and MDMX renders a more efficient E3 ligase activity towards p53 and this fact can help to explain the functional non-redundancy of MDM2 and MDMX observed in mouse models [48]. Human cancers frequently possess elevated levels of MDM2 leading to inhibition of p53 function. This phenomenon has been reported in sarcomas, gliomas, haematological malignancies, melanomas and carcinomas [49].

1.4.2. Targeting the p53-MDM2 interaction

Most of the small molecules developed which target the p53/ MDM2 complex mimic three aminoacids of p53 peptide which interacts with MDM2. Structural studies revealed hydrophobic clefts on MDM2 that are filled by three critical p53 amino acid residues which are Phe19, Trp23 and Leu26. This set of amino acids were found to interact with MDM2 and bind to its hydrophobic cleft, thus acting by steric hindrance [50]. Based on these findings, an impressive number of p53-MDM2 interaction inhibitors, from distinct chemical families, have been identified. Although many small-molecule MDM2 inhibitors have shown potent *in vitro* activity, only a limited number of compounds have demonstrated to possess acceptable pharmacokinetic properties for *in vivo* evaluation. To date, the most studied chemotypes have been cis-imidazolines (such as nutlins **21**), benzodiazepines, and spiro-oxindoles (like compound **22**). The cis-imidazoline **21** (Figure 1.5) were the first discovered potent and selective small-molecule inhibitors of the p53-MDM2 interaction and they continue to show therapeutic potential.

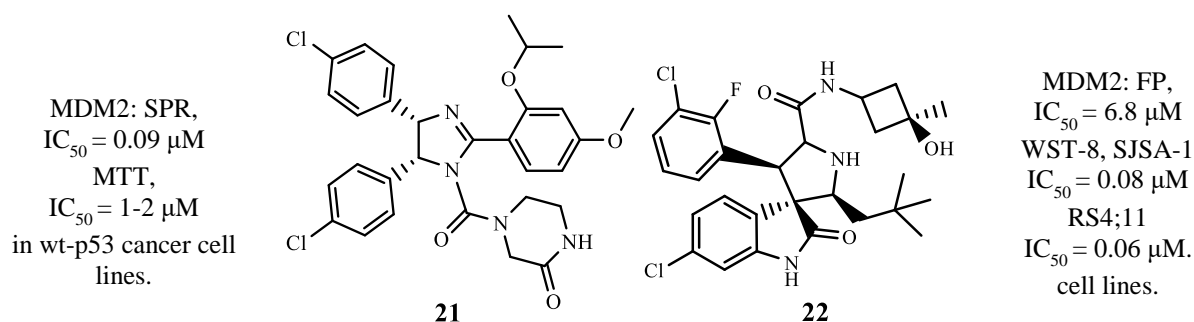
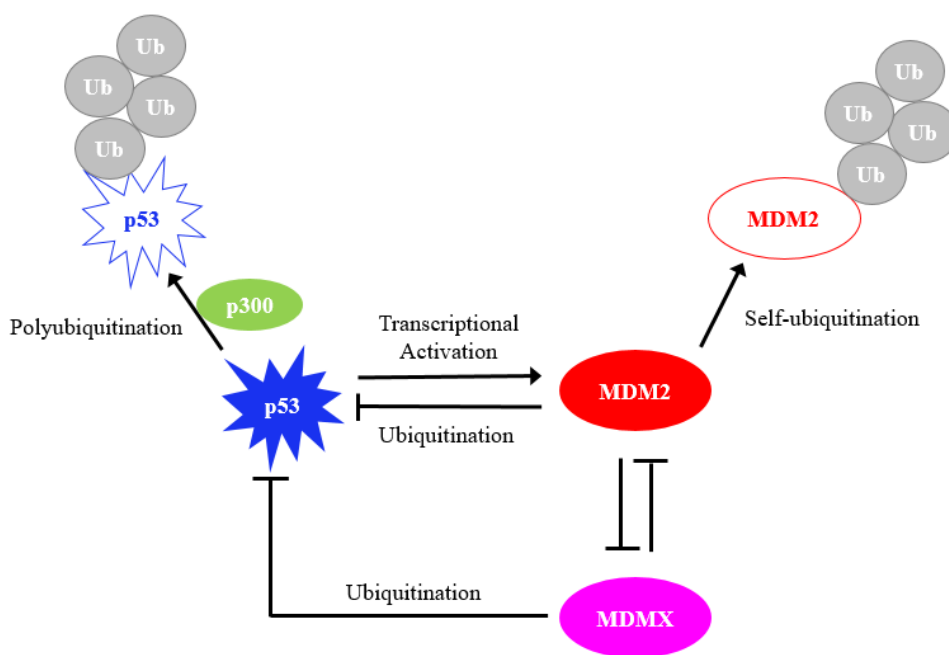


Figure 1.5. Two examples of small molecules **21** and **22** inhibitors of MDM2 [51] [52].



Scheme 1.5. MDM2- MDMX -p53 protein-protein interaction.

1.4.3. Targeting MDMX

One factor which compromises the efficiency of MDM2 inhibitors is the overexpression of another negative p53 regulator, MDMX. MDM2 and MDMX regulate p53 in a non-redundant fashion and act synergistically, as already mentioned (**Scheme 1.5**). Anyway, due to structural differences between the binding pockets in MDMX and MDM2, molecules which inhibit MDM2 have low affinity to MDMX [53]. Therefore, the inhibition of both MDM2 and MDMX is required for a full-scale p53 activation ([53], [54], [55]). A good example of small molecule targeting p53 binding site in MDMX is compound **23** (see **Figure 1.6**). It is found to not kill cancer cells on its own, but has an additive effect when combined with MDM2 inhibitors [56].

1.4.4. Blocking both MDM2 and MDMX

Recent efforts have been focused on the identification of dual MDM2/ MDMX antagonists, a ‘two-in-one’ inhibitors which can offer an effective therapy for a broader range of tumors. This idea has been pursued by Vassilev and colleagues who identified compound **24** (**Figure 1.6**). This compound was found to induce the formation of MDM2 and MDMX homo- or heterodimers which cannot bind p53. This leads to p53 activation, resulting in cell cycle arrest and apoptosis [57].

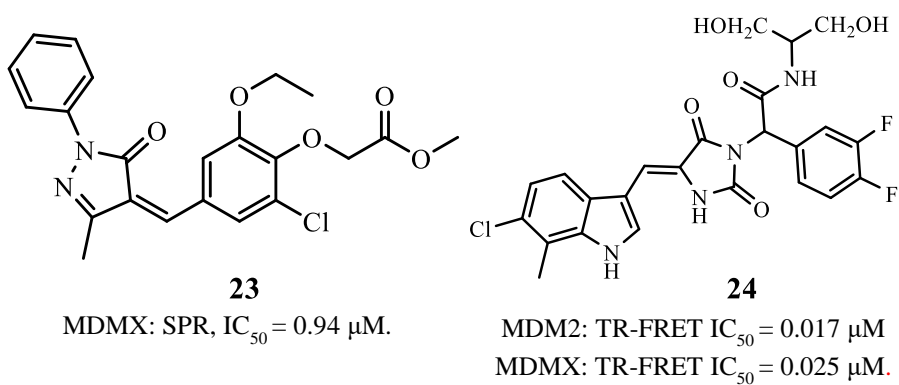


Figure 1.6. Examples of small molecules **23**, inhibitor of MDMX [56], and **24**, inhibitor of both MDM2 and MDMX interactions with p53 [48].

1.5. The World-wide problem of malaria: how does it work?

According to the latest information provided by the WHO about 1.2 billion people are at risk of malaria with the major burden disease carried by young children and pregnant women living in endemic areas [58]. Malaria is found to be caused by parasites of the genus *Plasmodium*, afflicting 350-500 million people annually and causing 800,000 deaths world-wide [59]. The human transmission is carried out by the bites of infected female *Anopheles* mosquitoes, which has the role of primary host. Once the parasite is introduced, it travels to the liver where it infects the hepatocytes cells. Hepatocytes make up 70-85% of the liver's mass. The parasite then grows and replicates within hepatocytes and ultimately spawns tons of daughter merozoites into blood stream (**Figure 1.7**). Now the infection passes from liver-stage to blood-stage, leading to symptomatic infection [60]. The genus *Plasmodium* is a member of the order Haemosporidia.

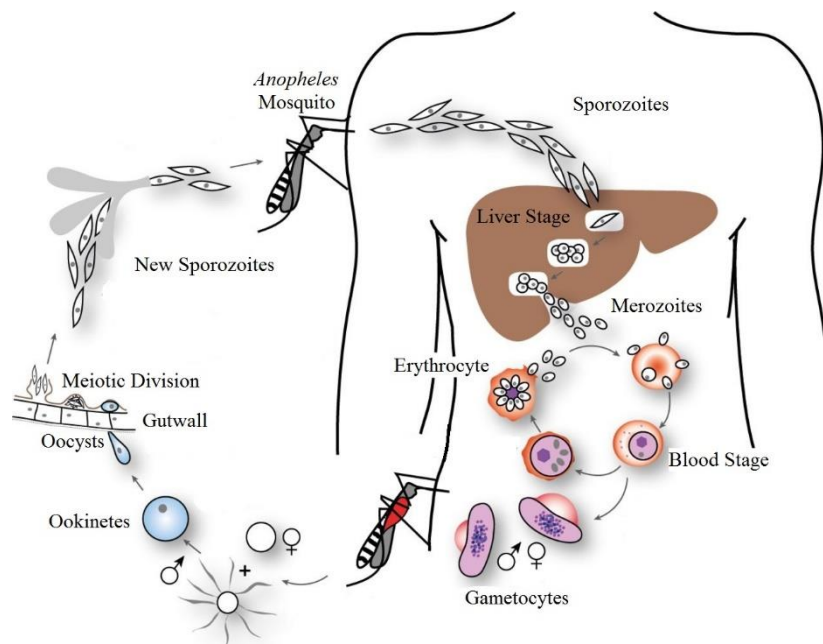


Figure 1.7. Life cycle of Malaria Parasite.

It is the largest genus within this order and currently consists of over 250 species. They cause malaria in many different vertebrates. There are 5 parasite species that cause malaria in humans [61]:

- *Plasmodium falciparum*, which is the responsible for most of the malaria deaths globally and it is the most prevalent species in sub-Saharan Africa. The remaining species are not typically as life threatening as *P. falciparum*.
- *Plasmodium vivax*, is the second most significant specie and is prevalent in Southeast Asia and Latin America. *P. vivax* and *Plasmodium ovale* have the added complication of a dormant liver

stage phase of the infection, which can be reactivated in the absence of a mosquito bite, leading to clinical symptoms.

- *P. ovale* and *Plasmodium malariae* represent only a small percentage of infections and with *P. vivax* are milder forms of Malaria.
- A fifth specie *Plasmodium knowlesi* is found to infect primates. Its exact mode of transmission remains unclear [59].

In order to study human malaria, in the context of this thesis, it was chosen to use as model organism *Plasmodium berghei* parasite. It represents a good tool because of its similarity to the *Plasmodium* species which cause human malaria. *P. berghei* has a very similar life-cycle to the species that infect humans, and it causes disease in mice which has signs similar to those seen in human malaria. Importantly, *P. berghei* can be genetically manipulated more easily than the species that infect humans, making it a useful model for research into *Plasmodium* genetics [62].

1.6. The common net of cancer and malaria

Even though still not clearly documented, from literature emerges a biological connection between cancer illness and the propagation of malaria starting from *Plasmodium* parasites infection at liver-stage and their replication inside hepatocytes before they invade erythrocytes and trigger clinical malaria [63]. Particularly, to understand the contact points, which link these two illnesses it is important to take as reference the system squared in **Figure 1.8**. In the network reported it is underlined a parasite-mediated signaling, which the adequate changes render the infected host cell more hospitable for the parasite. Zooming, when activated form of Akt and Bcl-2 increase and in contemporary the level of Bad decrease an input of survival response is ongoing and this assist the parasite in protecting its host cell. The process of autophagy is blocked and the parasite can follow its intracellular development.

From the other side, the activation of Rb suggests the infected hepatocyte is pushed towards a proliferative state. Finally, the decrease in p53 levels fits into both the proliferative and anti-apoptotic framework. Together, the observed perturbations are consistent with a general anti-apoptotic, pro-proliferative, anti-autophagic environment within the infected host cell. In a lysate array analysis, reported in literature, experiment where Nutlin-3 was used in order to exert its effects, where it binds selectively to the p53 - binding region of the E3-ubiquitin ligase MDM2 blocking the inhibitory interaction of MDM2 on p53, it is observed that protein levels of MDM2 were increased in response to parasite infection, indicating that the parasite might promote MDM2 mediated p53 degradation [64].

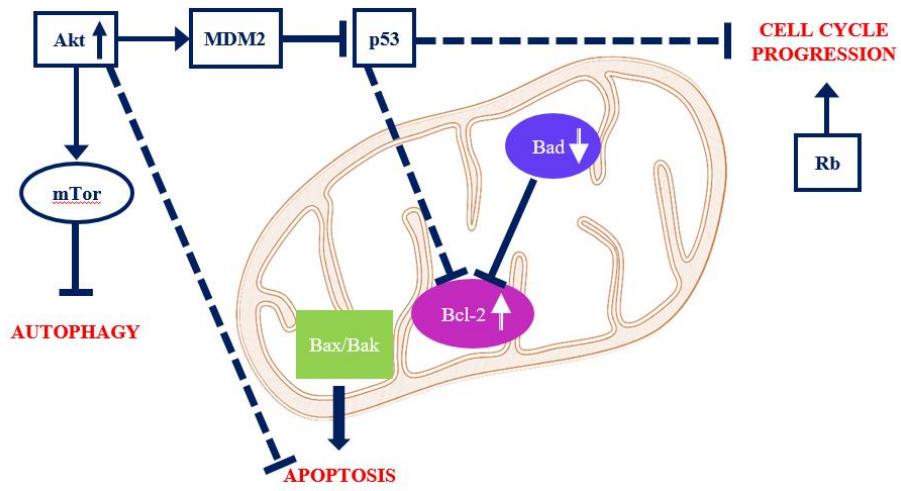
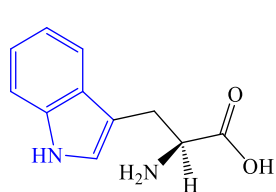


Figure 1.8. Key host signaling pathways in *Plasmodium* infected hepatocytes. Adapted from [64].

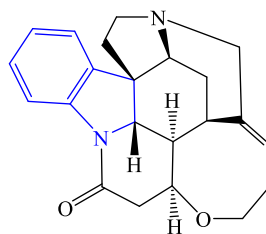
1.7. Biomedical importance of Indole-based small molecules

Compounds with heterocyclic rings are inextricably tissue into the most basic biochemical processes of life. Indole is the parent substance of many important compounds that occur in nature. It has a benzene ring and a pyrrole ring sharing one double bond. It is a heterocyclic system with 8 electrons from four double bonds and the lone pair from the nitrogen atom, for a total of 10 electrons delocalized along the framework, giving to the system aromatic character. Indole is an important heterocyclic system because it is built into proteins in the form of the amino acid tryptophan. As illustrated in **Figure 1.9**, it provides the skeleton of indole alkaloids, which figure as biologically active compounds from plants. Tryptophan **25**, Strychnine **26** and LSD **27** are two main examples. In animals, serotonin **28** is a very important neurotransmitter in the CNS as well as in cardiovascular and gastrointestinal systems. The structurally similar hormone melatonin **29** is thought to control the diurnal rhythm of physiological functions.



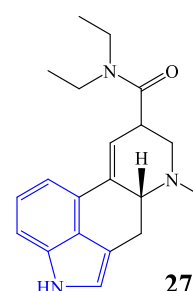
25

essential amino acid **Tryptophan**



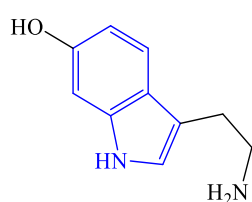
26

Strychnine, first alkaloid identified by Linnaeus in 1753



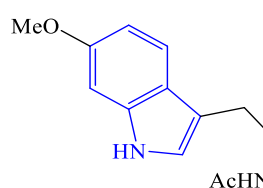
27

Lysergic acid diethylamide (LSD), a psychedelic drug



28

Serotonin, monoamine neurotransmitter



29

Melatonin, a hormone common in animals

Figure 1.9. Examples of compounds contain the indole frame, important in the biological world.

Innumerable biological functions are associated to indole-based compounds [64], including antimalarial and anticancer activity. Focusing only in anticancer properties of indole moiety, there are some reviews in the literature that report several compounds as antitumor agents containing an indole core ([64], [65], [66]) Xu research group designed a novel series of *N*-hydroxycinnamamide-based HDACIs **30** (histone deacetylase inhibitors) with an indole-containing cap group (**Figure 1.10**). Few synthesized molecules among them are reported to exhibited potent *in vitro* and *in vivo* antitumor activity, where the indole fragment turned to be an important structural element for antitumor drug design [66].

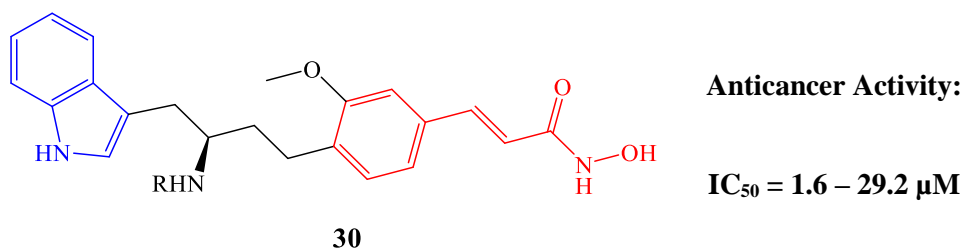


Figure 1.10. General formula for *N*-hydroxycinnamamide-based HDACIs **30** with an indole-containing cap group [67].

A series of 3-[(4-substitutedpiperazin-1-yl)methyl]-1H-indole derivatives **31** (**Figure 1.11**) were synthesized via Mannich reaction by Akkoc group. The cytotoxicity of the derivatives was studied on 3 cell lines and showed a variable extent of IC₅₀ values (less than 10 μM) [68].

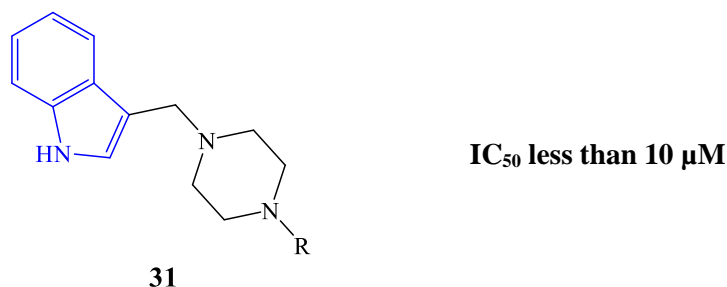
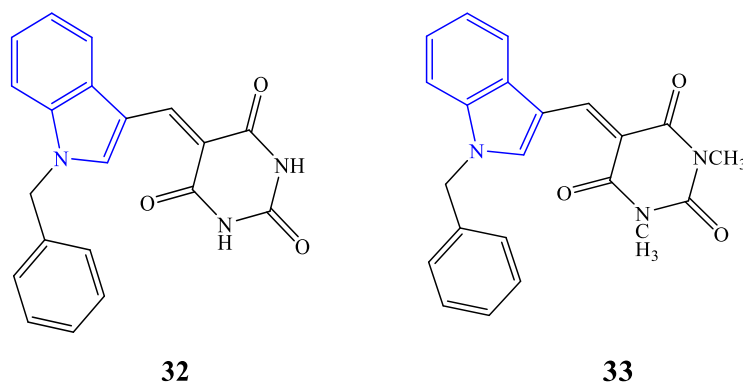


Figure 1.11. Indole-based 1,4-disubstituted piperazines **31** as cytotoxic agents [68].

Palwinder Singh *et al.* reported the synthesis and anticancer activities of hybrids of indole and barbituric acids (**Figure 1.12**) compounds **32** and **33**. They evaluated these molecules over 60 cell line panel of human cancer cells and they have identified two molecules with significant anticancer activities [69].



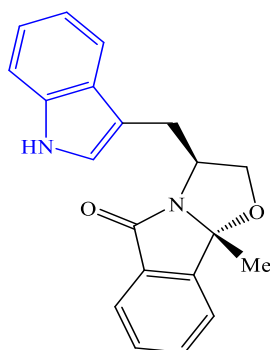
**Anticancer
activity
(GI₅₀):**

**A498 = 0.03 μM
MDA-MB-468 = 0.1 μM**

**IGROV1 = 0.03 μM
MDA-MB-468 = 0.02 μM**

Figure 1.12. Two examples of hybrids of indole and barbituric acids acting as anticancer agents [69].

Recent discoveries by Santos's group, led to the discovery of one enantiopure tryptophan-derived oxazoloisoindolinone, compound **34**, as novel anticancer small-molecule (**Figure 1.13**) [70]. The growth inhibitory potential of compound **34** and the contribution of p53 pathway to its activity were ascertained in p53^{+/+} and p53^{-/-} HCT116 tumor cells.



HCT116 p53^{+/+} GI₅₀ ~ 16 μM

HCT116 p53^{-/-} GI₅₀ ~ 34 μM

activator of wt p53

reactivator of mt p53

Figure 1.13. Structure of **34**.

From the other side, indole-based compounds show biological versatility as antimalarials, too [71]. Briefly, the spiroindolone from Novartis, compound **35**, which it is currently in phase I clinical trials as antimalarial, shows antiplasmodial activity against *P. falciparum* [72] and several indoloisoquinolines **36**, synthesized from enantiopure tryptophan were recently reported to have low micromolar activity against a chloroquine-resistant *P. falciparum* strain [73]. Also, benzindolizinoindolones **37** are found

to be inhibitors of *P. falciparum* erythrocytic-stage and *P. berghei* liver-stage parasites (see **Figure 1.14**) [28].

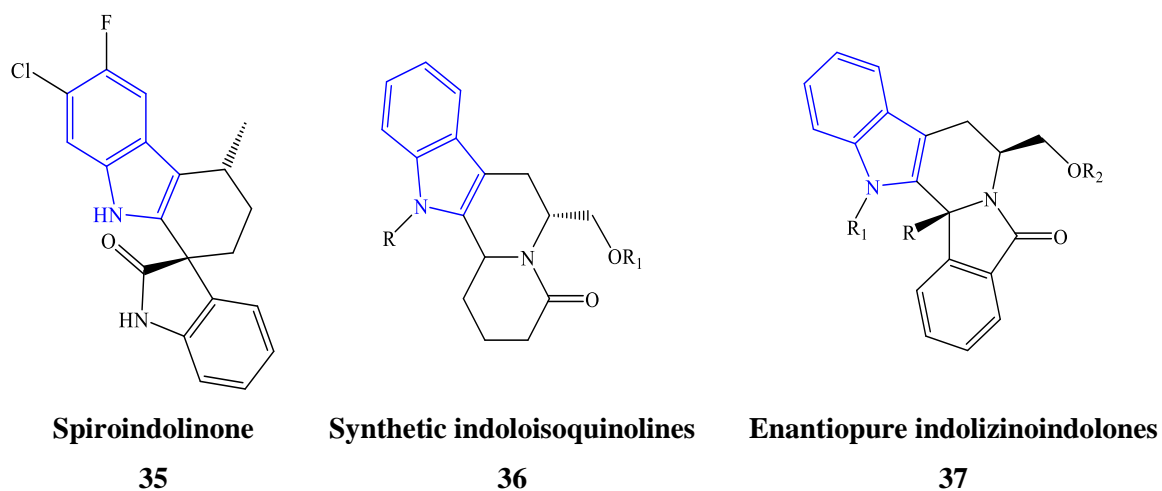


Figure 1.14. From left to right: Chemical structure of spiroindolinone **35**, of indoloisoquinolines **36** and enantiopure indolizinoindolones **37** general structures.

Our research group has been interested in the study of tryptophanol derivatives as a source of antitumor and antimalarial agents [74]. Based on the tools settled in terms of knowledge in this state of art, in this thesis it was studied the synthesis of tryptophanol-derived bicyclic lactams, the hit-to-lead optimization of the most promising candidates and their evaluation in terms of activity in cancer and malaria.

2. Results and Discussion

2.1. Synthesis of a library of enantiopure tryptophan-derived oxazoloisindolinones

As referred in chapter 1, from the analysis of a chemical library of novel enantiopure tryptophan derived oxazoloisindolinones, the small molecule **34** was recently identified as a novel activator of wild-type p53 and reactivator of mutant-type p53 (**Figure 2.1**) [75]. Therefore, the first objective of this thesis was the hit-to-lead optimization of derivative **34** to search for new leads acting as anticancer small molecules. Chemical modification of the nucleus present in the enantiopure tryptophan-derived oxazoloisindolinone was developed.

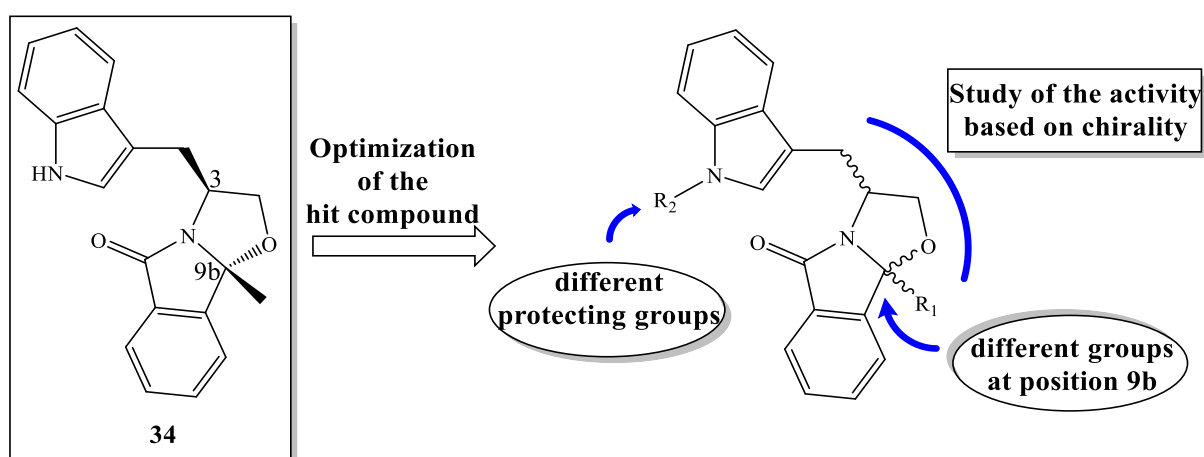
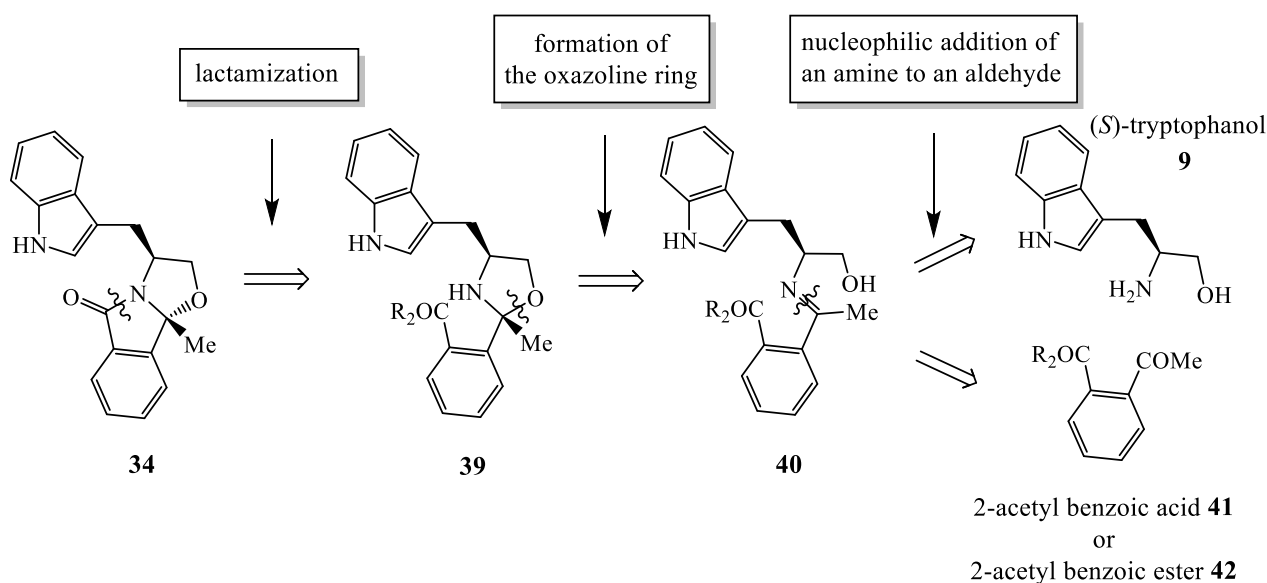


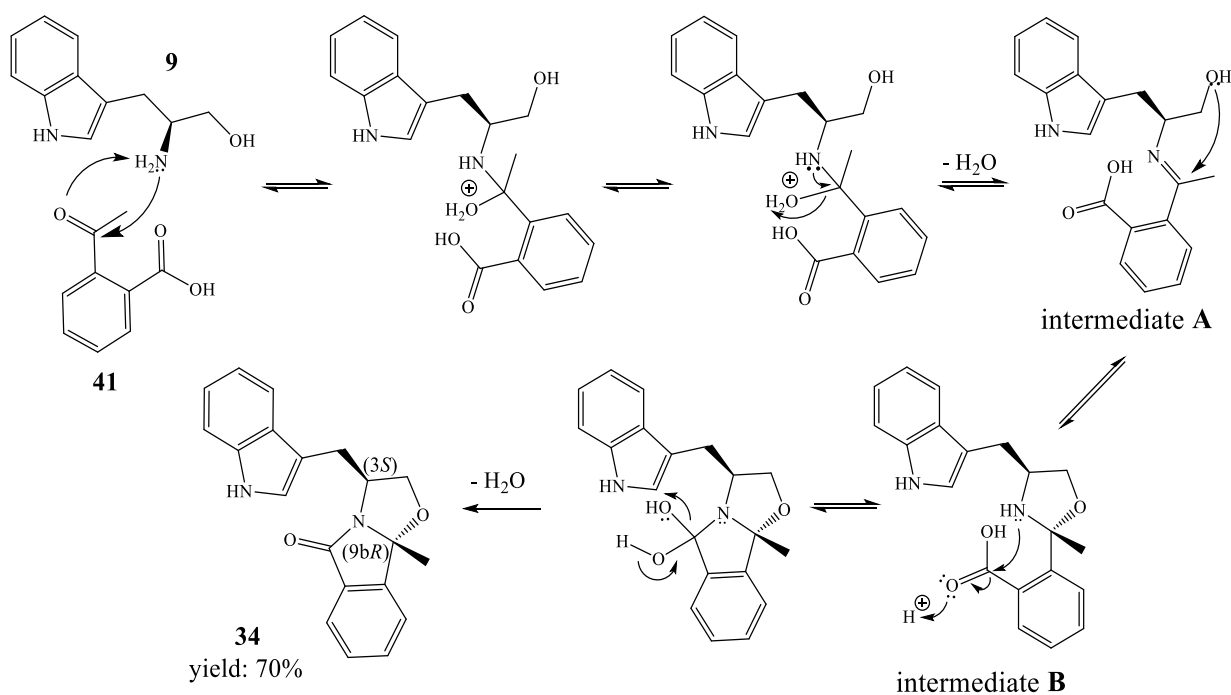
Figure 2.1. Strategy of hit-to-lead optimization of compound **34**.

Compound **34** was modified inserting different groups in positions 9b and different protecting substituents in the indole nitrogen. The stereochemistry of the final compounds was also considered. Particularly, several alkyl substituents with increasing size and electron withdrawing/donating groups were selected for the protection of the indole nitrogen. To assemble the library of new analogues, a retrosynthetic analysis of the hit compound **34** was rationalized, finding that it is possible to obtain the oxazolo-isindolinone skeleton, starting from commercially available amino alcohols and achiral oxoacids. As illustrated in **Scheme 2.1**, disconnection of the carbon-nitrogen bond through an opening ring process leads to intermediate **39**, and through a break-down of the oxazoline ring it is obtained the imine **40**. The imine can be obtained starting from (*S*)-tryptophan **9** and from 2-acetylbenzoic acid **41** or from the correspondent ester **42**.



Scheme 2.1. Example of retrosynthetic analysis of compound **34** for the oxazoloisindolinone library.

From a cyclocondensation reaction between racemic 2-acetyl benzoic acid **41** and (*S*)-tryptophanol **9**, and 2-benzoyl benzoic acid **43** and the enantiopure (*S*)- and (*R*)-tryptophanol **9** and **44** respectively, it was possible to build up the starting materials derivative **34**, **38** and **38'** for the development of the small library of bicyclic lactams (see **Scheme 2.3**, **Scheme 2.4** and **Scheme 2.5**). To guarantee that the chemical equilibrium of this reaction promotes the products formation it is required the use of a *dean-stark* apparatus which eliminates water from the reaction mixture. 1 equivalent of amino alcohol and a light excess of oxoacid (1.2 equivalents) are employed, affording the cyclocondensation products in good to excellent yields (70-80%). Since the products contain two chiral centres, it may be expected formation of two diastereoisomers, with *3S,9bS* and *3S,9bR* configurations respectively. In all the reactions, the exclusive formation of the *3S,9bR* epimer was observed. This can be explained through the analysis of the mechanism of reaction, designed for the cyclocondensation reaction and reported in **Scheme 2.2**. Nucleophilic attack by the amine group of the amino alcohol (*S*)-tryptophanol **9** to the carbonyl group of 2-acetyl benzoic acid **41** leads to imine intermediate **A**. In this stage of reaction, a first exit of water from the mixture of reaction takes place. Then, as illustrated in **Scheme 2.2**, intermediate **B** is formed by intramolecular attack of the hydroxyl function on the iminic carbon, where the hydroxyl group can promote formation of intermediate **B** through bottom attack or above attack. At last, the approach of the amine to the carbonyl group of the carboxylic acid leads to formation of oxazoloisindolinone **34**. The determining step that promotes product formation is the exit of water, which brings the chemical equilibrium dislocated in direction of the product of cyclocondensation.



Scheme 2.2. Mechanism of cyclocondensation reaction.

This reaction represents an interesting and functional synthetic methodology to access enantiomerically pure compounds. Amino alcohols, like (*S*)-tryptophan **9**, act as inductor of chirality where a new chiral centre is formed [76]. Starting from (*S*)-tryptophan **9**, the only product formed has configuration 3*S*,9*bR*. This fact is correlated by the presence of the amino alcohol tryptophan which acts as chiral inductor in this reaction. As it is possible to asseverate, the cyclocondensation reactions, performed in this work of thesis, are stereoselective. The control of the stereoselectivity was establish in first place with ¹H-NMR spectroscopy, where, through comparison of the most characteristic signals of hit-compound **34** with the ones of the derivatives obtained, it was possible to establish the stereochemistry formed. Indicated with blue arrows are reported in **Figure 2.2** the most characteristic protons for this class of bicyclic lactams. As illustrated specifically in the NMR spectrum of **Figure 2.3**, the multiplet at around 4.60 ppm is attributed to (H-3) hydrogen. Two doublet of doublets at around 4.30 ppm and around 4.18 ppm are associated respectively to the diastereotopic couple of hydrogens connected to carbon C-2 of the oxazolidine ring (they are indicated in **Figure 2.2** with the abbreviation H-2) and the other two doublet of doublets at around 3.43 ppm and around 3.18 ppm identify the second diastereotopic couple of

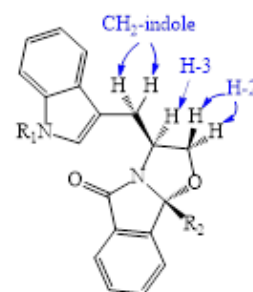


Figure 2.2. General structure of the (*S*)-tryptophan bicyclic lactams, where the more characteristic protons are reported.

hydrogens, connected to carbon C-10 located in the proximity of the indole nucleus (in **Figure 2.2** these hydrogens are indicated as CH₂-indole).

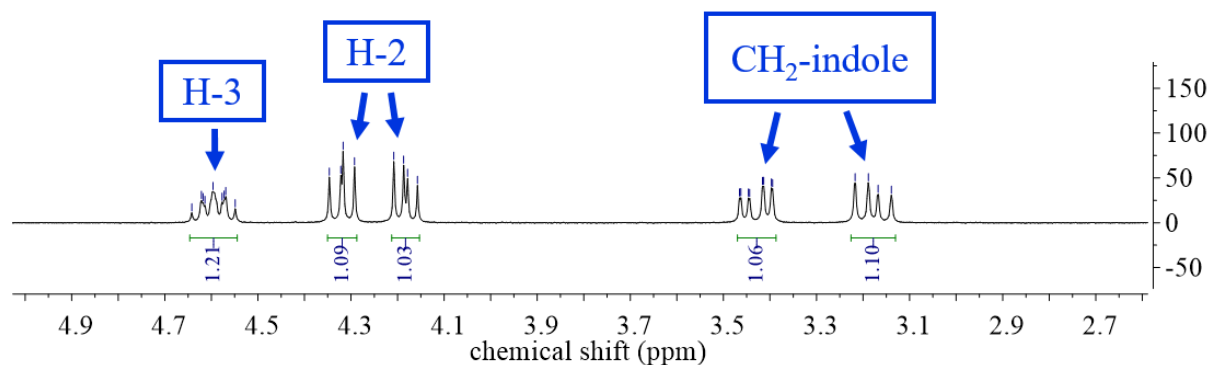
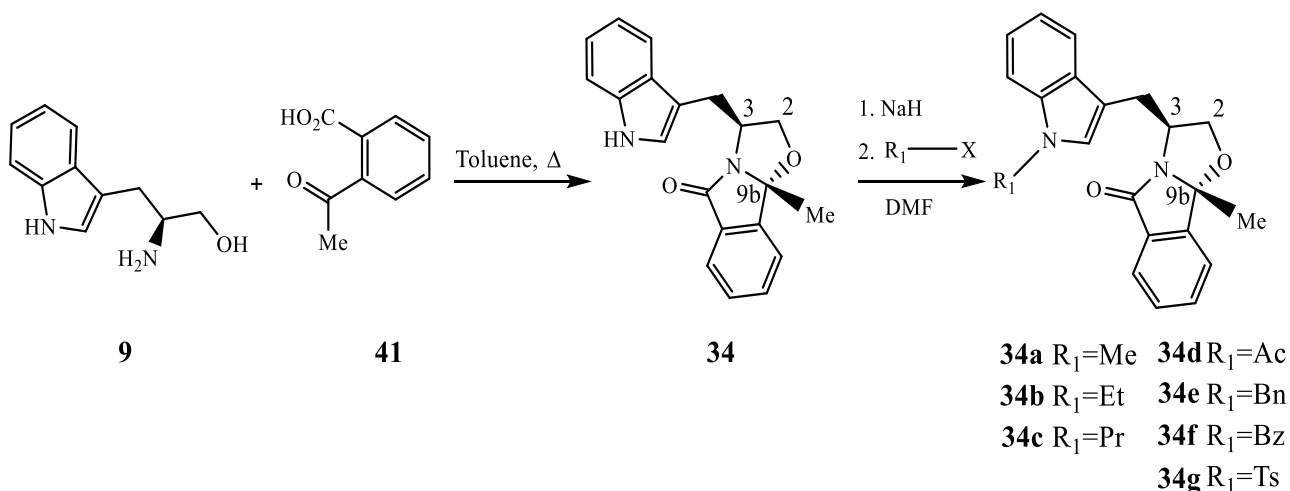


Figure 2.3. Expansion of ¹H-NMR spectrum of compound **34** in CDCl₃ between 5.0 and 2.6 ppm.

Finding correlation between the signals of the diversified derivatives is meaningful for the identification of the stereochemistry of these enantiopure bicyclic lactams. In addition, it was previously confirmed by X-ray analysis the structure of the bicyclic lactam **34** [77]. For this reason, decisive it results the analysis of the ¹³C-NMR peaks of compound **34** for the two stereogenic carbons in position 3 and 9b, where carbon C-3 is detected at 56 ppm and the new chiral centre formed, C-9b, at 98.9 ppm. Exceptionally for (*R*)-tryptophanol **44**, all amino alcohols and oxoacids were commercially purchased. (*R*)-tryptophanol **44** was obtained by reduction of the commercially available amino acid tryptophan with lithium aluminium hydride, which as reported in literature, it constitutes a recommended approach of preparation of this starting material [27]. After this first step of cyclocondensation, compounds **34a-g**, **38a-g** and **38a'-g'** were obtained after a second synthetic protection step. The chemical derivatization, that it was carried out, has the scope of discovering analogues, optimized leads generation of compound **34**, which, through a SAR study of this derivative, a more potency in terms of biological activity should be achieved. The products are obtained by first deprotonation on the nitrogen of the indole nucleus, promoted by sodium hydride. Secondly, a variety of electron withdrawing and electron donating protecting groups of different size are introduced to construct a chemical diverse library of compounds.

In **Scheme 2.3** and in **Scheme 2.4**, are presented the general procedures used to obtain the new bicyclic lactams derived from hit compound **34**.



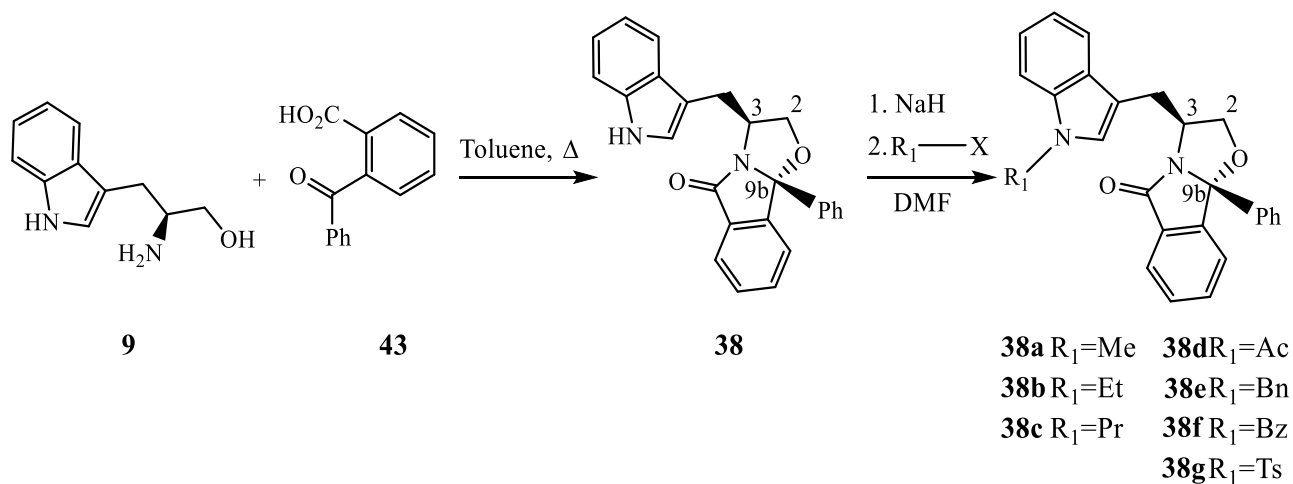
Scheme 2.3. General procedure for the synthesis of (*S*)-tryptophanol-derived bicyclic lactams **34a-g**.

The results obtained in terms of yields of reaction are included in **Table 2.1**, where compounds **34a-g** were obtained in yields between 71 and 90%. In the choice of studying exclusively the activity of (*S*)-tryptophanol based bicyclic lactams there is the fact that compound **34'**, enantiomer of compound **34**, was found to be not selective for HCT116 tumor cells [75] and so the hit-to-lead optimization process was focused only on the (*S*)-tryptophanol derivatives. The choice of introducing these specific protecting groups was based on the interest in testing if an increase in size can improve the potency of the hit compound **34** as well as if introducing electron donating/withdrawing groups can implement its biological activity. Anyway, a study of the activity was based even in changing the substituent in position 9b, introducing a phenyl group.

Table 2.1. Reaction yields for the *N*-protected (*S*)-tryptophanol derivatives **34a-g**.

Reference	(<i>S</i>)-tryptophanol derivatives	
	R ₁	η (%)
34a	Me	90.3
34b	Et	71.5
34c	Pr	75.3
34d	Ac	79.5
34e	Bn	83.9
34f	Bz	76.6
34g	Ts	85.4

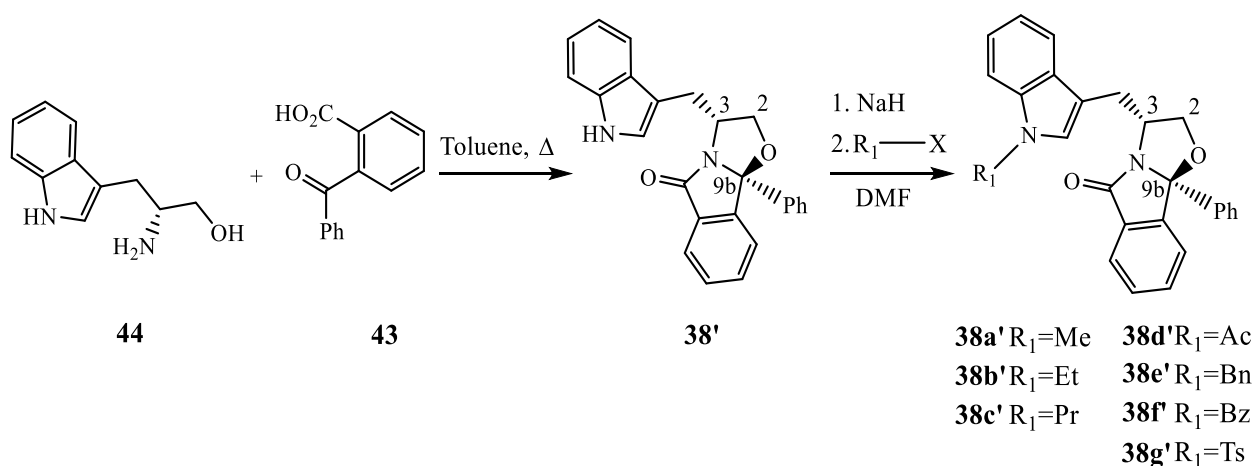
Compounds **38a-g** were afforded by cyclocondensation reaction of (*S*)-tryptophanol **9** and 2-benzoyl benzoic acid **44** (see **Scheme 2.4**) and the corresponding enantiomers **38a'-g'** are synthesized using the same route starting from (*R*)-tryptophanol **44**, as it is possible to see in **Scheme 2.5**. This first cyclocondensation step is followed by the protection on the nitrogen of the indole nucleus. The yields of reaction obtained are listed in **Table 2.3**.



Scheme 2.4. General procedure for the synthesis of (*S*)-tryptophanol derived bicyclic lactams **38a-g**.

Table 2.2. Reactions yields for the *N*-protected (*S*)-tryptophanol derivatives **38a-g**.

Reference	<i>(S)</i> - tryptophanol derivatives	
	R ₁	η (%)
38	H	81.3
38a	Me	89.5
38b	Et	70.6
38c	Pr	77.0
38d	Ac	84.2
38e	Bn	96.2
38f	Bz	76.6
38g	Ts	80.1



Scheme 2.5. General procedure for the synthesis of (*R*)-tryptophanol derived bicyclic lactams **38a'-g'**.

As reported in **Table 2.2** and **Table 2.3**, compounds **38a-g** compounds **38a'-g'** were obtained in good to excellent yields between 77 to 96% and between 60 to 88%, respectively. This datum reflects the efficacy of the synthetic route, through which the library of bicyclic lactams was built.

Table 2.3. Reaction yields and times for the *N*-protected (*R*)-tryptophanol derivatives **38a'-g'**.

Reference	<i>(R)</i> - tryptophanol derivatives	
	R ₁	η (%)
38'	H	79.1
38a'	Me	86.5
38b'	Et	82.0
38c'	Pr	70.0
38d'	Ac	74.5
38e'	Bn	75.5
38f'	Bz	60.0
38g'	Ts	87.6

All compounds were characterized by NMR spectroscopy. As shown in **Figure 2.4** and **Figure 2.5**, for bicyclic lactams the most characteristic signals appearing in ¹H-NMR spectra correspond to the proton connected to carbon 3 (H-3), the couple of protons linked to the carbon atom next to the oxygen of the oxazolidine ring (H-2), and the second couple of diastereotopic hydrogens connected with the carbon

directly linked to the indole core (CH₂-indole). For most of the compounds, it is observed that H-3 appears as the most deshielded alkyl proton, appearing as a multiplet between 4.34 and 4.12 ppm for compounds **34a-g**, and between 4.73 and 4.65 ppm for compounds **38a-g** and **38a'-g'**. Protons H-2 are diastereotopic protons, which means that each magnetic protonic nucleus has a different chemical and magnetic environment around. Since H-2 protons are diastereotopic, they also couple between each other. In the case of compounds **34a-g** the H-2 protons appear as two doublet of doublets around 4.34 and 4.12 ppm, while for compounds **38a-g** and **38a'-g'** these two signals appear between 4.54 and 3.90 ppm. The CH₂-indole protons are also diastereotopic. For the diastereotopic H-2 hydrogens the highest *J* value observed is of around 9 Hz and lowest *J* value of around 7.5 Hz meanwhile CH₂-indole hydrogens couple together with a coupling constant *J* of highest value of about 14 Hz and lowest value of 9 Hz. Sometimes H-2 protons are represented in the ¹H-NMR spectrum by an apparent triplet, resulting from a coalescence process, where the inner peaks of the doublet of doublets melt together originating the false triplet. The protons of CH₂-indole appear at upper fields, generally between 3.46-2.99 ppm and at 3.21-2.58 ppm for compounds **34a-g** and **38a-g**, respectively (**Figure 2.4** and **Figure 2.5**).

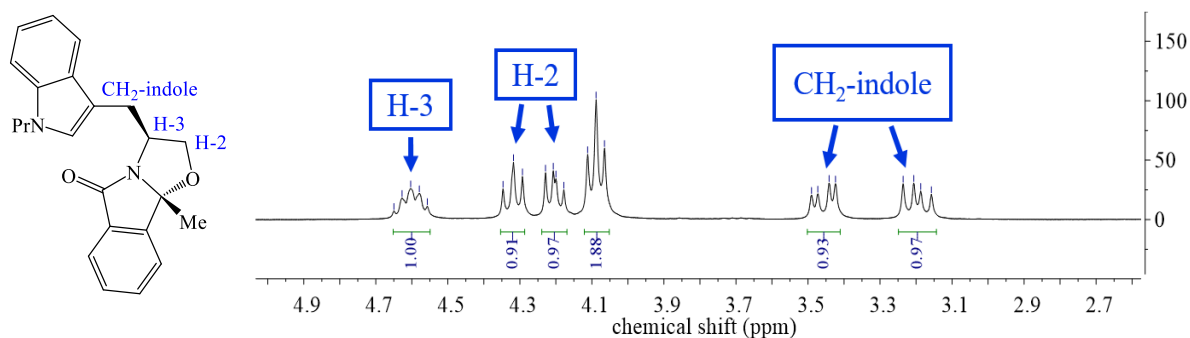


Figure 2.4. Expansion of ¹H-NMR spectrum of compound **34c** in CDCl₃ between 5.0 and 2.6 ppm.

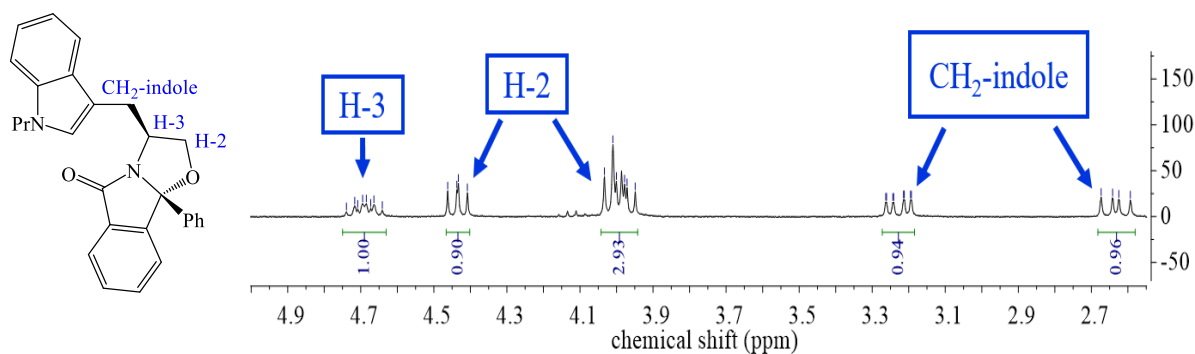


Figure 2.5. Expansion of ¹H-NMR spectrum of compound **38c** in CDCl₃ between 5.0 and 2.6 ppm.

To assess that the protection reaction occurred it is essential to identify the most characteristic signals related to the protecting substituents. In compounds **34a**, **38a** and **38a'**, the *N*-methyl group can be identified by a singlet at about 3.75 ppm related to the methyl substituent. The presence of the *N*-ethyl group in compounds **34b**, **38b** and **38b'** can be established by the presence of a triplet at about 4.12 ppm (triplet related to the two methylenic protons) and by the presence of a more shielded quartet at 1.46 ppm attributed to the methyl frame of the *N*-ethyl group. These two signals are found to be coupled by a *J* coupling constant of around 7.2 Hz. For the *N*-propylated products, it is observed a triplet at 4.09 ppm of the methylene protons beside the nitrogen of the indole core, a sextet at 1.89 ppm of the intermediary methylene protons, and a shielded triplet, at 0.96 ppm, from the methyl group of the propylic chain. Even for this case a *J* coupling constant of about 7 Hz is measured. Acetylation was confirmed by the presence of a deshielded singlet at about 2.60 ppm in the NMR spectra of compounds **34d**, **38d** and **38d'**. This signal is related to the methyl frame of the acetyl group. Quite diagnostic is the singlet at 5.25 ppm related to the 2 methylene protons of the benzyl substituent of compounds **34e**, **38e** and **38e'**. In the case of compounds **34g**, **38g** and **38g'**, tosylation was confirmed by the presence of a singlet at 2.30 ppm related to the methyl group connected to the phenyl ring of the tosyl group. The ¹³C-NMR is also helpful and it represents a useful tool to understand if the compound expected is the diastereoisomer desired. As reported in **Table 2.4** The signal of the new chiral centre, C-9b, appears always between 99 and 98 ppm for compounds **34a-g** and at 100 ppm for compounds **38a-g**, an indication that the specific diastereoisomers formed are the ones expected. The stereochemistry assessed is 3*S*, 9*bR* in the case of (*S*)-tryptophanol bicyclic lactams **34a-g** and **38a-g**. In **Table 2.1-4** the most characteristic chemical shifts are reported. As it is possible to observe, the greatest variation between compounds **34a-g** and **38a-g** in terms of chemical shift is notable for the signal related to the carbon connected with the diastereotopic protons, close to the indole frame. This means that this part of the framework of the molecules is more sensitive to the changes in terms of magnetic and chemical environment, based on the proximity of these nuclei to the part of the molecule that it is optimized. Other curious variation observed is related with the chemical shift of C-9b of compounds **34d** and **38d**, which appears more deshielded in comparison with the ones of the starting materials, compounds **34** and **38**, respectively.

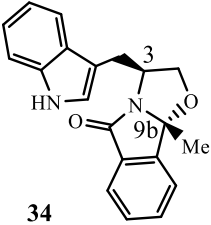
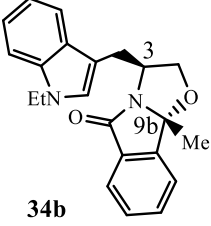
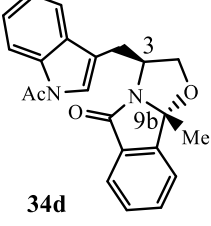
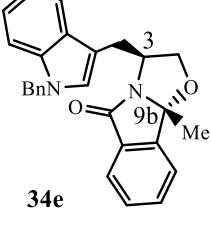
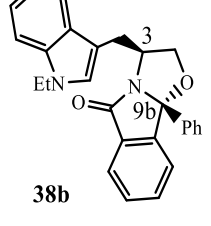
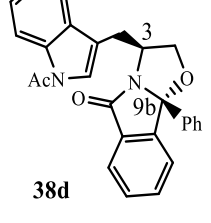
Table 2.4. Comparison between ^{13}C -NMR chemical shifts of the hit-to-lead optimization products, **34a-f** and **38a-f**.

^{13}C -NMR δ (ppm); R ¹ = Me				Reference		^{13}C -NMR δ (ppm); R ¹ = Ph			
C-9b	C-2	C-3	CH ₂ -indole			C-9b	C-2	C-3	CH ₂ -indole
98.87	74.65	55.95	30.84	34	38	100.79	76.24	55.87	30.31
98.96	74.80	56.22	30.67	34a	38a	100.95	76.32	55.79	30.04
98.97	74.75	56.23	30.60	34b	38b	100.94	76.35	55.78	30.15
98.97	74.72	56.24	30.59	34c	38c	100.93	76.32	55.78	30.12
99.22	74.91	54.97	30.64	34d	38d	101.18	76.24	54.50	29.68
99.05	74.79	56.23	30.72	34e	38e	100.93	76.27	55.74	30.14
98.99	74.54	55.33	30.72	34f	38f	100.99	75.93	55.07	29.68
98.98	74.39	55.09	30.35	34g	38g	100.95	76.00	54.61	29.88

2.1.1. Biological evaluation of a library of enantiopure tryptophanol-derived oxazoloisindolinones

The biological activity of compounds **34b**, **34d**, **34e**, **38b** and **38d** was evaluated using a yeast-based screening strategy [75]. The approach is based on the restoration of the wt-like activity of mut p53R280K, a mutated form of p53 where an amino acidic residue of Arginine is replaced in position 280 of the DNA binding domain of wt-p53 with a Lysine. Once the p53 is in its mutated form is tested how much the bicyclic lactams are able to restore the wt-like activity in this specific mutant form of p53. The expression of mutant was previously determined and no significative differences were observed compared to that of wt-p53 [75]. As expected, mut p53R280K did not considerably interfere with the yeast cell growth when compared to yeast transformed with the empty vector (control). Thereafter, this cell system was used to test 1-30 μM of compounds. Considering the activity of compound **34** as reactivator of mutant p53R280K [75], this compound was used as positive control. Results presented in **Table 2.5** correspond to the maximal effect obtained with these compounds at 10 μM . For lower concentrations, these compounds did not significantly interfere with the yeast growth; higher concentrations of compounds did not increase the growth inhibitory effect, and for 30 μM unspecific cytotoxic effects were detected on yeast cells transformed with the empty vector (data not shown). The results of this first screening are listed in **Table 2.5**. The obtained results are reported as percentage of re-establishment of wild-type p53 induced in yeast cells expressing mutant p53R280K. Considering the result, reported in literature for compound **34** [75], it is possible to conclude that between the compounds tested, the (*S*)-tryptophanol-derived oxazoloisindolinone **34d** is the most active of the tested compounds. Compound **34d** restores the wt-like growth inhibitory effect to mut p53R280K in a percentage of 86.8%. An explicative interpretation of the results obtained can be researched firstly in the diversified nature of the protecting groups on the nitrogen of the indole core. The free nitrogen of the pyrrole ring of compound **34** and the carbonyl of the acetyl group of compound **34d** are hydrogen bond donor and acceptor respectively. Therefore, one possibility is that some hydrogen bonding is established, modulating the activity and this leads to a consistent growth inhibitory effect. Anyway, this seems significant only when the (*S*)-tryptophanol oxazoloisindolinones derivatives include in their structures a methyl group in position 9b since in comparison compound **38d** has by far a minor effect in the restoration of the wt-like activity of mut p53R280K. Particularly, it emerged that the methyl group in carbon C-9b is believed to support the growth inhibitory effect in comparison to the bulky phenyl group present in the chemical structure of compounds **38b** and **38d**. For example, the (*S*)-tryptophanol bicyclic lactam **38d** restores the wt-like growth inhibitory effect just 13.1%, meanwhile compound **38b** of 9.5% only. Moreover, taking into consideration the two oxazoloisindolinone derivatives ethylated **34b** and **38b**, it results that the ethylation does not give effective contribution in terms of biological anti-cancer activity.

Table 2.5. Percentage of re-establishment of wild-type p53-induced yeast growth inhibition in yeast cells expressing mutant p53R280K; *p* indicates the result precision. Results correspond to 3-7 independent experiments.

Structure	% mutant Reactivation	SEM	<i>p</i>
 <p>34</p>	61.4	1.8	-
 <p>34b</p>	8.7	5.4	0.772
 <p>34d</p>	86.8	11.0	<0.0001
 <p>34e</p>	13.4	2.1	-
 <p>38b</p>	9.5	8.1	0.847
 <p>38d</p>	13.1	7.9	0.845

2.2. Stability studies in human and rat microsomes, in human plasma and in pH 7.4 phosphate buffer of oxazoloisindolinones **34 and **34e****

Biological assessment of chemical leads represents a fundamental step in drug development process. In this scenario, investigation of the stability profile of promising drug candidates provides important information about the behaviour of a compound in a certain biological context. Metabolic stability studies represent some of the earliest *in vitro* approaches, used to optimize pharmacokinetic parameters like bioavailability and clearance. From the other side, plasma stability plays an important role in drug discovery, where it is studied the degradation profile of a test compound. At last, pH-profile study is relevant to evaluate if the testing compound does not degrade at physiological conditions. As it emerged from literature and in this work of thesis, (*S*)-tryptophanol bicyclic lactam **34** was identified as promising anticancer agent [75]. Consequently, it become meaningful to investigate the *in vitro* stability of this class of compounds in rat and human microsomes in human plasma and at last in pH 7.4 phosphate buffer. Compounds **34** and **34e** were used as models.

2.2.1. Determination of the metabolic stability of compounds **34 and **34e**. Characterization of Phase I metabolites by LC-ESI-MS upon microsomes incubation**

Identification of metabolites is crucial in drug discovery and development process to optimize lead compounds for further development. The information generated in the early discovery phase of metabolic identification can be used to identify lead compounds and undesirable metabolic products, which can penalize a promising drug candidate. According to the knowledge available about these biological analyses, the experimental approach followed was based on determining the metabolic stability of compounds **34** and **34e** from *in vitro* incubations of thawed pooled male rat and pooled human liver microsomes in two different experiments. *In vitro* interspecies metabolism studies are functional in order to screen for qualitative similarities and differences in metabolism between human and animal species [78]. The general methodology for the screening involves a period of incubation of a total of 180 minutes in liver microsomes supplemented with NADPH regenerating system. Test compounds **34** and **34e** were assayed in duplicates and added at a low micromolar concentration (10 μ M) to a pH 7.4 phosphate buffer system. A NRS regenerating system was then added. The incubation was maintained at 37°C in a shaking water bath and the reaction was stopped by addition of a cold solution of Reserpine in acetonitrile, which it was used as internal standard for the determination of the relative amount of parent drug in each time point. The acetonitrile addition has the function of stopping the microsomal enzymatic activity, upon precipitation of proteins. To evaluate if the test compounds underwent any Phase I enzymatic modification a LC-ESI(+)-MS analytical methodology was used.

Particularly, the metabolic stability of compounds **34** and **34e** was assessed at times 0, 120 and 180 minutes. One additional incubation of Neviripine, a drug whose metabolic products are known, was used as a positive control to ensure a properly microsomal activity. In the case of compound **34**, it resulted that after 120 minutes of experiment 57.7% of the initial quantity went under metabolic Phase I chemical modifications. Moreover, after 180 minutes of incubation, almost 40% of compound resulted unmodified. A screening of the metabolites formed during the incubation time was then performed. For this purpose, it is very important to know the behaviour of the parent drug under the analytical conditions used. Compound **34** eluted at 28.3 minutes under the chromatographic conditions was used, and exhibits a signal at m/z 319, compatible with its the protonated molecule in the full scan mass spectrum. As illustrated in **Figure 2.6**, the full scan ESI-MS/MS spectrum of $[M+H]^+$ ion (m/z 319), of compound **34** displays abundant product ions at m/z 301 (that stems from the loss of water from the protonated molecule), m/z 174 (loss of the oxazoloisoindolinone moiety), m/z 156.01 (loss of the indole core and of the oxazolidine ring in protonated molecule form), m/z 130 (indole core). In **Figure 2.7** a proposed ESI(+)-MS/MS mechanism of fragmentation for the protonated molecule of **34** is reported.

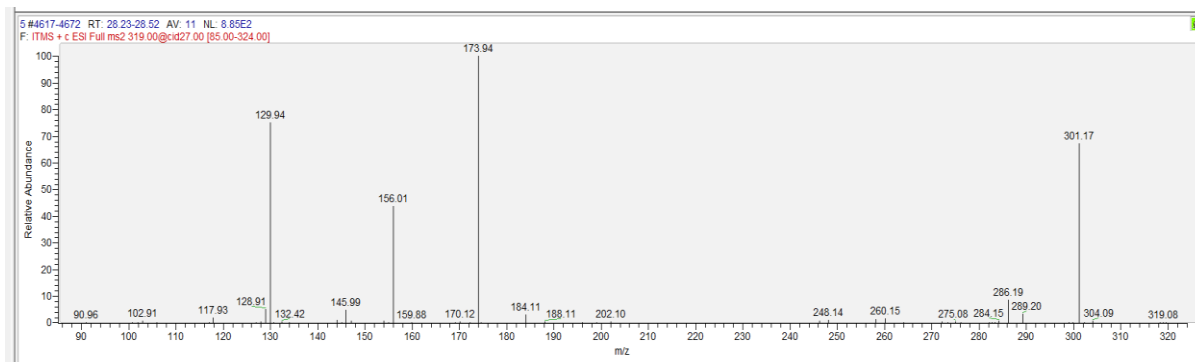


Figure 2.6. Tandem mass spectrum obtained upon LC-ESI(+)-MS/MS analysis of m/z 319 ion corresponding to the protonated molecule of compound **34**.

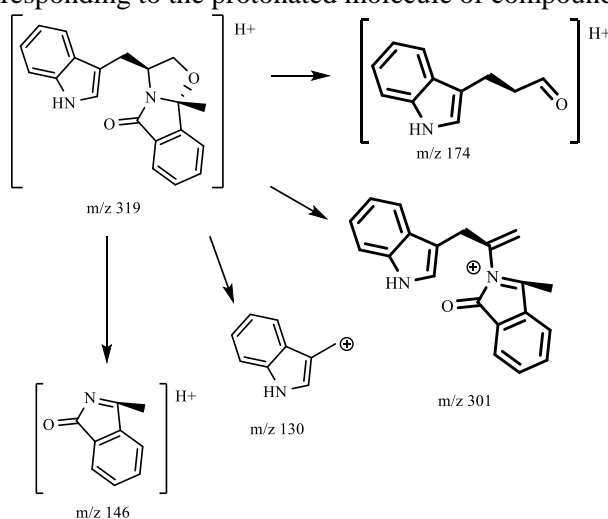


Figure 2.7. Proposed ESI(+)-MS/MS fragmentation mechanisms for the protonated molecule (m/z 319) of **34**.

All metabolic products of compound **34** are found to be eluted prior than the parent drug, which is compatible with the formation of more polar products. In fact, several mono-hydroxylated metabolites were distinguished for this (*S*)-tryptophanol bicyclic lactam. The extracted ion chromatogram of **Figure 2.9 C** presents three major peaks eluting at 22.90, 21.02 and 20.41 minutes. However, it was not possible to define precisely the site where the hydroxylation occurred in the three isomers due to the scarce fragmentation presented when analysed under tandem mass spectrometry conditions. Nonetheless, when subjected to tandem mass spectrometry, the monohydroxylated metabolite eluting at 22.90 minutes gives rise to several fragments which suggests that the hydroxylation occurred at the indole moiety (see **Figure 2.8 A and B**).

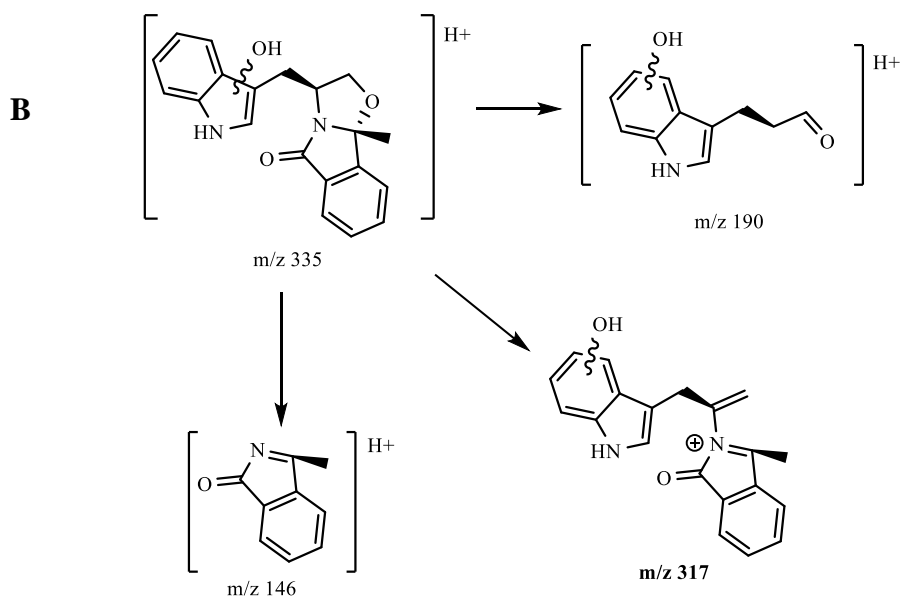
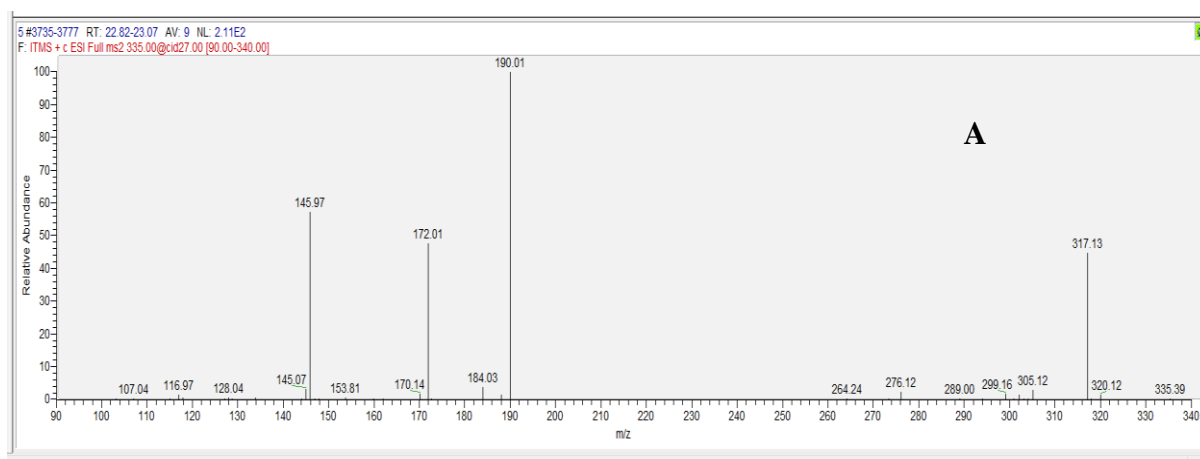


Figure 2.8. A) Tandem mass spectrum obtained by ESI(+) for the mono-hydroxylated metabolite of **34** eluting at 22.90 minutes; B) Proposed fragmentation mechanism for this metabolite.

Additionally, several di-hydroxylated metabolites of compound **34** were detected. As depicted in the extracted ion chromatogram of m/z 351 (**Figure 2.9 D**), six different di-hydroxylated metabolites were formed eluting at 19.6, 19.4, 18.3, 15.8, 15.2 minutes. The main peak, which it appears at 19.6 minutes was selected and its fragmentation pattern is reported in **Figure 2.11 B**. In this case, it can be suggested that di-hydroxylation occurs on the oxazolidine ring and on the carbon which links the indole core to the oxazoloisindolinone frame, based on the fragmentation pattern obtained under tandem ESI(+) analysis of this metabolite.

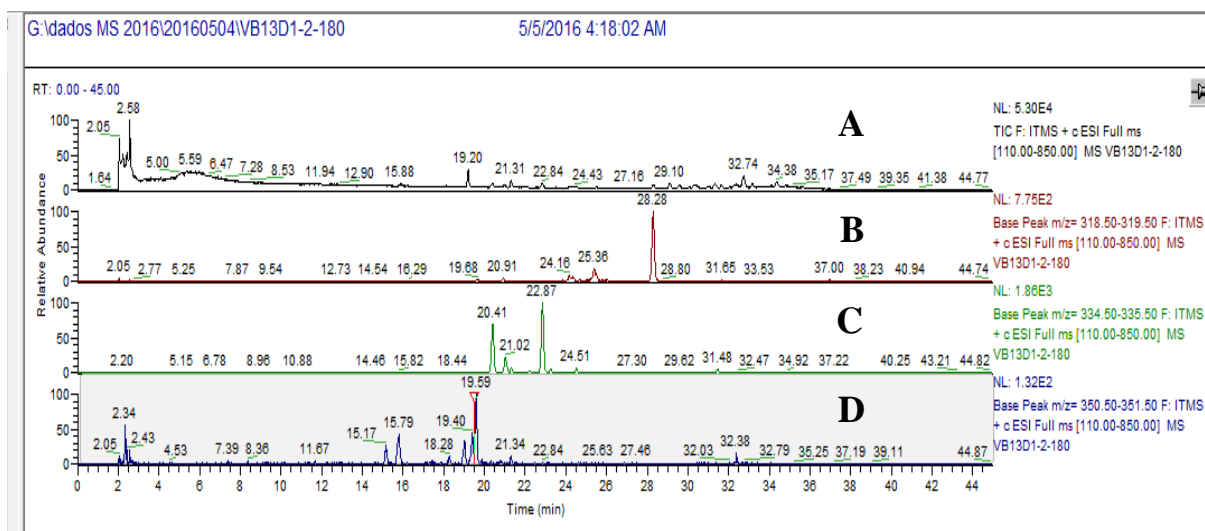


Figure 2.9. A) Total ion chromatogram obtained by LC-ESI(+)-MS of compound **34** under microsomes incubations; B) Extracted ion chromatogram of ion m/z 319 corresponding to the protonated molecule of **34**; C) Extracted ion chromatogram at m/z 335 corresponding to the protonated molecules of hydroxylated metabolites of **34**; D) Extracted ion chromatogram at m/z 351 corresponding to the protonated molecules of dihydroxylated metabolites of **34**.

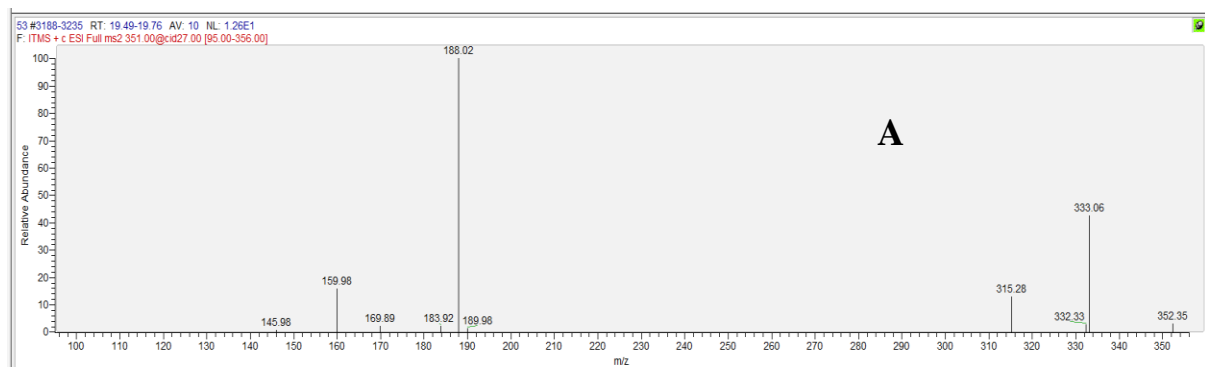


Figure 2.10. A) Tandem mass spectrum obtained by ESI(+) for the dihydroxylated metabolite of **34** eluting at 19.6 minutes;

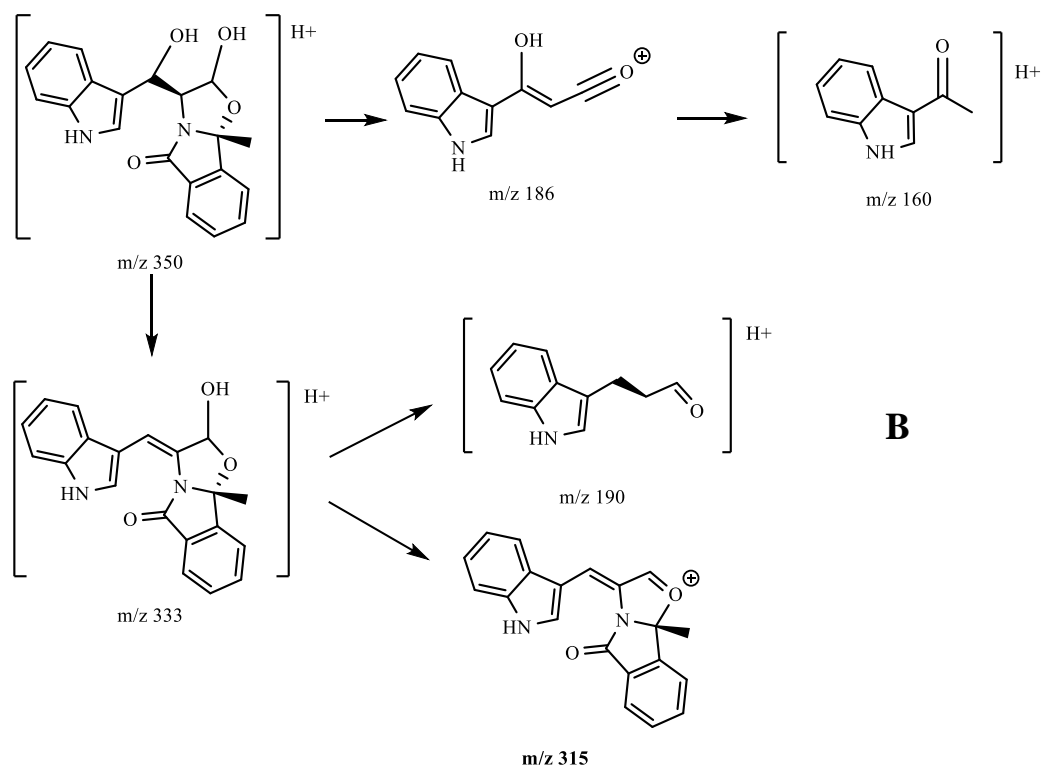


Figure 2.11. B) Proposed fragmentation mechanism for this metabolite.

A similar study was performed for compound **34e**. In first approach, the percentage of compound lost over the time in the presence of metabolically active microsomes was determined. In this case, in the first 120 minutes of experiment it was found that 69.3% of this compound is present in the samples analysed by LC-ESI-MS, and after 180 minutes of experiment only 26.3% of test molecule was found to remain unmetabolized. Subsequently, an attempt to identify some of the metabolites formed was undergone. Compound **34e** eluted at 35 minutes, under the chromatographic conditions used, and, as illustrated in **Figure 2.12**, the tandem mass spectrum of m/z 409 ion, corresponding to the protonated molecule of compound **34e** displays abundant product ions at: m/z 391 (loss of the oxygen on the oxazolidine ring as H_2O), m/z 264 (loss of the oxazoloisoindolinone frame) and m/z 220 (indole core benzylated). In **Figure 2.13**, is reported a possible mechanism of fragmentation for this specie.

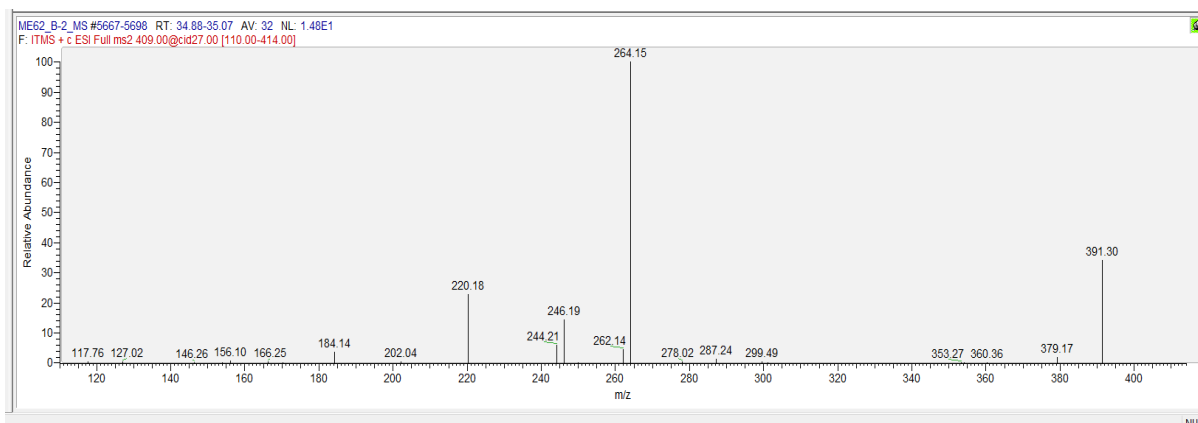


Figure 2.12. Tandem mass spectrum obtained by ESI(+) of ion at m/z 409, corresponding to the protonated molecule of compound **34e**.

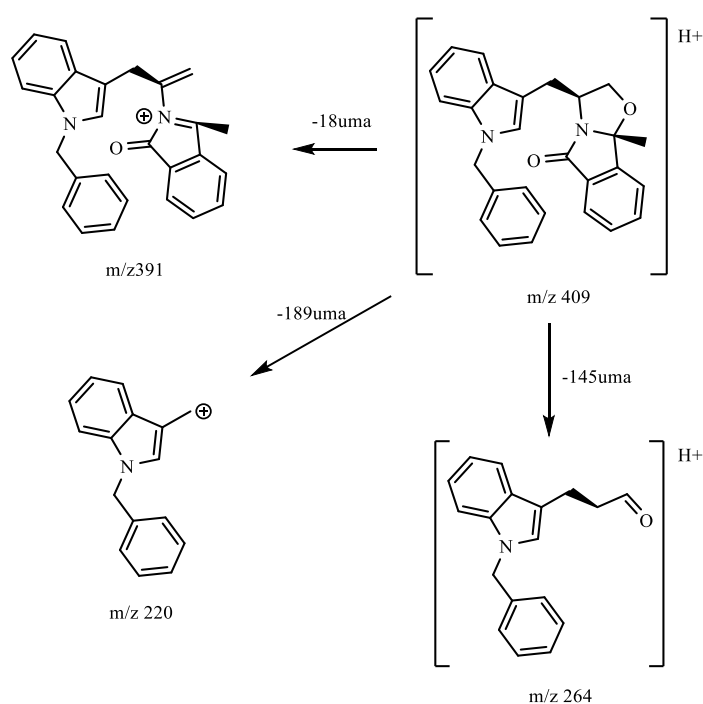


Figure 2.13. Proposed ESI(+)-MS fragmentation mechanism of compound **34e**.

From the extracted ion chromatogram of m/z 425 ion (**Figure 2.14 D**) it is possible to observe that several mono-hydroxylated metabolites of compound **34e** are formed. They eluted at 30.0, 31.1 and 32.5 minutes, where the main monohydroxylated metabolite is detected at retention time 30.0 minutes. From its fragmentation profile obtained upon ESI(+)-MS/MS, it emerges that probably the mono-hydroxylation occurs on the junction carbon between the indole core a fragmentation profile where abundant product ions at m/z 407, m/z 280, m/z 262, m/z 236 are observable (**Figure 2.15**). The mechanism of fragmentation is reported in **Figure 2.16**, where the proposed structure for fragments at m/z 262 and 236 are compatible with the position of hydroxylation assigned.

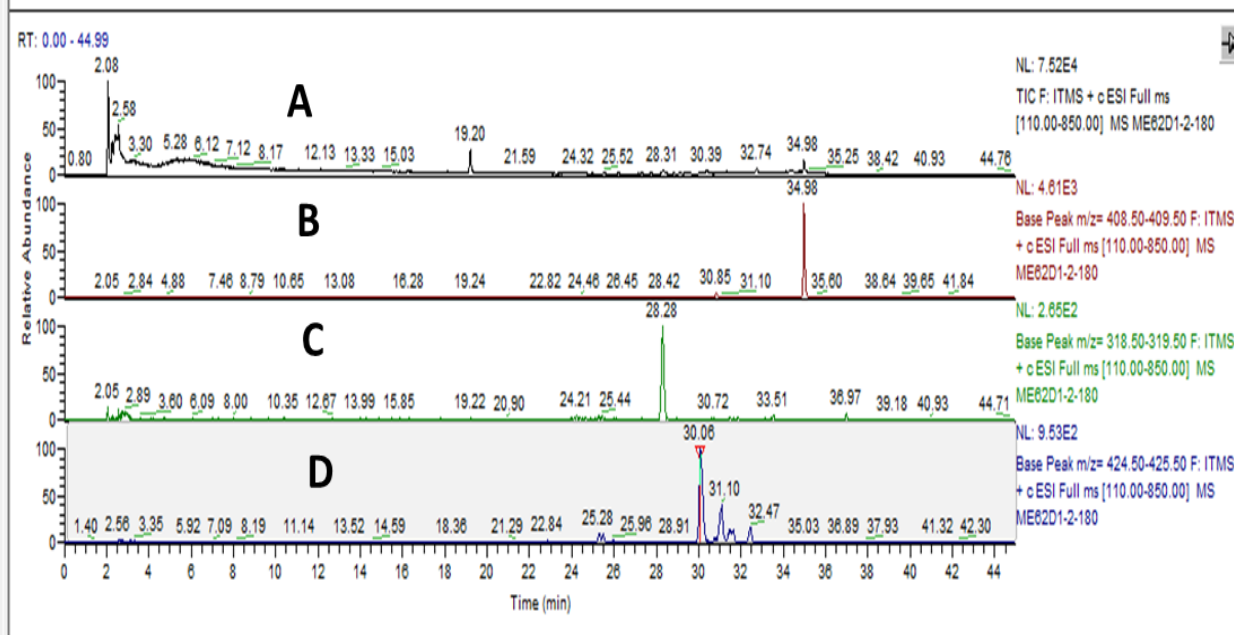


Figure 2.14. A) Total ion chromatogram obtained by ESI(+)-MS for **34e** incubations; B) Extracted ion chromatogram at m/z 409, corresponding to the protonated molecule of **34e**; C) Extracted ion chromatogram at m/z 319 corresponding to the debenzilation metabolic product of **34e** (corresponding to **34**); D) Extracted ion chromatogram at m/z 425 corresponding to the protonated molecule of hydroxylated metabolites of **34e**.

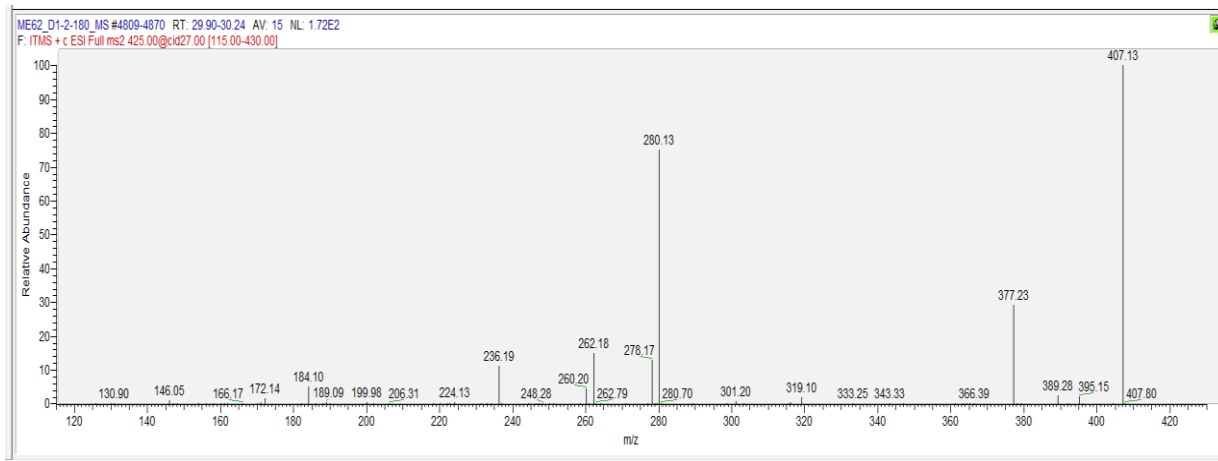


Figure 2.15. Fragmentation pattern obtained by LC-ESI-MS/MS of ion at m/z 425 eluting at 30.1 minutes.

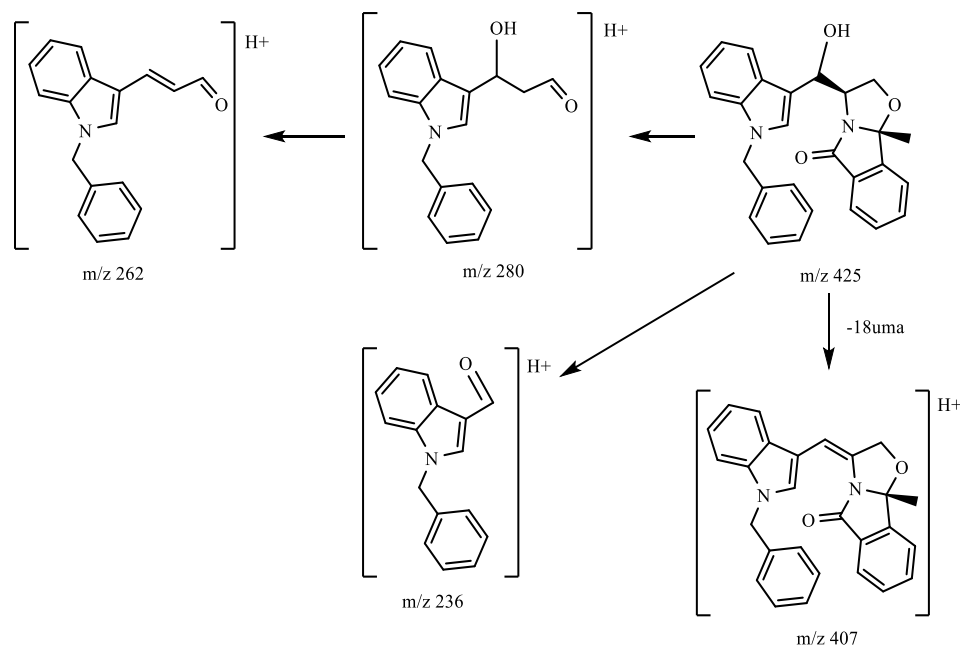


Figure 2.16. Proposed ESI(+)-MS/MS fragmentation mechanisms of ion m/z 425, eluting at 30.1 minutes, corresponding to the protonated molecule of the main hydroxylated metabolite of **34e**.

Unfortunately, the other two mono-hydroxylated metabolites of **34e** eluting at 31.1 and 32.5 minutes, despite exhibiting full mass spectra compatible with the occurrence of hydroxylation exhibited under tandem mass spectrometry only few product ions (**Figure 2.17**) which precluded the assignment of the position of hydroxylation.

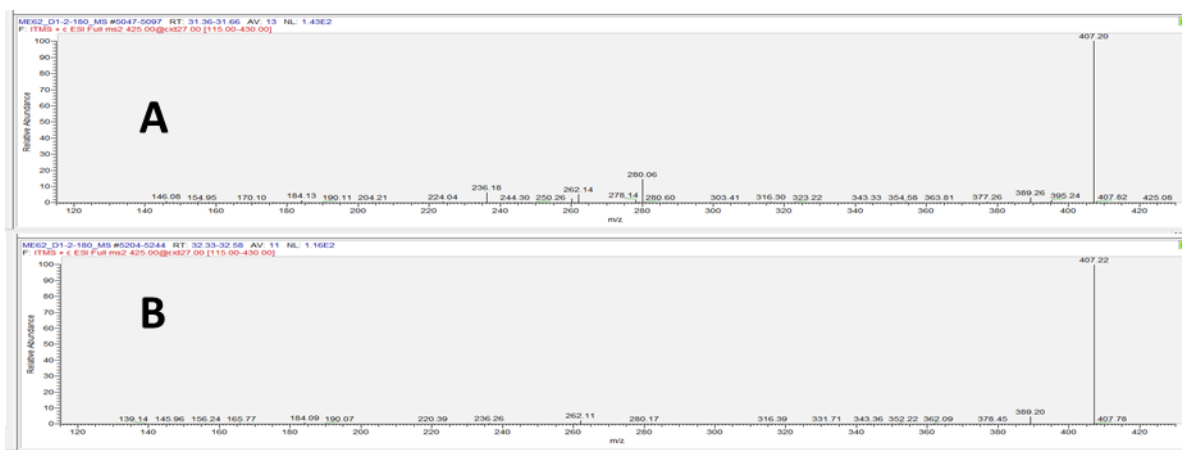


Figure 2.17. Tandem mass spectra obtained by ESI(+) of ion m/z 425 corresponding to the monohydroxylated metabolites of compound **34e** eluting at 31.10 min (**A**) and 32.47 min (**B**).

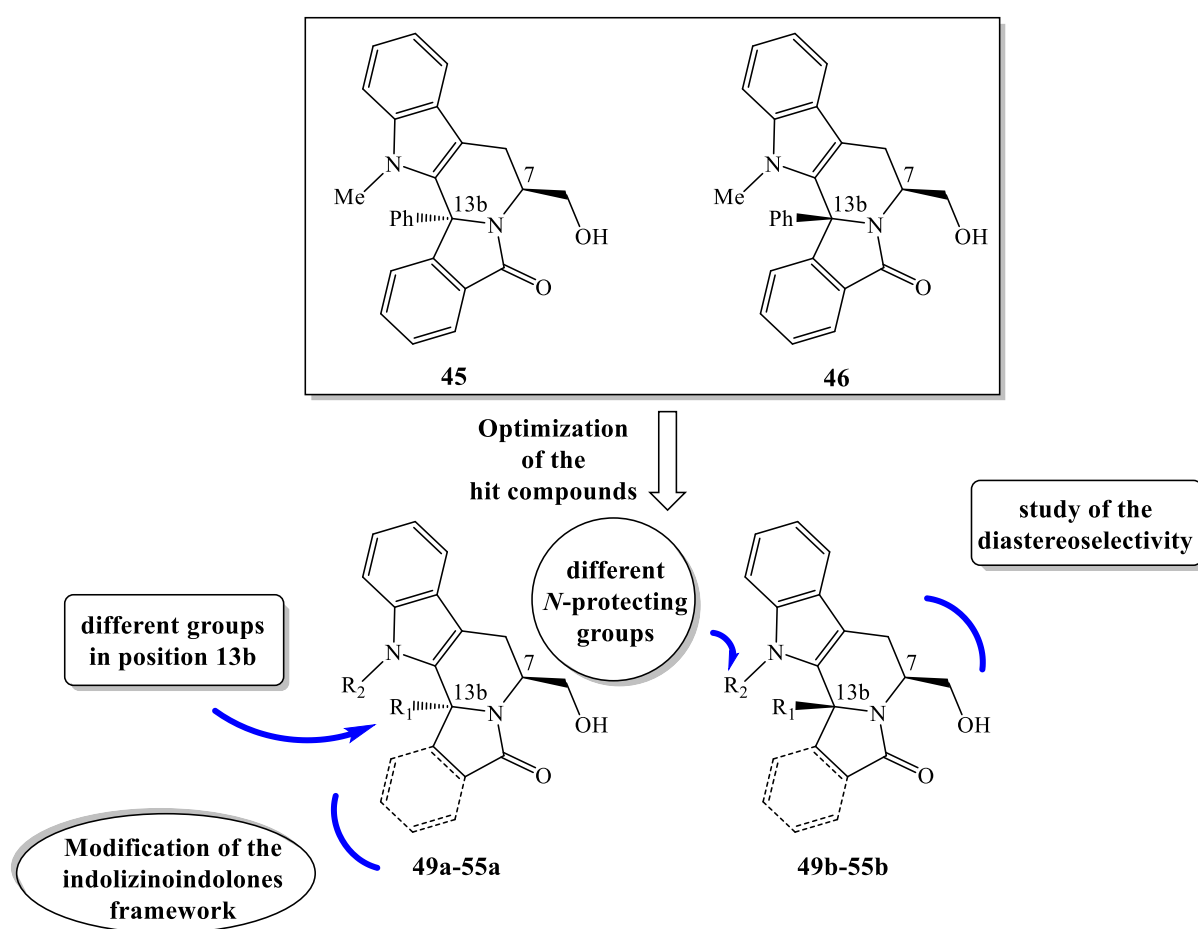
Additionally, it was detected at retention time of 26.4 minutes, a product of debenylation of the protonated molecule **34e**, exhibiting a signal in the full scan spectrum at m/z 319 (**Figure 2.14 C**) which corresponds to the protonated molecule of **34**. Nonetheless, no dihydroxylated metabolites were detected for this compound.

2.2.2. Determination of the stability of compounds **34** and **34e** in human plasma

In the early phase of drug discovery process, investigation of the stability in plasma is performed with the goal of evaluating the potential degradation of a new chemical entity by plasmatic enzymes. Compound **34** was identified as bioactive molecule, where after optimization of this hit compound, bicyclic lactam **34e** was used as model to determine the stability profile of the oxazoloisoindolinone bicyclic lactams. For this reason, it emerged of primary importance to study the stability profile of these two compounds. To assess the stability in human plasma of compounds **34** and **34e**, the standard experimental approach followed was based on the use of diluted thawed human plasma in pH 7.4 phosphate buffer [79]. It is important to adjust to physiological pH of the plasma since the result can be complicated by the pH effect. Furthermore, dilution of plasma reduces viscosity and increases pipetting accuracy [79]. Procaine was used as reference drug to verify the adequate plasmatic activity. Test compounds **34** and **34e** were assayed in duplicates and added at low micromolar concentration (40 μ M). This concentration was chosen to avoid any side effect of the substrate concentration on plasma activity. Moreover, a set of buffer samples were prepared in duplicate to test the stability of compound **34** and **34e** in the absence of plasma enzymes. The incubation was maintained at 37°C shaking water bath for a total time of 48 hours. This was possible since plasma is a quite robust biological component. Its enzymatic composition allows long incubation times, turning the plasma usefull to monitor slow degradation processes. In this experimental context plasma stability of compounds **34** and **34e** were studied at 0, 30, 60, 120, 180 minutes, 24 and 48 hours. To evaluate analytically if the test compounds underwent the usual plasma biotransformations both LC-ESI-MS and HPLC-DAD instrumental approaches were employed. A solution of Reserpine in acetonitrile was added at each aliquot. Acetonitrile is functional to arrest the enzymatic activity to proceed to further analysis. Calculations of the percentage of each testing compound were made as ratio of the peak areas obtained for each compound on the peak area of the internal standard Reserpine. As documented, the main chemical reactions in plasma that affect the stability of a drug are oxidation and hydrolysis. Hydrolysis is the most common pathway for drug breakdown and it was observed in this study. In general, both (*S*)-tryptophanol derivatives **34** and **34e** were found to be stable in human plasma, according to HPLC-DAD analysis and this result make of these compounds promising leads in anticancer research. Particularly, it was found that results obtained through LC-ESI-MS were not consistent since the buffer used was observed to suppress the signals. Derivatives **34** and **34e** were identified through their UV-vis profiles. The percentage of compound present unmodified was evaluated confirming the stability in plasma after the first 180 minutes of experiment.

Synthesis of a library of indolizinoindolones

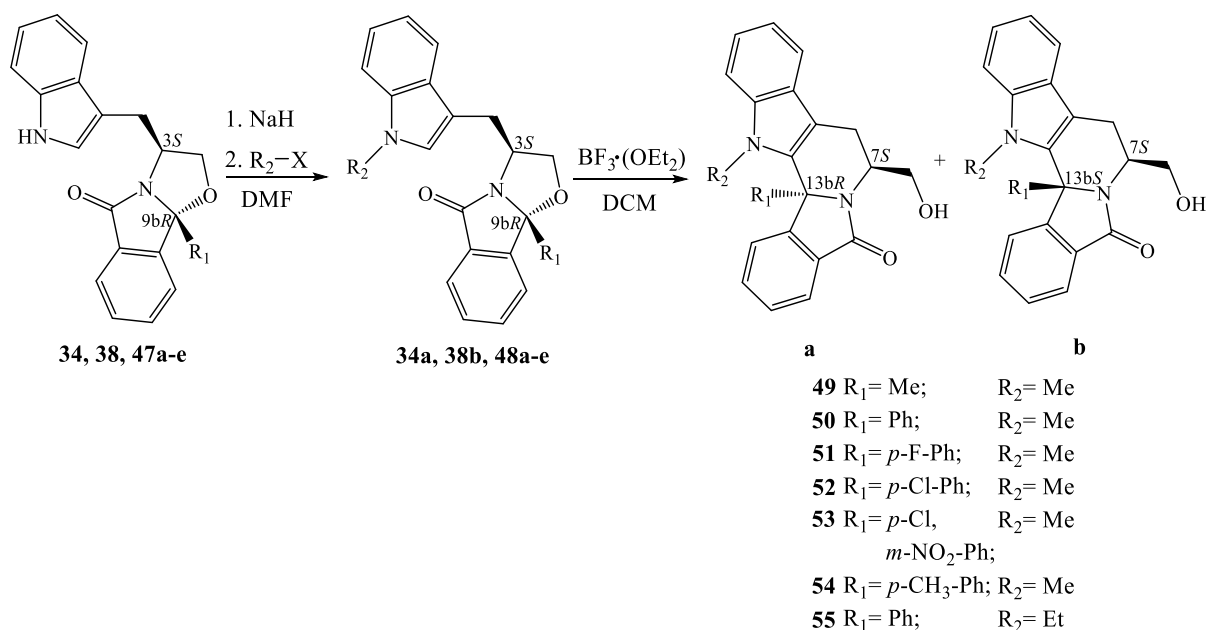
Indole-based compounds are known to possess a wide range of biological activities [80], including activity as antimalarials [81]. Moreover, a class of synthetic indoloisoquinolines as well as indolo[2,3-*a*]quinolizidines derivatives arose for their broad bioactivity profile [82]. Recently, our research group reported that enantiopure benzoindolizinoindolones, synthesized starting from (*S*)-tryptophan-derived bicyclic lactams display *in vitro* activity against erythrocytic and liver stages of malaria parasites [77]. Compounds **45** and **46** emerged as the most promising active derivatives. Taking advantage of the tryptophan-derived bicyclic lactams developed in chapter 2.1 of this thesis, we decided to develop a hit-to-lead optimization of compounds **45** and **46**, to develop more potent antimalarials, as reported in **Scheme 2.6**.



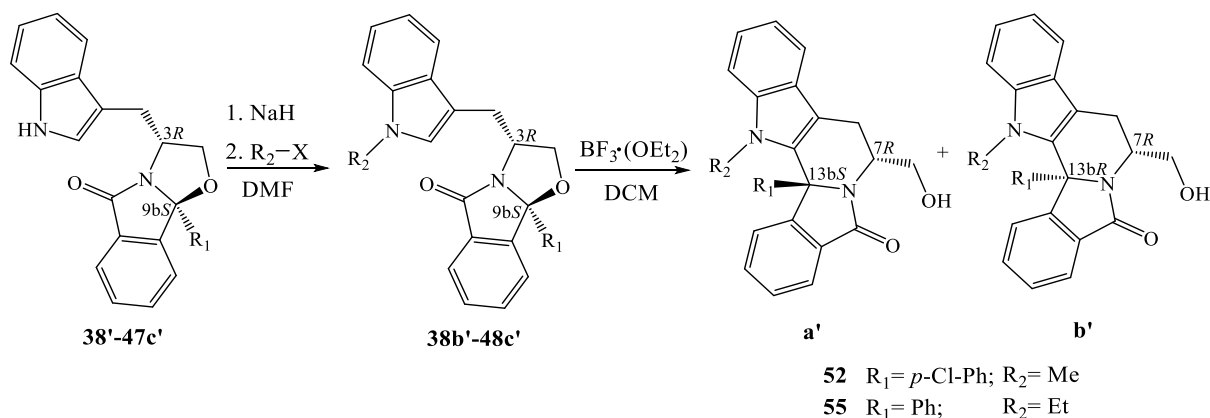
Scheme 2.6. Rational for the synthesis of the benzoindolizinoindolones library.

The indolizinoindolones were prepared by an enantioselective two-step route which involved in first place the stereoselective cyclocondensation of a racemic keto-acid with enantiopure (*S*)-tryptophan **9**, leading to compounds **34**, **38**, **38'** and from **47a** to **47e** and secondly a subsequent stereocontrolled

intramolecular cyclization on the aromatic ring occurs, taking advantage of the masked *N*-acyliminium, present in the tricyclic compounds. It is important to underline the fact that the amino alcohol tryptophanol used to obtain the cyclocondensation starting materials acts as chiral inductor that not only constitutes the source of chirality but it is also used to assemble the final polycyclic indolizinoindolones derivatives. Anyway, several methodologies are reported to succeed in the synthesis of these kind of complex indole-based compounds [83]. As reported in literature, when the intramolecular cyclization of tryptophanol-derived bicyclic lactams is moved by a starting material with 3*S*,9*bR* stereochemistry, BF₃·OEt₂-promoted α -amidoalkylation reaction on the indole 2-position takes place affording 7,13*b-cis* indole derivatives, as single stereoisomers and they are detectable by NMR experiment [77]. From the other side, it was discovered that 7,13*b-trans* indole derivatives can be obtained directly by cyclocondensation of (*S*)-tryptophanol **9** with 2-formylbenzoic acid [77]. To obtain both *cis*- and *trans*-diastereoisomers in one step reaction, it was found as promising synthetic approach the use of BF₃·OEt₂ on the correspondent oxazoloisoindolinone bicyclic lactams, **34a**, **38b** and **48a** to **48e**. In the case of compounds **45** and **46** it was found that after initial treatment of the relative cyclocondensation compound with the lewis acid the two epimeric indole derivatives were formed in a moderate diastereoselectivity (ratio of 2.5:1), where the *trans*-indolizinoindolone **45** was formed as major product [77]. For this reason, the first goal of the hit-to-lead optimization was to test different substituents in carbon 13*b* and study if this chemical modification improves the efficiency in terms of diastereoselectivity and biological activity. In particular, introduction of a methyl group and a set of diversified *para* and *meta* substituted phenyl groups led to synthesis of compounds **49a** and **49b** and **51a-51b** to **54a-54b**. Secondly, optimization of the indolinone framework led to compounds **50a** and **50b**. Cyclization of (*R*)-tryptophanol derived bicyclic lactam, compound **47c'**, led to formation of indolizinoindolones **52a'** and **52b'**, having stereochemistry (7*R*, 13*bS*) and (7*R*, 13*bR*), respectively. Elongation of the alkyl chain, protecting the indole core was experimented and, introduction of an ethyl group, on the indole nucleus of the cyclocondensation compound **38** led to product **38b**, which, cyclization led to synthesis of compounds **55a** and **55b**. Same synthetic route, starting from the (*R*)-tryptophanol-derived cyclocondensation product **38'** led to the formation of products **55a'** and **55b'**, after protection step forming compound **38b'**. The general procedures followed for the synthesis of the cyclized analogues are reported in **Scheme 2.7** and in **Scheme 2.8**.



Scheme 2.7. General procedure for the synthesis of indolizinoindolones **49-55a** and **49-55b**.



Scheme 2.8. General procedure for the synthesis of indolizinoindolones **52a'**, **55a'** and **52b'**, **55b'**.

The yields obtained, listed in **Table 2.6**, are good where *trans*-diastereoisomers **50-56a** were obtained between 17 to 80% and diastereoisomers *cis* **49-54b** were obtained in yields between 5 and 67%. The diastereoselectivity of these reactions is observed to depend strongly by the nature of the substituent inserted in position 13b. Particularly, the dimensions of the methyl group seem to promote medium stereoselectivity, and compounds **49a** and **49b** are formed in yields 40 and 28% (d.r. 1.5:1), respectively. When a phenyl group is introduced in the molecular framework it is noticed, as reported in literature that the indole derivatives **45** and **46** are formed in a ratio of 2.5:1 [77]. When the bulky phenyl ring is introduced substituted only in *para* position is observed a light increase in diastereoselectivity where for example *trans*-diastereoisomers **51a** and **54a** figure as major products obtained. At last, when the

phenyl group is substituted in *para* position with a chlorine atom and, in addition, in *meta* position with a nitro group the intramolecular cyclization promotes the massive formation of the *cis*-diastereoisomer **53b** with a yield of 67%. Moreover, when the indolizinoindolone framework is varied as in compounds **50a** and **50b**, the stereoselectivity increases significantly in favour of formation of the *trans*-isomer **50a**, which it is observed to form in a ratio 13:1, meaning that the phenyl frame, adjacent to the oxazolidine ring, is a decisive diastereoselective element of the cyclization reaction.

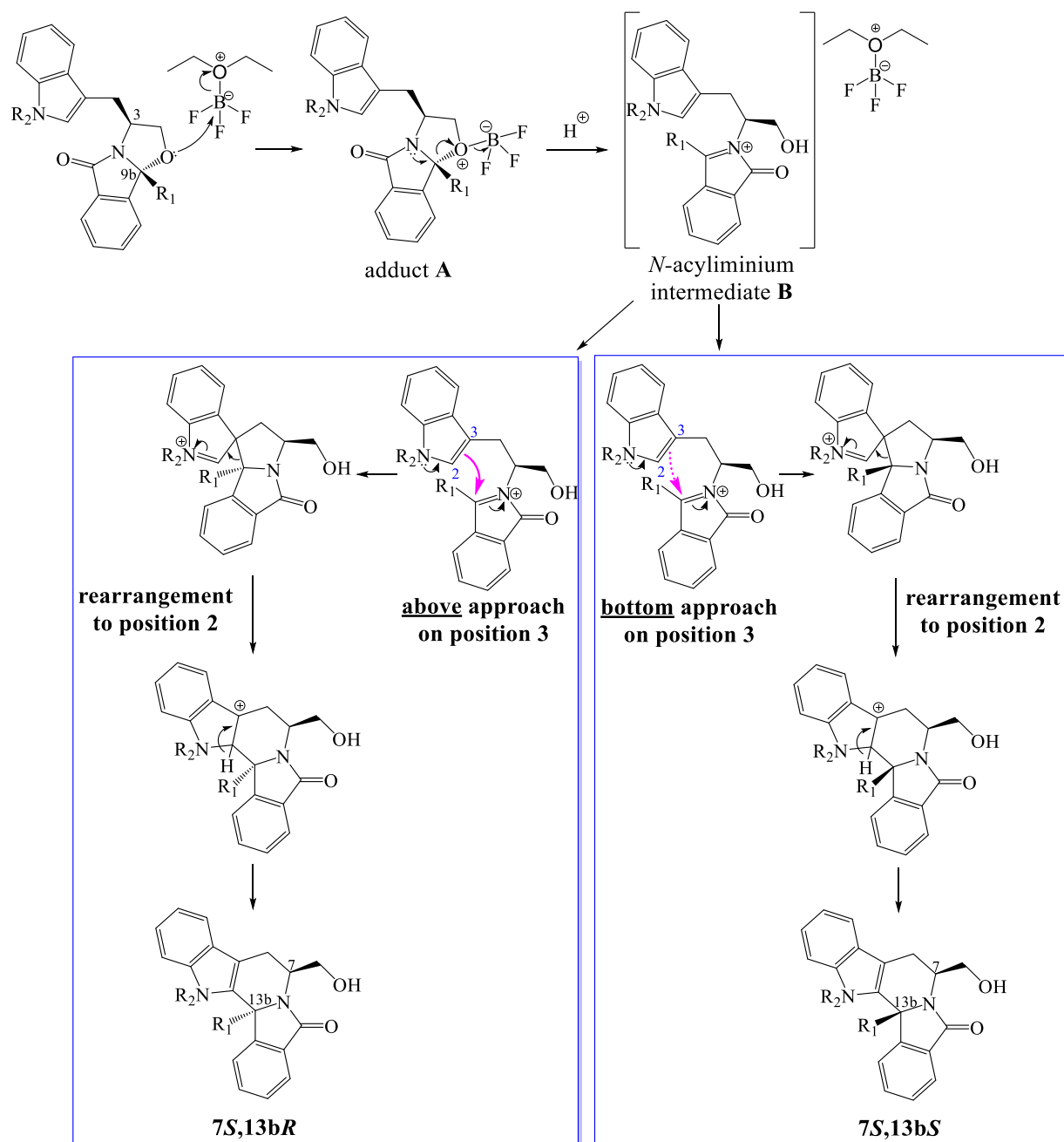
Table 2.6. Reaction yields for the diastereoselective intramolecular cyclized indolizinoindolones **49-55a** and **49-55b**.

Reference	R ₁	R ₂	η (%)		d.r.
			a (<i>trans</i>)	b (<i>cis</i>)	
49	Me	Me	40	28	1.5:1
50	Ph	Me	64.7	5.1	13:1
51	<i>p</i> -F-Ph	Me	51.1	25.2	2:1
52	<i>p</i> -Cl-Ph	Me	46.0	43.7	1:1
53	<i>p</i> -Cl, <i>m</i> -NO ₂ -Ph	Me	17.0	67.0	1:4
54	<i>p</i> -CH ₃ -Ph	Me	80.0	12.5	6.4:1
55	Ph	Et	68.0	ND	ND

Table 2.7. Reaction yields for the diastereoselective intramolecular cyclized indolizinoindolones **52a'**, **55a'** and **52b'** and **55b'**.

Reference	R ₁	R ₂	η (%)		d.r.
			a' (<i>trans</i>)	b' (<i>cis</i>)	
52	<i>p</i> -Cl-Ph	Me	59.6	28.4	2.1:1
55	Ph	Et	68.7	ND	ND

To understand clearly the stereochemistry of the products obtained the mechanism of reaction is reported in **Scheme 2.9**. First event, the oxygen of the oxazolidine ring attacks the boron atom of the lewis acid BF₃·OEt₂ by direct addition, where after formation of adduct **A**, boron trifluoride exits bringing to formation of an *N*-acyliminium intermediate **B** [84]. Cyclization can now occur by direct attack at the indole 3-position to generate, after rearrangement to position 2, diastereoisomers **a** and **b** [85].



Scheme 2.9. Mechanism of reaction of cyclization reaction.

The relative configuration of the formed products can be rationalized based on a stereoelectronically controlled axial approach [86] of the indole ring to the electrophilic carbon centre of the *N*-acyliminium specie **A**. The new ring can be formed by above approach, leading to **7S,13bR** product or by bottom approach, forming **7S,13bS** product. As it is possible to notice, the nature of R_1 group is functional element for the diastereoselectivity of this reaction as well as the hydroxymethyl substituent seems to play a decisive role as stereocontrol element in determining the relative stereochemistry of the chiral centres generated in the cyclization step [86]. As it is possible to notice even the dimensions of the

protecting group can affect the diastereoselectivity of this reaction. The yields obtained can be consistent based on what reported. The 15 benzoindolizinoindolones were characterized by $^1\text{H-NMR}$ and $^{13}\text{C-NMR}$ spectroscopy. The stereochemistry of products **49-51a** and **49-51b** was evaluated by comparing the $^1\text{H-NMR}$ chemical shifts with the ones obtained for derivatives **45** and **46**. The structures of these two compounds were previously determined by X-ray analysis [77]. An illustrative representation of the protons, which correspond to the most characteristic signals in the $^1\text{H-NMR}$ analysis, are given in **Figure 2.18**. In **Figure 2.19** is reported an $^1\text{H-NMR}$ spectrum expansion of compound **52a** $^1\text{H-NMR}$ spectrum, where the signals of these peaks can be identified. In specific, *trans*-diastereoisomers **49-55a** are characterized by a very deshielded triplet at around 5.00 ppm related to the hydroxylic proton. To this signal is associated a coupling constant J of about 6 Hz, typical of this kind of proton. A multiplet between 4.30 and 4.07 ppm is attributed to the diastereotopic couple of protons linked to the hydroxylic group, ($H-2$). When not overlapped by other signals, a multiplet which appears between 3.18 and 3.96 ppm is assigned to proton ($H-7$). A multiplet around 3.00 ppm is attributed to the diastereotopic protons next the indole core (see **Table 2.8**). Moreover, *N*-methyl indole derivatives are recognized by a singlet, deshielded at about 3.70 ppm related to the methyl group bounded to the nitrogen atom of the indole nucleus, while *N*-ethyl indole compound **55a** is identified by the presence of a triplet at 4.25 ppm, attributed to the methylene frame of the alkyl chain and a quartet at 1.10 ppm assigned to the terminal methyl group of the chain. These two signals show a coupling constant, J , of about 7 Hz, typical value for a simple alkyl chain.

Table 2.8. $^1\text{H-NMR}$ most characteristic signals for compounds **49-55a**.

Substitution in position 13b		<i>trans</i> -diastereoisomer a					
		OH	H-2		H-7	CH ₂ -indole	
45*	Ph¹	4.99	4.26	4.01	3.33	3.05	2.96
49a	Me¹	5.18	4.39-4.24		3.18	2.99-2.83	
50a	Ph²	4.86	3.86	3.09	3.96	2.99	2.90
51a	<i>p</i>-F-Ph¹	4.97	4.26	4.07	3.41	3.00	
52a	<i>p</i>-Cl-Ph¹	4.96	4.26	4.07	3.29	3.00	
53a	<i>p</i>-Cl, <i>m</i>-NO₂-Ph¹	4.91	4.23-4.13		ND	2.98	
54a	<i>p</i>-CH₃-Ph¹	5.00	4.28	4.00	ND	3.00	
55a	Ph³	4.98	4.25	4.02	3.26	3.02	

*compound reported in literature [77].

¹oxazoloisindoline framework; ²pyrrolidone ring only; ³R₂=Et;

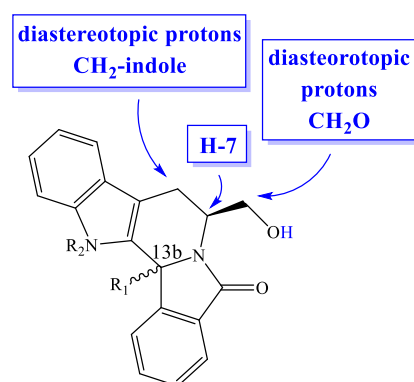


Figure 2.18. Most characteristic $^1\text{H-NMR}$ signals for the indolizinoindolones scaffold.

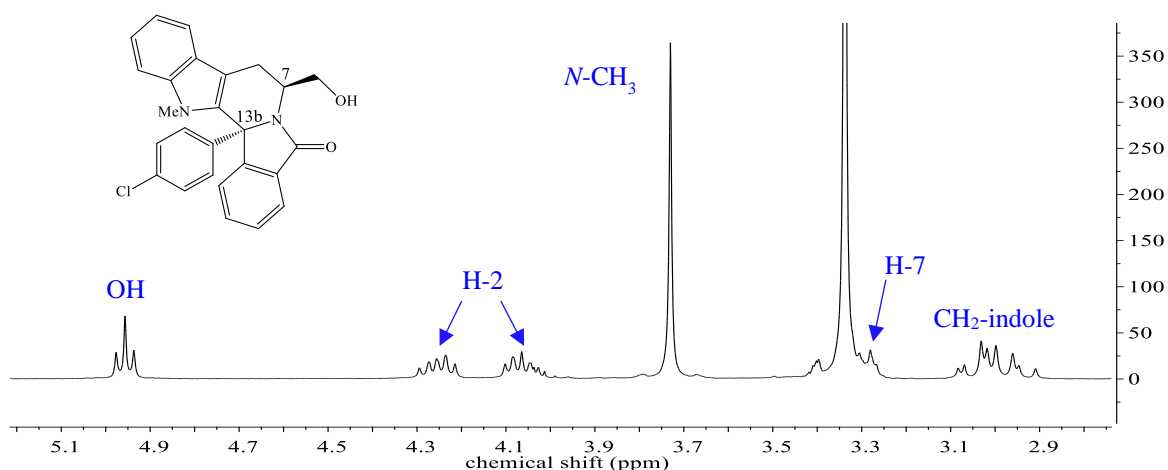


Figure 2.19. Expansion of $^1\text{H-NMR}$ spectrum of compound **52a** in DMSO between 5.2 and 2.8 ppm. At 3.33 ppm appears the signal of water of the solvent.

As illustrated in **Figure 2.20**, stereoisomerism *cis* is identified when, as in the case of compounds **49-55b**, (H-7) is observed as a doublet of a doublet of doublets at 4.90 ppm. This is valid limited to compounds **51b** to **54b**, which R_1 is a substituted phenyl ring meanwhile in the case of derivative **49b** this signal is shielded and it appears at 3.63 ppm. Moreover, peculiar is the multiplet at 4.75 ppm related to the hydroxylic proton (in **49b** this signal appears deshielded at 5.05 ppm). Multiplets at 2.68 and 2.92 ppm are assigned, respectively to each H-2 diastereotopic proton and to the two diastereotopic protons located next the indole moiety (see **Table 2.9**).

Table 2.9. $^1\text{H-NMR}$ most characteristic signals for compounds **49-54b**.

Substitution in		<i>cis</i> -diastereoisomer b					
position	13b	OH	H-2	H-7	CH ₂ -indole		
46*	Ph	4.75	3.12-3.05	2.61	4.90	3.12-3.05	2.92
49b	Me	5.05	4.97	3.63	2.98	2.78	
50b	Ph	ND	ND	ND	ND	ND	
51b	<i>p</i> -F-Ph	4.75	3.15-3.01	2.68	4.88	3.15-3.01	2.92
52b	<i>p</i> -Cl-Ph	4.76	3.14-3.01	2.68	4.88	3.14-3.01	2.92
53b	<i>p</i> -Cl, <i>m</i> -NO ₂ -Ph	4.74	3.01-2.94	2.80	4.91	3.14	3.01-2.94
54b	<i>p</i> -CH ₃ -Ph	4.88	3.14-3.01	2.68	4.76	3.14-3.01	2.92

*compound reported in literature [77].

In general, it was observed that *N*-methyl *cis*-indole derivatives, **49-54b** is detected by the presence of a singlet at 3.90 ppm, attributed to the methyl protecting group (see **Figure 2.20**).

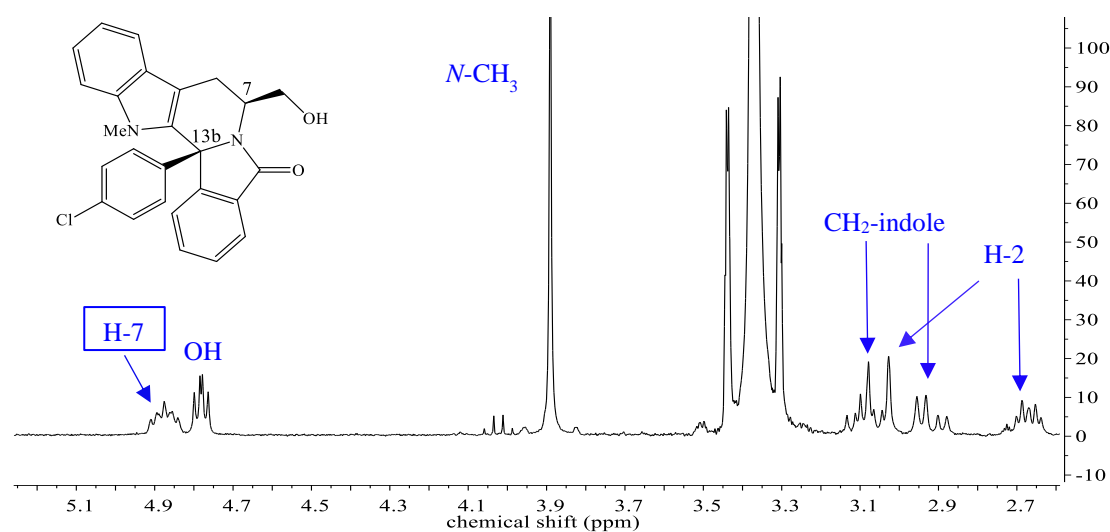


Figure 2.20. Expansion of ¹H-NMR spectrum of compound **52b** in DMSO between 5.2 and 2.6 ppm. At 3.33 ppm appears the signal of water of the solvent.

The ¹³C-NMR is also an essential tool to distinguish each diastereoisomer formed. The signal of the new chiral centre, C-13b, appears for compounds **49-55a** at about 72 ppm meanwhile for derivatives **49-54b** this signal is identified shielded at around 69 ppm. The second chiral centre C-7, introduced with the amino alcohol tryptophanol and present in the structure of the bicyclic lactams **48a-48e**, starting material of the cyclization reaction, appears at around 50 and 55 ppm for compounds **49a-55a** and **49-54b** respectively. More shielded, between 60 and 62 ppm are detectable the signals related to (C-2) independently from the stereochemistry of the products obtained. At last, the most shielded signal, characterizing this library of cyclized tryptophanol derivatives, appears at around 25 ppm in the case of *trans*-diastereoisomers **49-54a**, meanwhile for *cis*-diastereoisomers **49-54b** appears slightly shielded at 22 ppm. This last signal is attributed to CH₂-indole hydrogens. This spectral characterization finds coherence with the ¹³C-NMR description given for compounds **45** and **46** in literature [77].

2.2.3. Biological evaluation and SAR study of a library of indolizinoindolones

The 15 enantiopure indolizinoindolones were screened *in vitro* as liver-stage antimalarials by evaluating their ability to inhibit the infection of Huh7 human hepatoma cell line by rodent *P. berghei* parasites.

In an initial screening, it was determined the effect of all compounds at 1 μM , 5 μM and 10 μM concentrations on infection and cell-confluency.

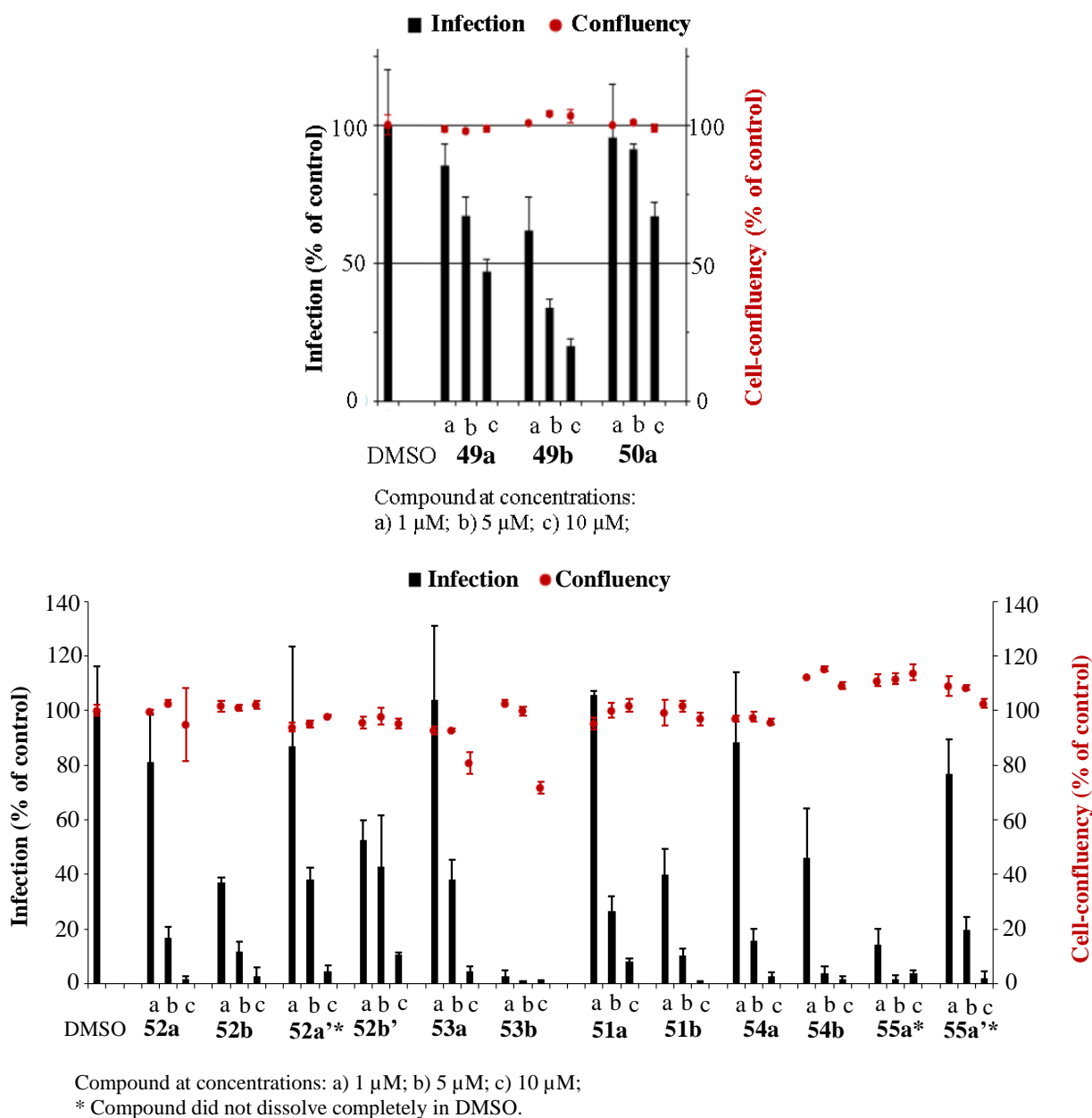


Figure 2.21. First *in vitro* screening of indolizinoindolones **49a**, **49b**, **50a**, **51a**, **51b**, **52a**, **52b**, **52a'**, **52b'**, **53a**, **53b**, **54a**, **54b**, **55a**, **55a'** against liver-stage *P. berghei* parasites. Activity (infection scale, bars) and toxicity to Huh-7 human hepatoma cells (cell-confluency scale, circles) are reported.

As illustrated in **Figure 2.21**, all compounds display good activity at concentrations of 5 and 10 μM . While indolizinoindolone **50a** seems to exhibit no significant effect at 10 μM concentration against the infection when compared to the respective control, compounds **49a**, **49b**, **51a**, **52a**, **52a'**, **52b'**, **53a**, **54a** and **55a'** exhibit a good to excellent effect at this concentration against the Huh-7 human hepatoma cell proliferation with little or no toxicity. As resulted in the first screening performed, the percentage of infection at 10 μM is at least below 50% for these derivatives and the IC_{50} values auspicated for these compounds are in the range of 1-5 μM [28]. Furthermore, it emerges that indolizinoindolones **51b**, **52b** and **54b** display somewhat higher activity than the compounds reported lately. For these three derivatives, the percentage of infection at 10 μM resulted to be decrease below 50% and the estimated IC_{50} values are probably equal or inferior to 1 μM . At last, compounds **53b** and **55a** present the strongest activity, with only derivative **53b** showing toxicity solely at 10 μM . Particularly, compound **53b** resulted to decrease the infection below 5% at all concentrations experimented, while indolizinoindolone **55a** resulted to bring the infection below 20% at concentration 1 μM , close to 5% at concentration 5 μM and below 10% at 10 μM . The expected IC_{50} values for these two testing-compounds is likely lower than 1 μM . The IC_{50} values were determined for the most active compounds. Since the screening results of this scaffold are quite recent, only for derivative **49b** the results of the second *in vitro* screening are available. In this case, the IC_{50} for the inhibition of hepatic *P. berghei* infection was determined and for compound **49b** it has a value of $0.56 \pm 0.17 \mu\text{M}$. The results obtained have been rationalized in a SAR study as illustrated in **Figure 2.22**, **Figure 2.23**, **Figure 2.24**. It emerges that *cis*-diastereoisomers **49b**, **51b**, **52b**, **52b'**, **53b**, and **54b** appear more active than the parental derivatives with *trans*- conformation. Beside this, all (*S*)-tryptophanol-derived indolizinoindolones seem to be more bioactive than the (*R*)-tryptophanol derivatives, suggesting that the (*S*)-stereochemistry of the chiral centre in position 7 is quite important. In particular, comparing compounds **56** with **60**, **59** with **63**, **57** with **61** and **62** with **58**, the (*S*)-tryptophanol derivatives report higher activity. Interestingly, once **52b** and **52b'** are compared it results that the (*7R*,13*bR*) indolizinoindolones **52b'** seems to be more bioactive than its enantiomer, compound **52b**. In this way, it is demonstrated the functionality of the presence of a bulky group in position 13*b*. Moreover, it emerges that the nature of the substituent on the new stereogenic centre, formed in position 13*b*, is of primary relevance. As a matter of fact, it appears that the presence of a Hydrogen atom in this position does not promote antiplasmodial activity. A methyl and a phenyl substitution ensures good to high activity, where a methyl substituent seems decisively to improve the bioactivity of compounds **60**, **61**, **62** and **49b**. A *para*-substituted phenyl ring, introduced in position 13*b*, show high activity, and at last bi-substitution, as it appears in compound **53b**, emerges to endorse significantly the antiplasmodial activity. This conclusion is consistent for both *cis*- and *trans*- diastereoisomers synthesized. The nature of the protection group on the nitrogen of the indole core is also crucial. *N*-methyl idole derivatives **46**

and **49b** show higher activity ($IC_{50}=0.6 \mu M$) than the moderately active, compounds **61** and **64**. Interestingly, an increase of the alkyl chain, protecting the indole moiety turns the *trans*-diastereoisomer **55a** strongly active. Considering, the result obtained for the correspondent *N*-methyl indole derivative **45**, and once compounds **61** and **64** are compared with compound **55a** it emerges that specifically in *trans*-diastereoisomers seem to be required a bulky group, protecting the indole core. Additionally, from comparison of the two enantiomers, compounds **55a** and **55a'**, it resulted that the biological activity is promoted by stereochemistry (*7S*, *13bR*). Moreover, it emerged that *N*-protected indole derivatives with the hydroxyl group unprotected show good to high activity. At last, modification of the indolinone framework, as it was experimented in compound **50a**, seems to be not functional and it does not improve the antiplasmodial activity of the correspondent hit compound **45**.

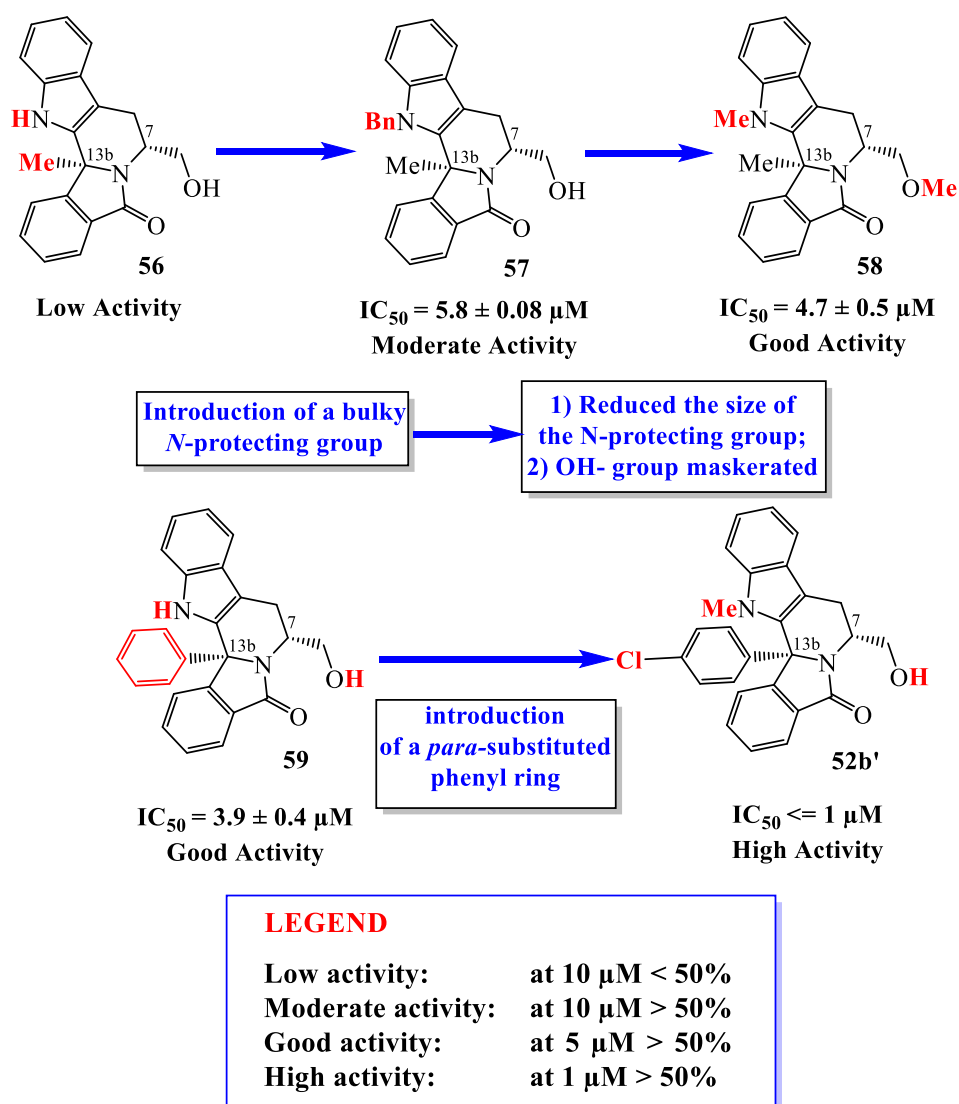


Figure 2.22. SARs (Structure-activity relationships) of (*7R*, *13bR*) indolizinoindolone derivatives. (Results reported in percentage of infection).

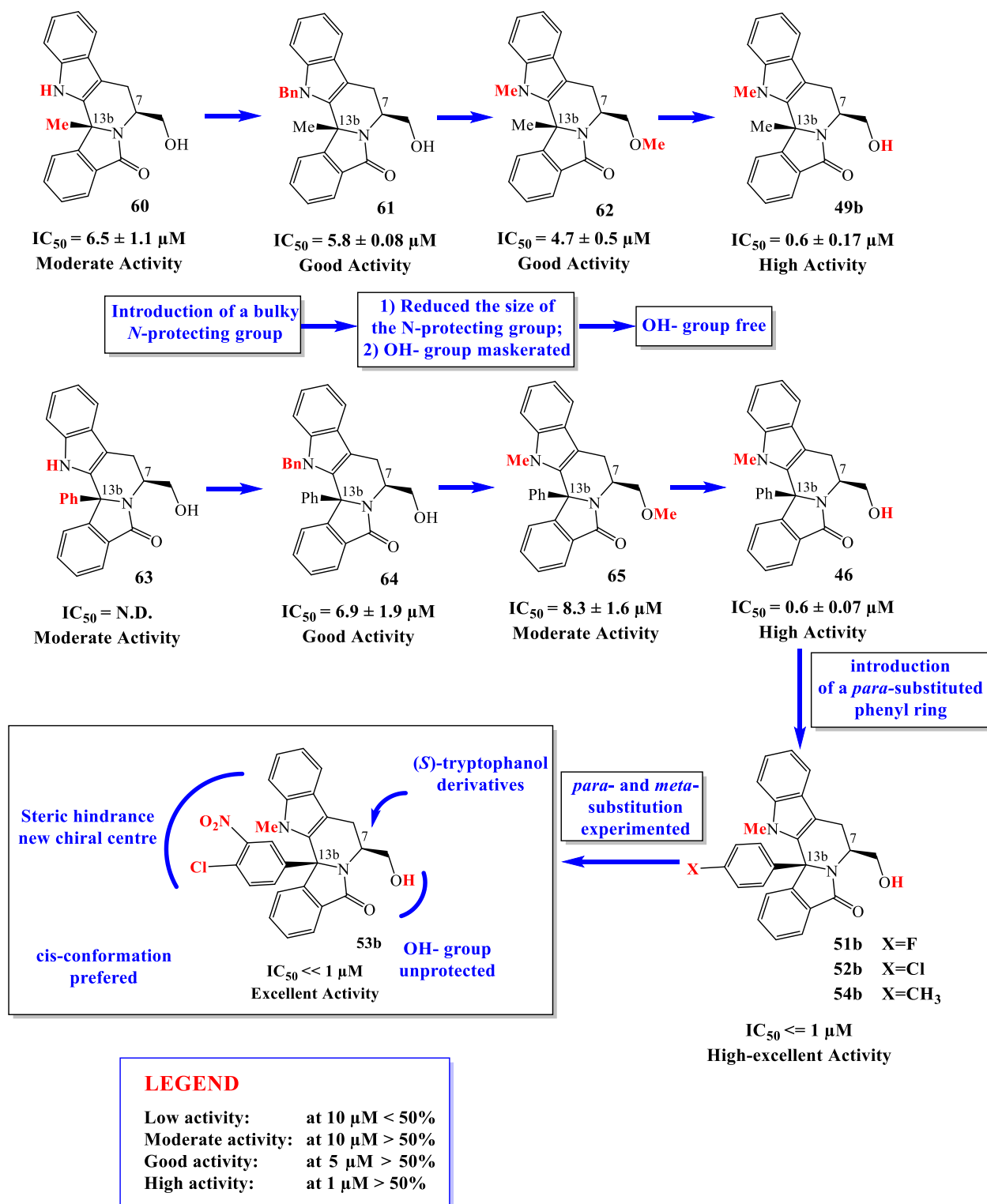


Figure 2.23. SARs (Structure-activity relationships) of (7*S*, 13*bS*) indolizinoindolone derivatives. (Results reported in percentage of infection).

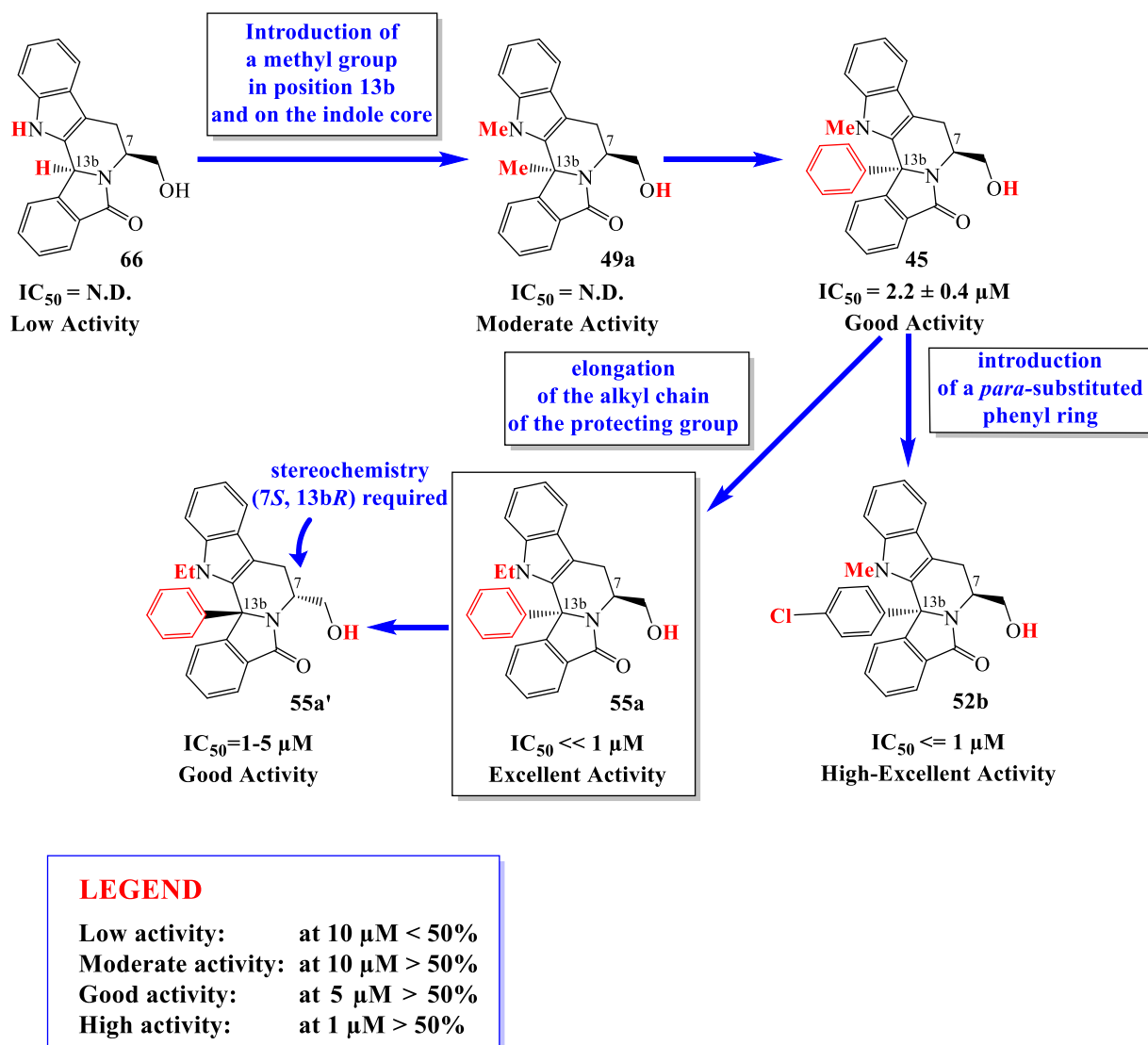


Figure 2.24. SARs (Structure-activity relationships) of (7*S*, 13*bR*) indolizinoindolone derivatives. (Results reported in percentage of infection.)

3. Conclusions

In this master thesis, a first objective settled consisted in the synthesis of a small set of (*S*)- and (*R*)-enantiopure tryptophanol-derived bicyclic lactams. These derivatives have been used to develop a leads generation where a diversified set of *N*-protected oxazoloisindolinones small molecules were obtained. The mechanism of reaction through which the amino alcohol tryptophanol, which acts as chiral inductor and the set of 2-substituted benzoic acids chosen bring to the cyclocondensation products was studied as well as the best procedure of protection on the nitrogen of the indole moiety was evaluated, resulting in a wide library of compounds, hit-to-lead optimization of compounds **34**.

The derivatives composing this scaffold were then biologically evaluated as anticancer agents, where through a yeast-based screening strategy it was found that compound **34d** at a concentration of 10 μ M increases the wt p53-induced yeast growth inhibition and it restores the wt-like growth inhibitory effect to mut p53R280K in about 86%.

Furthermore, the stability profile of compounds **34** and **34e** was assessed. Microsomal stability, plasma stability and buffer stability were evaluated. Biological verification of these two chemical leads represents a fundamental step in terms of drug development process and crucial in the drug discovery process to optimized lead compounds for further development.

At last, a novel library of enantiopure benzindolizinoindolones was synthesized. Cyclization of oxazoloisindolinones derived from enantiopure tryptophanol allowed the enantioselective synthesis of indolizinoindolones derivatives. In all cases both *trans*- and *cis*- diastereoisomers were isolated, where diastereoisomer *trans*- was found to be the major product formed. Only in case of compounds **53a** and **53b** it was found that the *cis*- stereochemistry was preferred.

Then, the *in vitro* activity against liver stages of *P. berghei* was tested for this class of compounds and from this study derivatives **53b** and **55a** emerged as most promising derivatives. This confirmed that there is a preference for the 7,13b-*cis* diastereoisomer, demonstrating that the stereochemistry of the target compounds has a critical role in the antiplasmodial activity in liver stage. In the case of *trans*-conformation emerged that elongation of the alkyl chain protecting the indole core favoured the antiplasmodial bioactivity.

4. Experimental Procedure

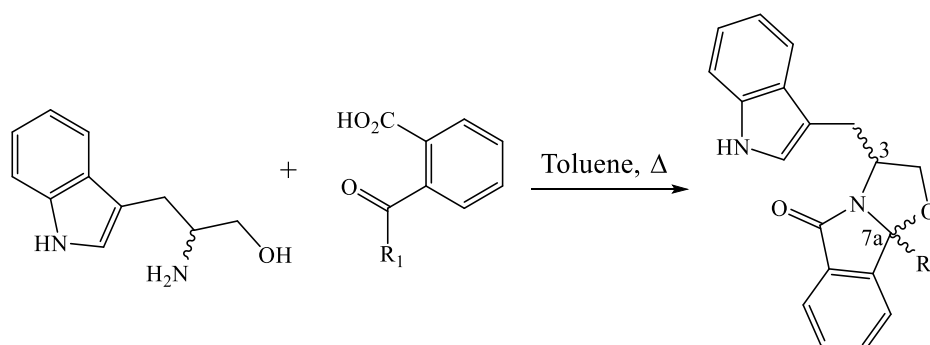
4.1. General Methods

All reagents and solvents were obtained from commercial suppliers and were used without further purification. (*R*)-tryptophanol **44** was obtained by reduction with Lithium Aluminium hydride. Melting points were determined using a Kofler camera Bock monoscope M. Analysis Merck Silica Gel 60 F254 plates were used as analytical thin layer chromatography and flash chromatography was performed on Merck Silica Gel (200- 400 mesh). ^1H and ^{13}C NMR spectra were recorded on a Bruker Magnet System 300 MHz/54mm Ultra-Shield, long hold time. ^1H nuclear magnetic resonance spectra were recorded at 300 MHz and ^{13}C nuclear magnetic resonance spectra were recorded at 100 MHz. ^1H and ^{13}C NMR chemical shifts are reported in parts per million (ppm, δ) referenced to the solvent used and the proton coupling constants J in hertz (Hz). Spectras were assigned using appropriate COSY, DEPT, HMQC and HMBC sequences. Microanalysis was performed in a Flash2000 ThermoScientific elemental analyzer and are within $\pm 0.4\%$ of theoretical values.

4.2. Experimental procedure chapter 2.1 Oxazoloisindolinones scaffold

4.2.1. General procedure for cyclocondensation reactions

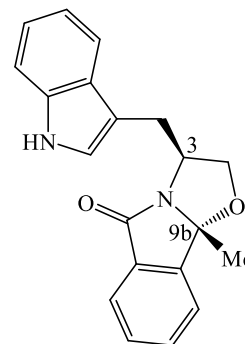
To a solution of a particular aminoalcohol (0.660mmol, 1 equivalent) in toluene (5ml) was added the appropriate oxocarboxylic acid (0.730mmol). The mixture was heated at reflux for 10-24h under *dean-stark* apparatus, until total consumption of the starting aminoalcohol. The solvent was evaporated and the residue was dissolved in ethylacetate. The organic phase was washed with saturated aqueous solutions of sodium monohydrogen carbonate, NaHCO_3 and sodium chloride, NaCl , dried with anhydrous magnesium sulfate, filtered and evaporated. The crude was absorbed on silica and purified by flash chromatography using ethyl acetate/ *n*-hexane as eluent.



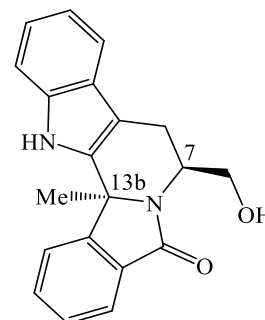
Scheme 4.1. General procedure for the preparation of (*S*)- and (*R*)-tryptophanol bicyclic lactams.

(3*S*,9*bR*)-3-((1*H*-indol-3-yl)methyl)-9*b*-methyl-2,3-dihydrooxazolo[2,3-*a*]isoindol-5(9*bH*)-one 34 and (7*S*,13*bS*)-7-(hydroxymethyl)-13*b*-methyl-7,8,13,13*b*-tetrahydro-5*H*benzo[1,2]indolizino[8,7-*b*]indol-5-one 66: Following the general procedure, to a solution of (*S*)-tryptophan **9** (0.218 g, 1.15 mmol) in toluene (10 mL) was added 2-acetylbenzoic acid (0.207 g, 1.38 mmol). Reaction time: 16.5 hours. Eluent for flash chromatography: ethyl acetate/ *n*-hexane, 1:1.

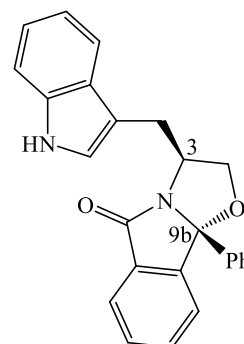
34: The product was obtained as a white solid (0.254 g, 70%). ¹H NMR (300 MHz, CDCl₃): δ 8.13 (s, 1H, *NH*), 7.78 (dd, *J* = 6.7, 1.9 Hz, 1H, *ArH*), 7.73 (d, *J* = 7.8 Hz, 1H, *ArH*), 7.64 – 7.57 (m, 1H, *ArH*), 7.54 (s, 1H, *ArH*), 7.50 (dd, *J* = 7.2, 1.3 Hz, 1H, *ArH*), 7.38 (d, *J* = 7.6 Hz, 1H, *ArH*), 7.26 (s, 1H, *ArH*), 7.23 (dd, *J* = 7.0, 1.2 Hz, 1H, *ArH*), 7.18 (dd, *J* = 3.9, 1.4 Hz, 1H, *ArH*), 7.14 (dd, *J* = 7.1, 1.1 Hz, 1H, *ArH*), 4.60 (m, 1H, *H*-3), 4.32 (dd, *J* = 8.8, 7.4 Hz, 1H, *H*-2), 4.18 (dd, *J* = 8.9, 6.4 Hz, 1H, *H*-2), 3.43 (dd, *J* = 14.8, 5.7 Hz, 1H, CH₂--indole), 3.18 (dd, *J* = 14.8, 8.6 Hz, 1H, CH₂--indole), 1.70 ppm (s, 3H, CH₃), as previously described in literature [75].



68: The product was obtained as white solid (0.0145 g, 4.20%). ¹H NMR (300 MHz, DMSO-*d*₆) δ 11.28 (s, 1H, *NH*), 8.29 (d, *J* = 7.7 Hz, 1H, *ArH*), 7.72 (td, *J* = 7.6, 1.1 Hz, 1H, *ArH*), 7.52 (t, *J* = 7.4 Hz, 1H, *ArH*), 7.40 (d, *J* = 7.7 Hz, 1H, *ArH*), 7.35 (d, *J* = 8.0 Hz, 1H, *ArH*), 7.08 (t, *J* = 8.2 Hz, 1H, *ArH*), 6.97 (t, *J* = 7.9 Hz, 1H, *ArH*), 5.15 (dd, *J* = 6.9, 5.5 Hz, 1H, *OH*), 4.32 (dd, *J* = 11.5, 6.1 Hz, 2H, *H*-2), 3.84 (ddd, *J* = 15.0, 9.3, 5.4 Hz, 1H, *H*-3), 2.93 (dd, *J* = 15.3, 3.7 Hz, 1H, CH₂--indole), 2.77 (dd, *J* = 15.3, 11.3 Hz, 1H, CH₂--indole), 1.88 (s, 3H, C13*b*-CH₃).



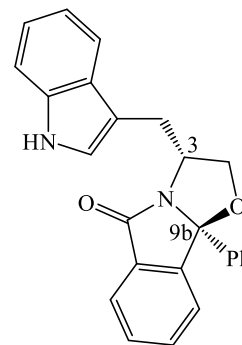
(3*S*,9*bR*)-3-((1*H*-indol-3-yl)methyl)-9*b*-phenyl-2,3-dihydrooxazolo[2,3-*a*]isoindol-5(9*bH*)-one 38: Following the general procedure, to a solution of (*S*)-tryptophan **9** (0.202 g, 1.06 mmol) in toluene (10 mL) was added 2-benzoylbenzoic acid (0.286 g, 1.26 mmol). Reaction time: 16 hours. Eluent for flash chromatography: ethyl acetate/ *n*-hexane 6:4. The product was obtained as white crystals (0.328 g, 81.3%). ¹H NMR (300 MHz, CDCl₃) δ 8.02 (s, 1H, *NH*), 7.84 – 7.79 (m, 1H, *ArH*), 7.69 – 7.62 (m, 2H, *ArH*), 7.54 – 7.48 (m, 3H, *ArH*), 7.46 – 7.33 (m, 4H, *ArH*), 7.19 (m, 5H, *ArH*), 4.73 (dddd, *J* = 13.9, 8.7, 7.29, 6.6 Hz, 1H, *H*-



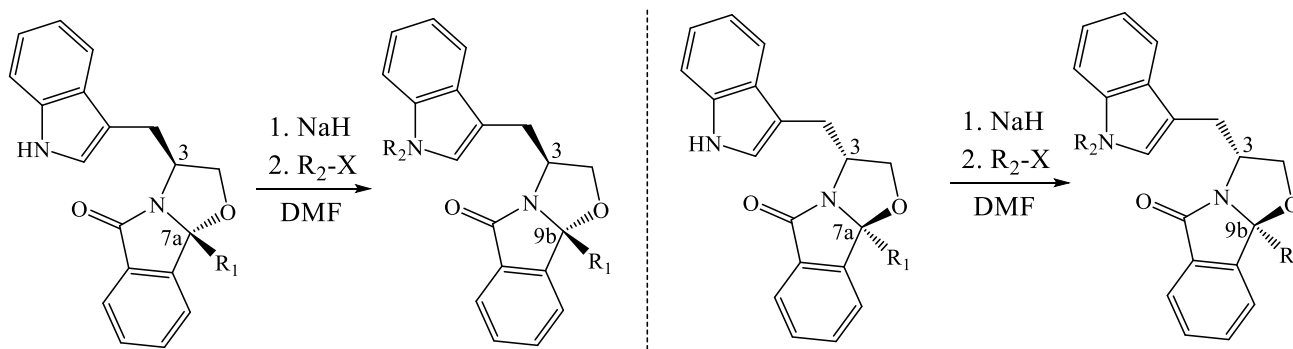
3), 4.49 (dd, $J = 8.6, 7.6$ Hz, 1H, $H-2$), 4.01 (dd, $J = 8.7, 6.7$ Hz, 1H, $H-2$), 3.19 (dd, 1H, $J = 14.7, 6.3$ Hz, CH_2 -indole), 2.68 ppm (dd, $J = 14.8, 9.1$ Hz, 3.19 (dd, 1H, $J = 14.7, 6.3$ Hz, CH_2 -indole), 2.68 ppm (dd, $J = 14.8, 9.1$ Hz, 1H, CH_2 -indole), as described in literature [28].

(3*R*,9*bS*)-3-((1*H*-indol-3-yl)methyl)-9*b*-phenyl-2,3-dihydrooxazolo[2,3-*a*]isoindol-5(9*bH*)-one

38': Following the general procedure to a solution of (*R*)-tryptophan **44** (0,199 g, 1.04 mmol) in toluene (10 mL) was added 2-benzoylbenzoic acid (0.286 g, 1.27 mmol). Reaction time: 19 hours. Eluent for flash chromatography ethyl acetate/ *n*-hexane, 1:1. The product was obtained as white powder (0.314 g, 79.1%). The ¹H-NMR spectrum was found to be identical to the one of compound **38**.



4.2.2. General procedure for indole protection reactions



Scheme 4.2. (*S*) and (*R*)-tryptophan-derived bicyclic lactams protected on the indole core.

4.2.2.1. General procedure for *N*-methylation

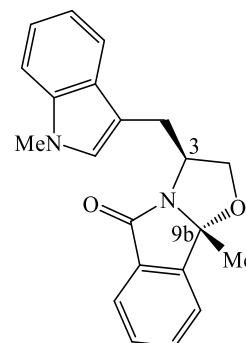
To a stirred solution of the appropriate (*S*)- or (*R*)- oxazoloisoindolinone derivative (0.320 mmol, 1 equivalent) in dry dimethylformamide, DMF (3 mL) under inert atmosphere of nitrogen and ice bath was added sodium hydride, NaH (2 equivalents, 95% anhydrous reagent). The mixture was allowed to stir for 30 minutes and then methyl iodide (2 equivalents) was added. The reaction was kept stirring at room temperature for 30 minutes. After this period, ethyl acetate was added to the crude of reaction and then extracted with room temperature deionized water. The organic phase was washed firstly with a aqueous saturated solution of sodium monohydrogen carbonate, NaHCO₃ and then with brine solution (saturated aqueous solution of sodium chloride, NaCl); dried with sodium sulphate, NaSO₄ and in the

end the solvent was evaporated. The crude was absorbed in silica, purified by flash chromatography using ethyl acetate/ *n*-hexane as eluent mixture and recrystallized.

(3*S*,9*bR*)-9*b*-methyl-3-((1-methyl-1*H*-indol-3-yl)methyl)-2,3-dihydrooxazolo[2,3-*a*]isoindol-

5(9*bH*)-one, 34a: Following the general procedure, starting from compound **34** (0.102 g, 0.320 mmol), sodium hydride, NaH 95%, (0.0154 g, 0.640 mmol) and methyl iodide (0.040 mL, 0.640 mmol, $d = 2.28 \text{ gmL}^{-1}$) were added.

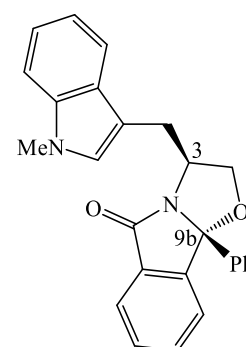
Reaction time: 1.5 hours. Eluent for flash chromatography: 7:3, *n*-hexane/ethyl acetate. Recrystallization: *n*-hexane/ethyl acetate. The product was obtained as a white light solid (0.0962 g, 90.3%); mp: 168 - 170 °C; ^1H NMR (300 MHz, CDCl_3) δ 7.78 (dd, $J = 7.0, 1.5$ Hz, 1H, Ar*H*), 7.72 (d, $J = 7.8$ Hz, 1H, Ar*H*), 7.64 – 7.57 (m, 1H, Ar*H*), 7.54 (s, 1H, Ar*H*), 7.51 (dd, $J = 7.1, 1.2$ Hz, 1H, Ar*H*), 7.31 (d, $J = 8.1$ Hz, 1H, Ar*H*), 7.28 – 7.21 (m, 1H, Ar*H*), 7.18 – 7.12 (m, 1H, Ar*H*), 7.11 (s, 1H, CH-indole), 4.63 – 4.53 (m, 1H, *H*-3), 4.30 (dd, $J = 8.8, 7.4$ Hz, 1H, *H*-2), 4.17 (dd, $J = 8.9, 6.3$ Hz, 1H, *H*-2), 3.78 (s, 3H, NCH₃), 3.44 (dd, $J = 14.8, 5.6$ Hz, 1H, CH₂-indole), 3.15 (dd, $J = 14.7, 8.9$ Hz, 1H, CH₂-indole), 1.72 (s, 3H, CH₃); ^{13}C NMR (75 MHz, CDCl_3) δ 174.37 (C=O), 147.42 (ArC), 136.96 (ArC), 133.19 (ArC), 131.71 (ArC), 130.13 (ArC), 128.10 (ArC), 127.19 (s), 124.29 (ArC), 122.11 (ArC), 121.76 (ArC), 119.06 (ArC), 119.00 (ArC), 110.21 (ArC), 109.24 (ArC), 98.96 (C-9*b*), 74.80 (C-2), 56.22 (C-3), 32.73 (N-CH₃), 30.67 (CH₂-indole), 23.22 (C-CH₃).



(3*S*,9*bR*)-3-((1-methyl-1*H*-indol-3-yl)methyl)-9*b*-phenyl-2,3-dihydrooxazolo[2,3-*a*]isoindol-

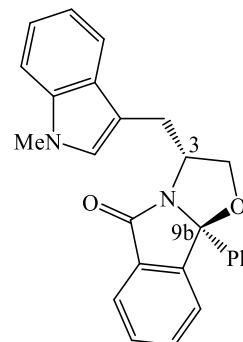
5(9*bH*)-one, 38a: Following the general procedure, starting from compound **38** (0.104 g, 0.273 mmol), sodium hydride, NaH 95%, (0.0140 g, 0.583 mmol) and methyl iodide (0.034 mL, 0.546 mmol, $d = 2.28 \text{ gmL}^{-1}$) were added.

Reaction time: one hour. Eluent for flash chromatography: 1:1, *n*-hexane/ethyl acetate. Recrystallization: *n*-hexane/ethyl acetate. The product was obtained as a white crystalline solid (0.0963 g, 89.5%); mp: 132-136 °C; ^1H NMR (300 MHz, CDCl_3) δ 7.83 – 7.79 (m, 1H, Ar*H*), 7.65 – 7.61 (m, 2H, Ar*H*), 7.49 (ddd, $J = 5.5, 3.0, 1.9$ Hz, 3H, Ar*H*), 7.40 (d, $J = 1.8$ Hz, 1H, Ar*H*), 7.38 (d, $J = 2.0$ Hz, 1H, Ar*H*), 7.28 – 7.17 (m, 2H, Ar*H*), 7.08 (m, 1H, Ar*H*), 6.96 (s, 1H, CH-indole), 4.69 (ddd, $J = 13.4, 9.2, 6.7$ Hz, 1H, *H*-3), 4.45 (dd, $J = 8.7, 7.5$ Hz, 1H, *H*-2), 3.98 (dd, $J = 8.7, 6.7$ Hz, 1H, *H*-2), 3.72 (s, 3H, NCH₃), 3.21 (dd, $J = 14.6, 5.9$ Hz, 1H, CH₂-indole), 2.65 (dd, $J = 14.7, 9.3$ Hz, 1H, CH₂-indole), as described in literature [28].



(3R,9bS)-3-((1-methyl-1H-indol-3-yl)methyl)-9b-phenyl-2,3-dihydrooxazolo[2,3-a]isoindol-

5(9bH)-one 38a': Following the general procedure, starting from compound **38'** (0.060 g, 0.158 mmol), sodium hydride, NaH 95%, (0.008 g, 0.315 mmol) and methyl iodide (0.022 mL, 0.347 mmol, $d = 2.28 \text{ gmL}^{-1}$) were added. Reaction time: 2 hours. Eluent for flash chromatography: ethyl acetate/ *n*-hexane, 3:7. Recrystallization: ethyl acetate/ *n*-hexane. The compound was obtained as a white crystalline solid (0.0591 g, 86.5%); mp: 148-150 °C; $^1\text{H NMR}$ (300 MHz, CDCl_3) δ 7.83 – 7.79 (m, 1H, ArH), 7.63 (m, 2H, ArH), 7.52 – 7.45 (m, 3H, ArH), 7.42 – 7.36 (m, 3H, ArH), 7.29 – 7.17 (m, 3H, ArH), 7.12 – 7.05 (m, 1H, ArH), 6.96 (s, 1H, CH-indole), 4.69 (ddd, $J = 13.4, 9.2, 6.7 \text{ Hz}$, 1H, H-3), 4.46 (dd, $J = 8.7, 7.5 \text{ Hz}$, 1H, H-2), 3.99 (dd, $J = 8.7, 6.7 \text{ Hz}$, 1H, H-2), 3.72 (s, 3H, NCH_3), 3.21 (dd, $J = 14.6, 5.9 \text{ Hz}$, 1H, CH_2 -indole), 2.65 ppm (dd, $J = 14.7, 9.3 \text{ Hz}$, 1H, CH_2 -indole); $^{13}\text{C NMR}$ (75 MHz, CDCl_3) δ 174.61 (C=O), 147.18 (Cq), 138.86 (Cq), 136.87 (Cq), 133.27 (ArC), 131.11 (Cq), 130.09 (Cq), 128.77 (ArC), 128.65 (ArC), 127.90 (ArC), 126.90 (CH-indole), 125.81 (ArC), 124.37 (ArC), 123.45 (ArC), 121.64 (ArC), 118.90 (ArC), 110.18 (Cq), 109.15 (ArC), 100.95 (C-9b), 76.32 (CH-2), 55.79 (CH-3), 32.67 (s), 30.04 (CH₂-indole).



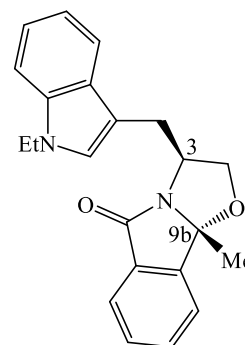
4.2.2.2. General procedure for N-ethylation

To a stirred solution of the appropriate (*S*)- or (*R*)-oxazoloisoindolinone derivative (0.320 mmol, 1 equivalent) in anhydrous dimethylformamide, DMF (3 mL) under inert atmosphere of nitrogen and ice bath was added sodium hydride, NaH (2 equivalents, 95% anhydrous reagent). The mixture was allowed to stir for 30 minutes and then ethyl iodide (2 equivalents, $d = 1.95 \text{ gmL}^{-1}$) was added. The reaction was kept stirring at room temperature till total consumption of the limitant reagent. After this period, ethyl acetate was added to the crude of reaction and then extracted with deionized water. The organic phase was washed then with a saturated aqueous solution of sodium chloride, NaCl (brine), dried with sodium sulphate, NaSO_4 and at least, the solvent was evaporated. The crude was absorbed in silica and purified by flash chromatography using ethyl acetate/ *n*-hexane as mixture of eluent and recrystallized.

(3S,9bR)-3-((1-ethyl-1H-indol-3-yl)methyl)-9b-methyl-2,3-dihydrooxazolo[2,3-a]isoindol-

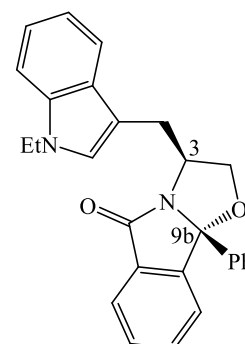
5(9bH)-one 34b: Following the general procedure starting from compound **34** (0.0509 g, 0.157 mmol), dissolved in dimethylformamide, DMF (2 mL) sodium hydride, NaH 95% (0.008 g, 0.315 mmol) and ethyl iodide (0.025 mL, 0.314 mmol, $d = 1.95 \text{ gmL}^{-1}$) were added. Reaction time: 2 hours. Eluent for flash chromatography: ethyl acetate/ *n*-hexane, 3:7. Recrystallization solvents: ethyl acetate/ *n*-hexane.

The product was obtained as white crystalline solid (0.0398g, 71.5%); mp: 161-164 °C; $[\alpha]_D^{20} = +24.7^\circ$ ($c = 0.39$, CH_2Cl_2); $^1\text{H NMR}$ (300 MHz, CDCl_3) δ 7.80 – 7.69 (m, 2H, ArH), 7.64 – 7.57 (m, 1H, ArH), 7.55 – 7.48 (m, 2H, ArH), 7.34 (d, $J = 8.1$ Hz, 1H, ArH), 7.26 – 7.19 (m, 1H, ArH), 7.17 (s, 1H, ArH), 7.16 – 7.10 (m, 1H, ArH), 4.62 – 4.52 (m, 1H, H-3), 4.30 (dd, $J = 8.85, 7.35$ Hz, 1H, H-2), 4.16 (q, $J = 7.24$ Hz, 3H, H-2 and CH_2CH_3 aliphatic), 3.43 (dd, $J = 14.7, 5.3$ Hz, 1H, CH_2 -indole), 3.17 (dd, $J = 14.7, 8.8$ Hz, 1H, CH_2 -indole), 1.68 (s, 3H, C-9b CH_3), 1.46 ppm (t, $J = 7.24$ Hz, 3H, CH_2CH_3); $^{13}\text{C NMR}$ (75 MHz, CDCl_3) δ 174.33 (C=O), 147.33 (Cq), 135.88 (Cq), 133.14 (ArC), 131.67 (Cq), 130.09 (ArC), 128.20 (Cq), 125.44 (ArC), 124.24 (ArC), 122.06 (ArC), 121.55 (ArC), 119.06 (ArC), 118.96 (ArC), 110.16 (Cq), 109.27 (ArC), 98.91 (C-9b), 74.69 (C-2), 56.17 (C-3), 40.80 (CH_2CH_3), 30.54 (CH_2 -indole), 23.09 (C-9b CH_3), 15.50 (CH_2CH_3). Anal. Calc. ($\text{C}_{22}\text{H}_{22}\text{N}_2\text{O}_2$): C, 76.28%; H, 6.40%; N, 8.09%. Found C, 76.34%; H, 6.50%; N, 8.08%.



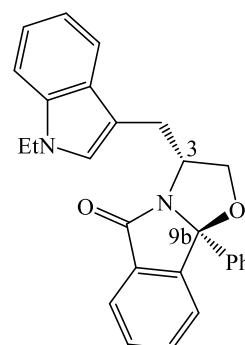
(3S,9bR)-3-((1-ethyl-1H-indol-3-yl)methyl)-9b-phenyl-2,3-dihydrooxazolo[2,3-a]isoindol-5(9bH)-one 38b:

To a solution of compound **38** (0.0533 g, 0.140 mmol) in anhydrous dimethylformamide, DMF (3 mL), sodium hydride, NaH 95%, (0.007 g, 0.280 mmol) and ethyl iodide (0.022 mL, 0.280 mmol, $d = 1.95 \text{ g mL}^{-1}$) were added. Reaction time: 30 minutes. Eluent for flash chromatography: ethyl acetate/ *n*-hexane, 3:7. The product was obtained as a light white solid (0.0404 g, 70.6%). The $^1\text{H-NMR}$ spectrum was found to be identical to the one of compound **38b'**.



(3R,9bS)-3-((1-ethyl-1H-indol-3-yl)methyl)-9b-phenyl-2,3-dihydrooxazolo[2,3-a]isoindol-5(9bH)-one 38b':

To a solution of compound **38'** (0.150 g, 0.394 mmol) in anhydrous dimethylformamide, DMF (3 mL), sodium hydride, NaH 95%, (0.019 g, 0.789 mmol) and ethyl iodide (0.063 mL, 0.789 mmol, $d = 1.95 \text{ g mL}^{-1}$) were added. Reaction time: 3 hours. Eluent for flash chromatography: ethyl acetate/ *n*-hexane, 2:8. The product was obtained as a light white solid (0.132 g, 82.0%); mp: 58 - 61 °C; $^1\text{H NMR}$ (300 MHz, CDCl_3) δ 7.85 – 7.78 (m, 1H, ArH), 7.67 – 7.62 (m, 2H, ArH), 7.52 – 7.45 (m, 3H, ArH), 7.43 – 7.37 (m, 3H, ArH), 7.29 (d, $J = 8.2$ Hz, 1H, ArH), 7.26 – 7.21 (m, 1H, ArH), 7.18 (d, $J = 8.1$ Hz, 1H, ArH), 7.08 (t, $J = 7.5$ Hz, 1H, ArH), 7.03 (s, 1H, CH-indole), 4.70 (dq, $J = 13.4, 6.8$ Hz, 1H, H-3), 4.45 (t, $J = 8.1$ Hz, 1H, H-2), 4.10 (q, $J = 7.3$ Hz, 2H, CH_2CH_3), 3.99 (dd, $J = 8.2, 7.2$ Hz, 1H, H-2), 3.23 (dd, $J = 14.6, 5.8$ Hz, 1H, CH_2 -indole), 2.65 (dd, $J = 14.6, 9.4$ Hz, 1H, CH_2 -indole), 1.42 (t, $J =$



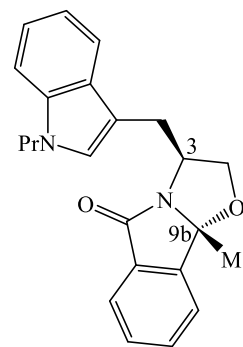
7.3 Hz, 3H, CH₂CH₃); ¹³C NMR (75 MHz, CDCl₃) δ 174.60 (C=O), 147.16 (ArC), 138.88 (ArC), 135.90 (ArC), 133.27 (ArC), 131.12 (ArC), 130.09 (ArC), 128.78 (ArC), 128.68 (ArC), 128.01 (ArC), 125.82 (ArC), 125.10 (CH-indole), 124.38 (ArC), 123.45 (ArC), 121.51 (ArC), 119.01 (ArC), 118.86 (ArC), 110.27 (ArC), 109.23 (ArC), 100.94 (C-9b), 76.35 (CH-2), 55.78 (CH-3), 40.79 (CH₂CH₃), 30.15 (CH₂-indole), 15.49 (CH₂CH₃).

4.2.2.3. General procedure for *N*-propylation

To a stirred solution of the appropriate (*S*)- or (*R*)- oxazoloisindolinone derivative (0.320 mmol, 1 equivalent) in anhydrous dimethylformamide, DMF (3 mL) under inert atmosphere of nitrogen and in ice bath was added sodium hydride, NaH (2 equivalents, 95% anhydrous solid reagent). The mixture was allowed to stir for 30 minutes and then propyl bromide (2 equivalents, *d* = 1.35 gmL⁻¹) was added. The reaction was kept stirring at room temperature till total consumption of the limitant reagent. After this period of time, ethyl acetate was added to the crude of reaction and then extracted with deionized water. The organic phase was washed then with bicarbonate of sodium, NaHCO₃, then with a saturated aqueous solution of sodium chloride, NaCl (brine), dried with sodium sulphate, NaSO₄ solid reagent and at last, the solvent was evaporated, after filtration of the drying solid agent. The crude was absorbed in silica and purified by flash chromatography using ethyl acetate/ *n*-hexane as mixture of eluent, and when required recrystallized using ethyl acetate/ *n*-hexane mixture of solvents.

(3*S*,9*bR*)-9*b*-methyl-3-((1-propyl-1*H*-indol-3-yl)methyl)-2,3-dihydrooxazolo[2,3-*a*]isindol-5(9*bH*)-one 34c:

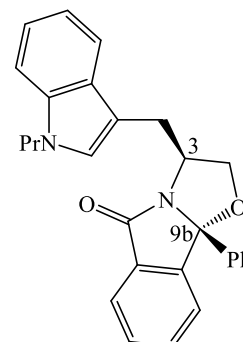
Following the general procedure starting from compound **34** (0.0628 g, 0.197 mmol), dissolved in dimethylformamide, DMF (3 mL) sodium hydride, NaH 95%, (0.0096 g, 0.400 mmol) and propyl bromide (0.036 mL, 0.396 mmol, *d* = 1.35 gmL⁻¹) were added. Reaction time: 1 hour. Eluent of flash chromatography: ethyl acetate / *n*-hexane, 3:7. The solid was obtained as a white crystalline solid (0.0535 g, 75.3%); mp: N. D.; ¹H NMR (300 MHz, CDCl₃) δ 7.81 (d, *J* = 7.2 Hz, 1H, Ar*H*), 7.75 (d, *J* = 7.8 Hz, 1H, Ar*H*), 7.66 – 7.58 (m, 1H, Ar*H*), 7.57 – 7.50 (m, 2H, Ar*H*), 7.36 (d, *J* = 8.1 Hz, 1H, Ar*H*), 7.28 – 7.21 (m, 1H, Ar*H*), 7.20 – 7.12 (m, 2H, Ar*H*), 4.65 – 4.54 (m, 1H, *H*-3), 4.32 (t, *J* = 8.1 Hz, 1H, *H*-2), 4.20 (dd, *J* = 8.8, 6.5 Hz, 1H, *H*-2), 4.09 (t, *J* = 7.2 Hz, 2H, CH₂CH₂CH₃), 3.46 (dd, *J* = 14.7, 5.3 Hz, 1H, CH₂-indole), 3.20 (dd, *J* = 14.7, 8.9 Hz, 1H, CH₂-indole), 1.89 (sextet, *J* = 7.2 Hz, 2H, CH₂CH₂CH₃), 1.71 (s, 3H, C9*b*-CH₃), 0.96 (t, *J* = 7.2 Hz, 3H, CH₂CH₂CH₃); ¹³C NMR (75 MHz, CDCl₃) δ 174.39 (C=O), 147.43 (C*q*), 136.30 (C*q*), 133.20 (ArC), 131.74 (ArC), 130.14 (ArC), 128.22 (C*q*), 126.34 (ArC), 124.30 (ArC), 122.13 (ArC), 121.59 (ArC), 119.09 (ArC), 118.98 (ArC), 110.02



(Cq), 109.48 (ArC), 98.97 (C-9b), 74.72 (CH-2), 56.24 (CH-3), 47.96 (CH₂CH₂CH₃), 30.59 (CH₂-indole), 23.61 (CH₂CH₂CH₃), 23.16 (C9b-CH₃), 11.59 (CH₂CH₂CH₃).

(3*S*,9*bR*)-9*b*-phenyl-3-((1-propyl-1*H*-indol-3-yl)methyl)-2,3-dihydrooxazolo[2,3-*a*]isoindol-

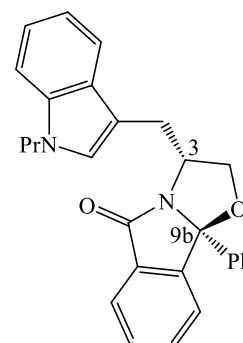
5(9*bH*)-one 38c: Following the general procedure starting from compound **38** (0.0592 g, 0.156 mmol), dissolved in dimethylformamide, DMF (3 mL) sodium hydride, NaH, 95% (0.008 g, 0.311 mmol) and propyl bromide (0.028 mL, 0.311 mmol, $d = 1.35 \text{ gmL}^{-1}$) were added. Reaction time: 1 hour. Eluent for flash chromatography: ethyl acetate/ *n*-hexane, 3:7. The compound was obtained as a white crystalline solid (0.0506 g, 77.0%); ¹H NMR (300 MHz, CDCl₃) δ 7.83 – 7.79 (m, 1H, Ar*H*), 7.65 (dd, $J = 2.7, 1.9 \text{ Hz}$, 1H, Ar*H*), 7.63



(d, $J = 1.8 \text{ Hz}$, 1H, Ar*H*), 7.51 – 7.46 (m, 3H, Ar*H*), 7.41 (dd, $J = 4.9, 1.9 \text{ Hz}$, 1H, Ar*H*), 7.38 (d, $J = 1.8 \text{ Hz}$, 2H, Ar*H*), 7.28 (d, $J = 8.3 \text{ Hz}$, 1H, Ar*H*), 7.25 – 7.21 (m, 1H, Ar*H*), 7.21-7.15 (m, 1H, Ar*H*), 7.07 (ddd, $J = 7.9, 7.0, 1.1 \text{ Hz}$, 1H, Ar*H*), 7.01 (s, 1H, CH-indole), 4.69 (ddd, $J = 13.2, 9.4, 6.9 \text{ Hz}$, 1H, *H*-3), 4.43 (dd, $J = 8.7, 7.5 \text{ Hz}$, 1H, *H*-2), 4.01 (t, $J = 7.26 \text{ Hz}$, 2H, CH₂CH₂CH₃), 3.97 (dd, $J = 8.8, 6.7 \text{ Hz}$, 1H, *H*-2), 3.23 (ddd, $J = 14.6, 5.8, 0.7 \text{ Hz}$, 1H, CH₂-indole), 2.63 (dd, $J = 14.6, 9.4 \text{ Hz}$, 1H, CH₂-indole), 1.89 – 1.75 (sextet, $J = 7.26 \text{ Hz}$, 2H, CH₂CH₂CH₃), 1.57 (s, 3H, C9*b*-CH₃), 0.90 (t, $J = 7.26 \text{ Hz}$, 3H, CH₂CH₂CH₃), the ¹H-NMR spectrum was found to be identical to the one of compound **38c**'.

(3*R*,9*bS*)-9*b*-phenyl-3-((1-propyl-1*H*-indol-3-yl)methyl)-2,3-dihydrooxazolo[2,3-*a*]isoindol-

5(9*bH*)-one 38c': Following the general procedure starting from compound **38'** (0.080 g, 0.210 mmol), dissolved in dimethylformamide, DMF (3 mL) sodium hydride, NaH 95%, (0.012 g, 0.500 mmol) and propyl bromide (0.0386 mL, 0.311 mmol, $d = 1.35 \text{ gmL}^{-1}$) were added. Reaction time: 3 hours. Eluent for flash chromatography: ethyl acetate/ *n*-hexane, 3:7. The product was obtained as a white crystalline solid (0.0619 g, 70.0%); mp: 54-56 °C; ¹H NMR (300 MHz, CDCl₃) δ 7.83 – 7.79 (m, 1H, Ar*H*), 7.65 (dd, $J = 2.7, 1.9 \text{ Hz}$, 1H, Ar*H*), 7.63 (d, $J = 1.8 \text{ Hz}$, 1H, Ar*H*), 7.51 – 7.46 (m, 3H, Ar*H*), 7.41 (dd, $J =$



4.9, 1.9 Hz, 1H, Ar*H*), 7.38 (d, $J = 1.8 \text{ Hz}$, 2H, Ar*H*), 7.28 (d, $J = 8.2 \text{ Hz}$, 1H, Ar*H*), 7.25 – 7.21 (m, 1H, Ar*H*), 7.21 – 7.15 (m, 1H, Ar*H*), 7.07 (ddd, $J = 7.9, 7.0, 1.1 \text{ Hz}$, 1H, Ar*H*), 7.01 (s, 1H, CH-indole) 4.69 (ddd, $J = 13.2, 9.4, 6.7 \text{ Hz}$, 1H, *H*-3), 4.44 (dd, $J = 8.7, 7.5 \text{ Hz}$, 1H, *H*-2), 4.01 (t, $J = 7.26 \text{ Hz}$, 2H, CH₂CH₂CH₃), 3.98 (dd, $J = 8.8, 6.7 \text{ Hz}$, 1H, *H*-2), 3.23 (dd, $J = 14.6, 5.9 \text{ Hz}$, 1H, CH₂-indole), 2.64 (dd, $J = 14.7, 9.5 \text{ Hz}$, 1H, CH₂-indole), 1.83 (sextet, $J = 7.26 \text{ Hz}$ 2H, CH₂CH₂CH₃), 0.90 (t, $J = 7.26 \text{ Hz}$, 3H, CH₂CH₂CH₃); ¹³C NMR (75 MHz, CDCl₃) δ 174.57 (C=O), 147.18 (Cq), 138.90 (Cq), 136.20 (Cq), 133.25 (ArC), 131.11 (ArC), 130.07 (ArC), 128.77 (ArC), 128.66 (ArC), 127.94 (ArC),

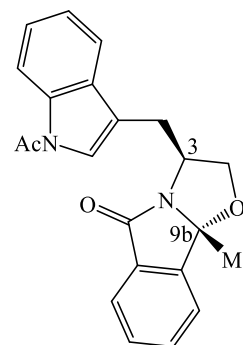
125.94 (Cq), 125.81 (CH-indole), 124.37 (ArC), 123.44 (ArC), 121.46 (ArC), 118.96 (ArC), 118.80 (ArC), 110.04 (Cq), 109.36 (ArC), 100.93 (C-9b), 76.32 (CH-2), 55.78 (CH-3), 47.90 (CH₂CH₂CH₃), 30.12 (CH₂-indole), 23.51 (CH₂CH₂CH₃), 11.54 (CH₂CH₂CH₃).

4.2.2.4. General procedure for *N*-acetylation

To a stirred solution of the appropriate (*S*)- or (*R*)-oxazoloisoindolinone derivative (0.32 mmol, 1 equivalent) in dry dimethylformamide, DMF (5 mL) under inert atmosphere of nitrogen and ice bath was added sodium hydride, NaH (2 equivalents, 95% anhydrous reagent). The mixture was allowed to stir for 30 minutes and then acetic anhydride (2 equivalents, $d = 1.08 \text{ gmL}^{-1}$) was added. The reaction was kept stirring at room temperature for 3 hours. After this period of time, ethyl acetate was added to the crude of reaction and then dimethylformamide was extracted with room temperature deionized water. The organic phase was washed then with brine, dried with sodium sulphate, NaSO₄, solid reagent and at last the solvent was evaporated. The crude was absorbed in silica and purified by flash chromatography using ethyl acetate/ *n*-hexane as mixture of eluents. Recrystallization was made using ethyl acetate/ *n*-hexane as solvents.

(3*S*,9*bR*)-3-((1-acetyl-1*H*-indol-3-yl)methyl)-9*b*-methyl-2,3-dihydrooxazolo[2,3-*a*]isoindol-

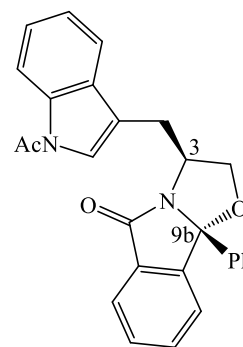
5(9*bH*)-one 34d: To a solution of compound **34** (0.0517 g, 0.162 mmol) in anhydrous DMF (5 mL) sodium hydride, NaH 95%, (0.00779 g, 0.325 mmol) and acetic anhydride (0.0307 mL, 0.280 mmol, $d = 1.08 \text{ gmL}^{-1}$) were added. Reaction time: 3 hours. Eluent for flash chromatography: ethyl acetate/ *n*-hexane, 3:7. Recrystallization: ethyl acetate/ *n*-hexane. The product was obtained as a white light solid (0.0465g, 79.5%); mp: 65-68 °C; $[\alpha]^{20}_{\text{D}} = +25.3^{\circ}$ ($c = 0.53$, CH₂Cl₂); ¹H NMR (300 MHz, CDCl₃) δ 8.38 (d, $J = 7.8$ Hz,



4H, ArH), 7.33 – 7.17 (m, 2H, ArH), 4.62 – 4.52 (m, 1H, *H*-3), 4.34 (dd, $J = 8.7, 7.6$ Hz 1H, *H*-2), 4.10 (dd, $J = 8.8, 5.8$ Hz, 1H, *H*-2), 3.23 (dd, $J = 14.7, 7.9$ Hz, 1H, CH₂-indole), 2.99 (dd, $J = 14.4, 6.2$ Hz, 1H, CH₂-indole), 2.60 (s, 3H, NCH₃), 1.68 ppm (s, 3H, C-9*b*CH₃); ¹³C NMR (75 MHz, CDCl₃) δ 174.62 (ring-C=O), 168.84 (protecting acylic group-C=O), 147.26 (Cq), 135.80 (Cq), 133.49 (ArC), 131.34 (Cq), 130.68 (Cq), 130.32 (ArC), 125.41 (ArC), 124.36 (ArC), 123.60 (ArC), 123.34 (ArC), 122.20 (ArC), 118.66 (Cq), 118.46 (ArC), 116.77 (ArC), 99.22 (C-9*b*), 74.91 (CH-2), 54.97 (CH-3), 30.64 (CH₂-indole), 24.15 (CH₃C=O), 23.33 (C-9*b*CH₃); Anal. Calc. (C₂₂H₂₀N₂O₃): C, 73.32%; H, 5.59%; N, 7.77%. Found C, 73.11%; H, 5.67%; N, 7.71%.

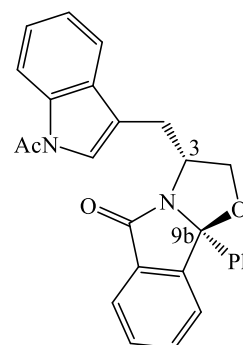
(3*S*,9*bR*)-3-((1-acetyl-1*H*-indol-3-yl)methyl)-9*b*-phenyl-2,3-dihydrooxazolo[2,3-*a*]isoindol-

5(9*bH*)-one 38*d*: To a solution of compound **38** (0.0522 g, 0.137 mmol) in anhydrous dimethyl formamide, DMF (5 mL), sodium hydride, NaH 95%, (0.00395 g, 0.165 mmol) and acetic anhydride (0.0150 mL, 0.159 mmol, $d = 1.08 \text{ g mL}^{-1}$) were added. Reaction time: 3 hours. Eluent for flash chromatography: ethyl acetate/ *n*-hexane, 3:7. The product was obtained as a white light solid (0.0488g 84.2%); mp: 140-143 °C; $[\alpha]_D^{20} = +141.3^\circ$ ($c = 0.56$, CH_2Cl_2); $^1\text{H NMR}$ (300 MHz, CDCl_3) δ 8.33 (d, $J = 7.4$ Hz, 1H, H-ar), 7.71 (dd, $J = 5.3, 2.9$ Hz, 1H, H-ar), 7.65 (s, 1H, H-ar), 7.49 – 7.36 (m, 6H, H-ar H-ar), 7.26 (d, $J = 0.9$ Hz, 7H, H-ar), 7.20 – 7.11 (m, 4H, H-ar), 4.68 (ddd, $J = 14.2, 7.5, 6.4$ Hz, 1H, *H*-3), 4.54 (dd, $J = 8.4, 7.6$ Hz, 1H, *H*-2), 3.92 (dd, $J = 8.5, 6.4$ Hz, 1H, *H*-2), 2.81 (dd, $J = 15.6, 8.1$ Hz, 1H, CH_2 -indole), 2.62 (dd, $J = 15.3, 6.2$ Hz, 1H, CH_2 -indole), 2.57 ppm (s, 3H, Ac- CH_3), the $^1\text{H-NMR}$ spectrum was found to be identical to the one of compound **38*c*'**; Anal. Calc. ($\text{C}_{27}\text{H}_{22}\text{N}_2\text{O}_3$): C, 76.76%; H, 5.25%; N, 6.63%. Found C, 76.91%; H, 5.31%; N, 6.69%.



(3*R*,9*bS*)-3-((1-acetyl-1*H*-indol-3-yl)methyl)-9*b*-phenyl-2,3-dihydrooxazolo[2,3-*a*]isoindol-

5(9*bH*)-one 38*d*': To a solution of compound **38'** (0.081 g, 0.210 mmol) in anhydrous DMF (5 mL), sodium hydride, NaH 95%, (0.00102 g, 0.426 mmol) and acetic anhydride (0.0403 mL, 0.426 mmol, $d = 1.08 \text{ g mL}^{-1}$) were added. Reaction time: 3 hours. Eluent for flash chromatography: ethyl acetate/ *n*-hexane, 2:8. The product was obtained as a white light solid (0.067g, 74.5%); mp: 85-87 °C; $^1\text{H NMR}$ (300 MHz, CDCl_3) δ 8.33 (d, $J = 7.9$ Hz, 1H, Ar*H*), 7.71 (dd, $J = 5.3, 2.9$ Hz, 1H, Ar*H*), 7.64 (s, 1H, CH-indole), 7.44 (dt, $J = 5.8, 2.3$ Hz, 2H, Ar*H*), 7.39 (dd, $J = 5.4, 3.3$ Hz, 2H, Ar*H*), 7.31 – 7.20 (m, 5H, Ar*H*), 7.19--7.10 (m, 2H, Ar*H*), 4.68 (ddd, $J = 14.2, 7.5, 6.4$ Hz, 1H, *H*-3), 4.54 (dd, $J = 8.4, 7.6$ Hz, 1H, *H*-2), 3.92 (dd, $J = 8.5, 6.4$ Hz, 1H, *H*-2), 2.81 (dd, $J = 15.6, 8.1$ Hz, 1H, CH_2 -indole), 2.62 (dd, $J = 15.3, 6.2$ Hz, 1H, CH_2 -indole), 2.56 (s, 3H, Ac- CH_3); $^{13}\text{C NMR}$ (75 MHz, CDCl_3) δ 174.79 (ring-C=O), 168.76 (Ac-C=O), 146.98 (Cq), 138.44 (Cq), 135.71 (Cq), 133.49 (ArC), 130.75 (Cq), 130.62 (ArC), 130.25 (ArC), 128.83 (ArC), 125.80 (ArC), 125.66 (ArC), 125.27 (CH-indole), 124.41 (ArC), 123.50 (Cq), 123.46 (ArC), 123.20 (ArC), 118.59 (ArC), 118.45 (ArC), 116.66 (ArC), 101.18 (C-9*b*), 76.24 (CH-2), 54.50 (CH-3), 29.68 (CH_2 -indole), 24.13 ($\text{CH}_3\text{C}=\text{O}$).

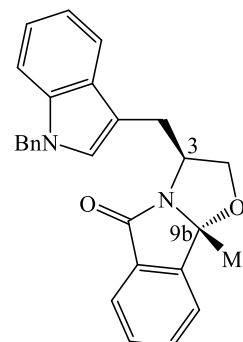


4.2.2.5. General procedure for *N*-benzylation

To a stirred solution of 1 equivalent of the adequate (*S*)- or (*R*)- oxazoloisindolinone derivative (0.320 mmol, 1 equivalent) in pure dimethylformamide, DMF (3 mL), under inert atmosphere and ice bath sodium hydride, NaH (2.2 equivalents, 95% anhydrous reagent) was added and the mixture was stirred for 30 minutes. After this period benzyl bromide (1.5 equivalents) was added and the reaction was allowed to stand at room temperature till total consumption of the limitant reagent. At the end of the reaction an aliquot of 20 mL of ethyl acetate was added to the mixture or reaction and extracted with room temperature deionized water. The organic phase was washed then with brine (saturated aqueous solution of NaCl), dried with sodium sulphate, NaSO₄, solid reagent and at last the solvent was evaporated. The crude was absorbed in silica and purified by flash chromatography using ethyl acetate/ *n*-hexane as mixture of eluent, and when required recrystallized using ethyl acetate/ *n*-hexane mixture of solvents.

(3*S*,9*bR*)-3-((1-benzyl-1-*H*-indol-3-yl)methyl)-9*b*-methyl-2,3-dihydrooxazolo[2,3-*a*]isoindol-

5(9*bH*)-one 34e: To a solution of compound **34** (0.100 g, 0.310 mmol) in anhydrous dimethylformamide, DMF (3 mL), sodium hydride, NaH 95%, (0.028 g, 0.690 mmol) and benzyl bromide (0.0560 mL, 0.470 mmol, $d = 1.44 \text{ gmL}^{-1}$) were added. Reaction time: 3 hours. Eluent for flash chromatography: ethyl acetate/ *n*-hexane, 1:2. The product was obtained as a pale yellow solid (0.108g, 83.9%); mp: 50-52 °C; ¹H-NMR (300 MHz, CDCl₃) δ 7.80 – 7.72 (m, 2H, Ar*H*), 7.64 – 7.57 (m, 1H, Ar*H*), 7.54 – 7.49 (m, 2H, Ar*H*), 7.34 – 7.24

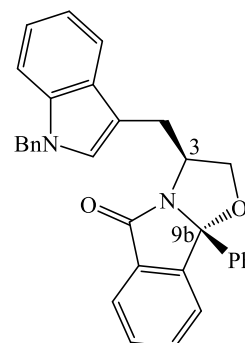


(m, 4H, Ar*H*), 7.14 – 7.11 (m, 5H, Ar*H*), 5.31 (s, 2H, benzyl-CH₂), 4.64 – 4.51 (m, 1H, *H*-3), 4.30 (dd, $J = 8.9, 7.4 \text{ Hz}$, 1H, *H*-2), 4.17 (dd, $J = 8.9, 6.5 \text{ Hz}$, 1H, *H*-2), 3.44 (dd, $J = 14.7, 5.3 \text{ Hz}$, 1H, CH₂-Indole), 3.17 (dd, $J = 14.7, 8.9 \text{ Hz}$, 1H, CH₂-Indole), 1.68 (s, 3H, C-9*b*CH₃), ¹³C-NMR (75 MHz, CDCl₃) δ 174.48 (C=O), 147.45 (Cq), 137.66 (ArC), 136.70 (Cq), 133.31 (ArC), 131.80 (Cq), 130.25 (ArC), 128.88 (ArC), 128.47 (ArC), 127.73 (Cq), 126.92 (ArC), 126.71 (ArC), 124.41 (ArC), 122.22 (ArC), 122.10 (ArC), 119.46 (ArC), 119.28 (ArC), 111.01 (ArC), 109.86 (Cq), 99.05 (C-9*b*), 74.79 (CH-2), 56.23 (CH-3), 50.10 (benzyl-CH₂), 30.72 (CH₂-Indole), 23.23 (C-9*b*CH₃). MS (ESI) m/z calcd for C₂₇H₂₄N₂O₂: 408, found 409 [M + H]⁺.

(3*S*,9*bR*)-3-((1-benzyl-1-*H*-indol-3-yl)methyl)-9*b*-phenyl-2,3-dihydrooxazolo[2,3-*a*]isoindol-

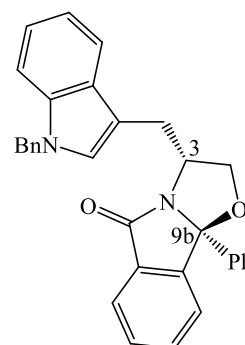
5(9*bH*)-one, 38e: according to the general procedure, to a solution of 0.0636 g of **38** (0.167 mmol) in dimethylformamide, DMF (3 mL) in ice bath and under inert atmosphere of nitrogen, 0.0089 g of

sodium hydride, NaH 95%, (0.368 mmol) were added. After stirring for 30 minutes 0.030 mL of benzyl bromide (0.251 mmol, 1.44 g mL^{-1}) were added. Reaction time: 2 hours. Eluent for flash chromatography: ethyl acetate/ *n*-hexane, 3:7. Recrystallization: in acetate/ *n*-hexane. The product was obtained as a white light solid (0.0757 g, 96.2%); mp: 61- 64 °C; ^1H NMR (300 MHz, CDCl_3) δ 7.84 – 7.77 (m, 1H, ArH), 7.67 – 7.60 (m, 2H, ArH), 7.53 (d, $J = 7.6$ Hz, 1H, ArH), 7.48 (dd, $J = 5.6, 3.1$ Hz, 2H, ArH), 7.42 – 7.35 (m, 4H, ArH), 7.28 (m, 1H, ArH), 7.25 – 7.20 (m, 3H, ArH), 7.17 (dd, $J = 6.9, 1.0$ Hz, 1H, ArH), 7.13 (dd, $J = 5.6, 1.3$ Hz, 1H, ArH), 7.08 (d, $J = 7.6$ Hz, 2H, ArH), 7.01 (s, 1H, CH-indole), 5.25 (s, 2H, Bn- CH_2), 4.70 (dq, $J = 9.4, 6.8$ Hz, 1H, *H*-3), 4.44 (dd, $J = 8.6, 7.5$ Hz, 1H, *H*-2), 3.99 (dd, $J = 8.7, 6.7$ Hz, 1H, *H*-2), 3.23 (dd, $J = 14.5, 5.9$ Hz, 1H, CH_2 -indole), 2.66 (dd, $J = 14.6, 9.5$ Hz, 1H, CH_2 -indole); ^{13}C NMR (75 MHz, CDCl_3) δ 174.55 (C=O), 147.18 (Cq), 138.89 (Cq), 137.59 (Cq), 136.56 (Cq), 133.26 (ArC), 131.09 (Cq), 130.08 (ArC), 128.77 (ArC), 128.74 (ArC), 128.67 (ArC), 128.12 (Cq), 127.56 (Cq), 126.75 (ArC), 126.26 (CH-indole), 125.80 (ArC), 124.37 (ArC), 123.45 (ArC), 121.89 (ArC), 119.21 (ArC), 119.04 (ArC), 110.97 (ArC), 109.66 (ArC), 100.93 (C-9b), 76.27 (CH-2), 55.74 (CH-3), 49.93 (Bn- CH_2), 30.14 (CH_2 -indole).



(3R,9bS)-3-((1-benzyl-1H-indol-3-yl)methyl)-9b-phenyl-2,3-dihydrooxazolo[2,3-a]isoindol-5(9bH)-one, 38e': To a solution of compound **38'** (0.0619 g, 0.210 mmol) in

anhydrous dimethylformamide, DMF (3 mL), sodium hydride, NaH 95%, (0.0091 g, 0.158 mmol) and benzyl bromide (0.0280 mL, 0.237 mmol, $d = 1.44 \text{ g mL}^{-1}$) were added. Reaction time: 1.5 hours. Eluent for flash chromatography: ethyl acetate/ *n*-hexane, 3:7. The product was obtained as a white light solid (0.0578 g, 75.5%); mp: 61- 64 °C; ^1H NMR (300 MHz, CDCl_3) δ 7.82 – 7.78 (m, 1H, ArH), 7.65 – 7.61 (m, 2H, ArH), 7.53 (d, $J = 7.6$ Hz, 1H, ArH), 7.48 (dd, $J = 5.6, 3.1$ Hz, 2H, ArH), 7.42 – 7.35 (m, 4H, ArH), 7.28 (m, 1H, ArH), 7.25 – 7.20 (m, 3H, ArH), 7.17 (dd, $J = 6.9, 1.0$ Hz, 1H, ArH), 7.13 (dd, $J = 5.6, 1.3$ Hz, 1H, ArH), 7.08 (d, $J = 7.6$ Hz, 2H, ArH), 7.01 (s, 1H, CH-indole), 5.25 (s, 2H, Bn- CH_2) 4.70 (dq, $J = 9.4, 6.8$ Hz, 1H, *H*-3), 4.44 (dd, $J = 8.7, 7.5$ Hz, 1H, *H*-2), 3.98 (dd, $J = 8.7, 6.7$ Hz, 1H, *H*-2), 3.23 (dd, $J = 14.7, 5.9$, 1H, CH_2 -indole), 2.65 ppm (dd, $J = 14.6, 9.5$ Hz, 1H, CH_2 -indole), the ^1H -NMR spectrum was found to be identical to the one of compound **38e**.

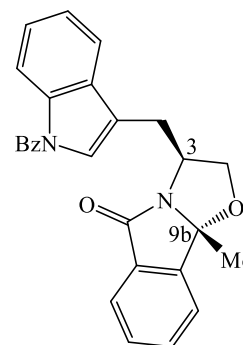


4.2.2.6. General procedure for *N*-benzylation

To a stirred solution of the appropriate (*S*)- or (*R*)-oxazoloisoindolinone derivative (0.320 mmol, 1 equivalent) in dry dimethylformamide, DMF (5 mL) under inert atmosphere of nitrogen and ice bath was added sodium hydride, NaH (2 equivalents 95% anhydrous reagent). The mixture was allowed to stir for 30 minutes and then acetic anhydride (2 equivalents, $d = 1.08 \text{ g mL}^{-1}$) was added. The reaction was kept stirring at room temperature for 3 hours. After this period, ethyl acetate was added to the crude of reaction and then dimethylformamide was extracted quantitatively with room temperature deionized water. The organic phase was washed then with brine, dried with sodium sulphate, NaSO_4 , solid reagent and at last the solvent was evaporated. The crude was absorbed in silica and purified by flash chromatography using ethyl acetate/ *n*-hexane as mixture of eluent, and when required recrystallized using ethyl acetate/ *n*-hexane mixture of solvents.

(3*S*,9*bR*)-3-((1-benzoyl-1*H*-indol-3-yl)methyl)-9*b*-methyl-2,3-dihydrooxazolo[2,3-*a*]isoindol-

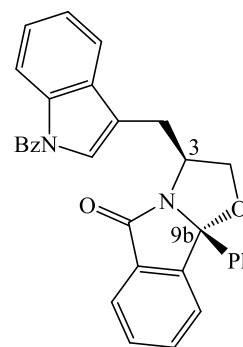
5(9*bH*)-one 34f: To a solution of compound **34** (0.0558 g, 0.175 mmol) in anhydrous dimethylformamide, DMF (3 mL), sodium hydride, NaH 95%, (0.0097g, 0.158 mmol) and benzoyl chloride (0.0408 mL, 0.351 mmol, $d = 1.21 \text{ g mL}^{-1}$) were added. Reaction time: 2 hours. Eluent for flash chromatography: ethyl acetate/ *n*-hexane, 3:7. The product was obtained as a white light solid (0.0567g, 76.6%); mp: 56- 58 °C; $^1\text{H NMR}$ (300 MHz, CDCl_3) δ 8.39 (dd, $J = 7.0, 1.3 \text{ Hz}$, 1H, Ar*H*), 7.78 – 7.70 (m, 4H, Ar*H*), 7.66



– 7.49 (m, 6H, Ar*H*), 7.45 – 7.33 (m, 3H, Ar*H*), 4.54 (dq, $J = 8.3, 6.2 \text{ Hz}$, 1H, *H*-3), 4.31 (dd, $J = 8.9, 7.4 \text{ Hz}$, 1H, *H*-2), 4.12 (dd, $J = 8.9, 6.2 \text{ Hz}$, 1H, *H*-2), 3.34 (dd, $J = 14.9, 6.0 \text{ Hz}$, 1H, CH_2 -indole), 3.08 (dd, $J = 14.9, 8.5 \text{ Hz}$, 1H, CH_2 -indole), 1.72 (s, 3H, C-9*b* CH_3); $^{13}\text{C-NMR}$ (75 MHz, CDCl_3) δ 174.36 (ring-C=O), 168.51 (Bz-C=O), 147.26 (Cq), 136.32 (Cq), 134.57 (Cq)133.37 (ArC), 131.93 (Cq), 131.41 (ArC), 130.89 (ArC), 130.59 (Cq), 130.24 (ArC), 129.23 (ArC), 128.89 (ArC), 128.66 (ArC), 125.34 (ArC), 125.25 (Cq), 124.34 (ArC), 123.99 (ArC), 122.17 (ArC), 119.05 (ArC), 117.86 (s), 116.59 (ArC), 98.99 (C-9*b*), 74.54 (CH-2), 55.33 (CH-3), 30.52 (CH_2 -indole), 23.25 (C-9*b* CH_3).

(3*S*,9*bR*)-3-((1-benzoyl-1*H*-indol-3-yl)methyl)-9*b*-phenyl-2,3-dihydrooxazolo[2,3-*a*]isoindol-

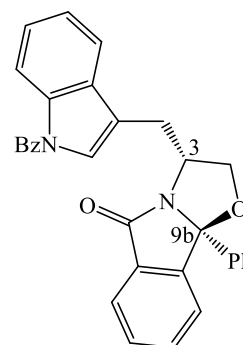
5(9*bH*)-one 38*f*: To a solution of compound **38** (0.0558 g, 0.175 mmol) in anhydrous dimethylformamide, DMF (3 mL), sodium hydride, NaH 95%, (0.0097g, 0.158 mmol) and benzoyl chloride (0.0408 mL, 0.351 mmol, d = 1.21 g mL⁻¹) were added. Reaction time: 2 hours. Eluent for flash chromatography: ethyl acetate/ *n*-hexane, 3:7. The product was obtained as a white light solid (0.0567g, 76.6%); mp: 55- 57 °C; ¹H NMR (300 MHz, CDCl₃) δ 8.37 (d, *J* = 8.2 Hz, 1H, *ArH*), 7.80 – 7.76 (m, 1H, *ArH*), 7.72 (t, *J* = 1.4 Hz,



1H, *ArH*), 7.70 (t, *J* = 1.9 Hz, 1H, *ArH*), 7.61 (dt, *J* = 2.9, 2.1 Hz, 1H, *ArH*), 7.55 (dd, *J* = 7.5, 1.4 Hz, 3H, *ArH*), 7.51 (dd, *J* = 2.6, 1.4 Hz, 2H, *ArH*), 7.48 (dd, *J* = 5.5, 3.2 Hz, 3H, *ArH*), 7.42 – 7.35 (m, 1H, *ArH*), 7.35 – 7.30 (m, 4H, *ArH*), 7.22 – 7.19 (m, 1H, *ArH*), 7.19 (s, 1H, *CH*-indole), 4.65 (ddd, *J* = 14.7, 8.0, 6.6 Hz, 1H, *H*-3), 4.50 (dd, *J* = 8.6, 7.5 Hz, 1H, *H*-2), 3.94 (dd, *J* = 8.7, 6.7 Hz, 1H, *H*-2), 3.02 (dd, *J* = 14.8, 6.4 Hz, 1H, *CH*₂-indole), 2.67 (dd, *J* = 14.7, 8.8 Hz, 1H, *CH*₂-indole), the ¹H-NMR spectrum was found to be identical to the one of compound **38*f*'**.

(3*R*,9*bS*)-3-((1-benzoyl-1*H*-indol-3-yl)methyl)-9*b*-phenyl-2,3-dihydrooxazolo[2,3-*a*]isoindol-

5(9*bH*)-one 38*f*': To a solution of compound **38'** (0.0830 g, 0.220 mmol) in anhydrous dimethylformamide, DMF (3 mL), sodium hydride, NaH 95%, (0.0120g, 0.500 mmol) and benzoyl chloride (0.0488 mL, 0.420 mmol, d = 1.21 g mL⁻¹) were added. Reaction time: 1.5 hours. Eluent for flash chromatography ethyl acetate/ *n*-hexane, 2:8. The product was obtained as a white light solid (0.0567g, 60.0%); mp: 55- 57 °C; ¹H NMR (300 MHz, CDCl₃) δ 8.37 (d, *J* = 8.2 Hz, 1H, *ArH*), 7.80 – 7.76 (m, 1H, *ArH*), 7.72 (t, *J* = 1.4 Hz,



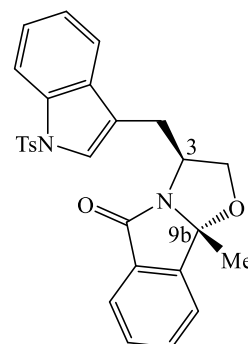
1H, *ArH*), 7.70 (t, *J* = 1.9 Hz, 1H, *ArH*), 7.61 (dt, *J* = 2.9, 2.1 Hz, 1H, *ArH*), 7.55 (dd, *J* = 7.5, 1.4 Hz, 3H, *ArH*), 7.51 (dd, *J* = 2.6, 1.4 Hz, 2H, *ArH*), 7.48 (dd, *J* = 5.5, 3.2 Hz, 3H, *ArH*), 7.42 – 7.35 (m, 1H, *ArH*), 7.35 – 7.30 (m, 4H, *ArH*), 7.22 – 7.19 (m, 1H, *ArH*), 7.19 (s, 1H, *CH*-indole), 4.65 (ddd, *J* = 14.7, 8.0, 6.6 Hz, 1H, *H*-3), 4.50 (dd, *J* = 8.6, 7.5 Hz, 1H, *H*-2), 3.94 (dd, *J* = 8.7, 6.7 Hz, 1H, *H*-2), 3.02 (dd, *J* = 14.8, 6.4 Hz, 1H, *CH*₂-indole), 2.67 (dd, *J* = 14.7, 8.8 Hz, 1H, *CH*₂-indole); ¹³C NMR (75 MHz, CDCl₃) δ 174.65 (ring-C=O), 168.43 (Bz-C=O), 147.13 (Cq), 138.65 (Cq), 136.24 (Cq), 134.59 (Cq), 133.43 (ArC), 131.86 (ArC), 130.84 (Cq), 130.78 (ArC), 130.18 (ArC), 129.24 (ArC), 128.79 (ArC), 128.74 (ArC), 128.61 (ArC), 125.65 (ArC), 125.22 (ArC), 125.11 (ArC), 124.39 (ArC), 123.88 (Cq), 123.50 (Cq), 118.96 (ArC), 117.77 (ArC), 116.53 (ArC), 100.99 (C-9*b*), 75.93 (*CH*-2), 55.07 (*CH*-3), 29.68 (*CH*₂-indole).

4.2.2.7. General procedure for *N*-tosylation

To a stirred solution of the appropriate (*R*)-oxazoloisindolinone derivative (0.320 mmol, 1 equivalent) in anhydrous dimethylformamide, DMF (2 mL) under inert atmosphere of nitrogen and ice bath was added sodium hydride, NaH (2 equivalents, 95% anhydrous reagent). The mixture was allowed to stir for 30 minutes and then *p*-toluene sulfonyl chloride (2 equivalents) was added. The reaction was kept stirring at room temperature for 1 hour and a half. After this period, ethyl acetate was added to the crude of reaction and then extracted at room temperature with deionized water. The organic phase was washed then with a saturated aqueous solution of sodium chloride, NaCl (brine), dried with sodium sulphate, NaSO₄ and in the end the solvent was evaporated in rotavapor. The crude was absorbed in silica and purified by flash chromatography using ethyl acetate/ *n*-hexane as mixture of eluent.

(3*S*,9*bR*)-9*b*-methyl-3-((1-tosyl-1*H*-indol-3-yl)methyl)-2,3-dihydrooxazolo[2,3*a*]isoindol-5(9*bH*)-one **34g**:

To a solution of compound **34** (0.1 g, 0.263 mmol) in anhydrous dimethylformamide, DMF (2 mL), sodium hydride, NaH 95%, (0.0013 g, 0.542 mmol) and *p*-toluenesulfonyl chloride (0.0501 g, 0.263 mmol) were added. Reaction time: 3 hours. Eluent for flash chromatography: ethyl acetate/ *n*-hexane, 3:7. The product was obtained as a white light solid (0.0967g, 77.8%). Recrystallization in ethyl acetate/ *n*-hexane provided 0.0854g of the compound; mp: 220 - 222 °C; ¹H NMR (400 MHz, CDCl₃) δ 8.00 (d, *J* = 8.2

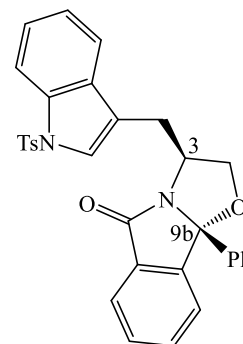


Hz, 1H, *ArH*), 7.81 – 7.75 (m, 3H, *ArH*), 7.65 – 7.59 (m, 3H, *ArH*), 7.53 (t, *J* = 7.0 Hz, 2H, *ArH*), 7.36 – 7.30 (m, 1H, *ArH*), 7.29 – 7.23 (m, 1H, *ArH*), 7.20 (d, *J* = 8.1 Hz, 2H, *ArH*), 4.55 – 4.47 (m, 1H, *H*-3), 4.31 (dd, *J* = 8.8, 7.6 Hz, 1H, *H*-2), 4.10 (dd, *J* = 8.9, 6.5 Hz, 1H, *H*-2), 3.28 (dd, *J* = 14.9, 5.0 Hz, 1H, *CH*₂-indole), 3.09 (dd, *J* = 14.9, 8.3 Hz, 1H, *CH*₂-indole), 2.32 (s, 3H, phenyl-*CH*₃), 1.61 (s, 3H, C-9*bCH*₃); ¹³C NMR (101 MHz, CDCl₃) δ 174.39 (ring-C=O), 147.21 (*C*_q), 144.87 (*C*_q), 135.20 (*C*_q), 133.37 (*ArC*), 131.43 (*C*_q), 130.91 (*C*_q), 130.26 (*ArC*), 129.84 (*ArC*), 126.83 (*ArC*), 124.94 (*ArC*), 124.36 (*ArC*), 124.07 (*ArC*), 123.97 (*C*_q), 123.32 (*ArC*), 122.17 (*ArC*), 119.62 (*ArC*), 118.54 (*C*_q), 113.79 (*ArC*), 98.98 (C-9*b*), 74.39 (*CH*-2), 55.09 (*CH*-3), 30.35 (*CH*₂-indole), 22.97 (phenyl-*CH*₃), 21.57 (C-9*bCH*₃).

(3*S*,9*bR*)-9*b*-phenyl-3-((1-tosyl-1*H*-indol-3-yl)methyl)-2,3-dihydrooxazolo[2,3-*a*]isoindol-5(9*bH*)-one **38g**:

To a solution of compound **38** (0.101 g, 0.266 mmol) in anhydrous dimethylformamide, DMF

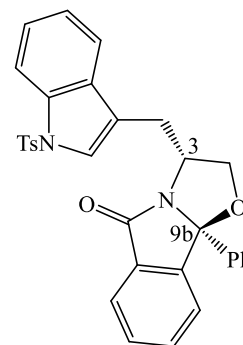
(2 mL), sodium hydride, NaH, 95% (0.0013 g, 0.531 mmol) and p-toluenesulfonyl chloride (0.0506 g, 0.266 mmol) were added. Reaction time: 3 hours. Eluent for flash chromatography: ethyl acetate/ *n*-hexane, 3:7. The product was obtained as a white light solid (0.0987g, 70.5%). Recrystallization in ethyl acetate/ *n*-hexane provided 0.0844g of the compound; mp: 218 - 220 °C; ¹H NMR (400 MHz, CDCl₃) δ 7.96 (d, *J* = 8.3 Hz, 1H, Ar*H*), 7.81 (d, *J* = 3.5 Hz, 1H, Ar*H*), 7.73 (d, *J* = 7.9 Hz, 2H, Ar*H*), 7.58 – 7.45 (m, 5H, Ar*H*),



7.41 (d, *J* = 7.8 Hz, 1H, Ar*H*), 7.37 (s, 3H, Ar*H*), 7.30 (t, *J* = 7.7 Hz, 1H, Ar*H*), 7.22 (d, *J* = 7.5 Hz, 2H, Ar*H*), 7.17 (d, *J* = 7.9 Hz, 2H, Ar*H*), 4.81 – 4.54 (m, 1H, *H*-3), 4.46 (t, *J* = 8.0 Hz, 1H, *H*-2), 4.00 – 3.79 (dd, *J* = 8.5, 6.5 Hz, 1H, *H*-2), 3.01 (dd, *J* = 14.9, 6.5 Hz, 1H, CH₂-indole), 2.58 (dd, *J* = 14.9, 8.5 Hz, 1H, CH₂-indole), 2.29 (s, 3H, phenyl-CH₃); ¹³C NMR (101 MHz, CDCl₃) δ 174.51 (ring-C=O), 147.07 (Cq), 144.78 (Cq), 138.55 (Cq), 135.20 (Cq), 135.17 (ArC), 133.44 (ArC), 130.79 (Cq), 130.71 (Cq), 130.20 (ArC), 129.78 (ArC), 128.84 (ArC), 128.82 (ArC), 126.80 (ArC), 125.64 (ArC), 124.84 (ArC), 124.39 (ArC), 123.79 (ArC), 123.51 (Cq), 123.21 (ArC), 119.38 (ArC), 118.64 (Cq), 113.79 (ArC), 100.95 (C-9*b*), 76.00 (CH-2), 54.61 (CH-3), 29.88 (CH₂-indole), 21.55 (phenyl-CH₃).

(3*R*,9*bS*)-9*b*-phenyl-3-((1-tosyl-1*H*-indol-3-yl)methyl)-2,3-dihydrooxazolo[2,3-*a*]isoindol-5(9*b**H*)-one 38g'**

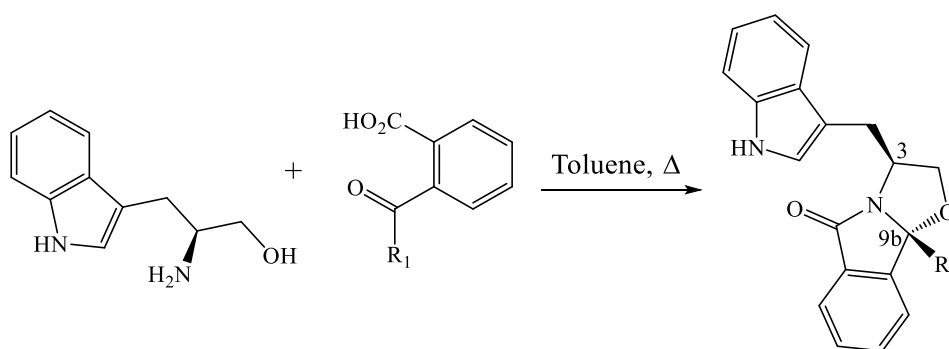
To a solution of compound **38'** (0.0694 g, 0.182 mmol) in anhydrous dimethylformamide, DMF (2 mL), sodium hydride, NaH 95%, (0.00102 g, 0.425 mmol) and p-toluenesulfonyl chloride (0.0603 g, 0.280 mmol) were added. Reaction time: 1.5 hours. Eluent for flash chromatography: ethyl acetate/ *n*-hexane, 3:7. The product is obtained as a white light solid (0.0854g, 87.6%). Recrystallization in ethyl acetate/ *n*-hexane provided 0.0554g of the compound; mp: 215 - 217 °C; ¹H NMR (300 MHz, CDCl₃) δ 7.96 (d, *J* = 8.1 Hz, 1H, Ar*H*), 7.81 (dd, *J* = 5.6, 3.1 Hz, 1H, Ar*H*), 7.73 (d, *J* = 8.3 Hz, 2H, Ar*H*), 7.58 – 7.45 (m, 5H, Ar*H*), 7.44 – 7.28 (m, 6H, Ar*H*), 7.24 – 7.14 (m, 4H, Ar*H*), 4.71 – 4.60 (m, 1H, *H*-3), 4.49 – 4.42 (dd, *J* = 8.8, 7.4 Hz, 1H, *H*-2), 3.93 (dd, *J* = 8.83, 6.4 Hz, 1H, *H*-2), 3.01 (dd, *J* = 14.9, 6.7 Hz, 1H, CH₂-indole), 2.58 (dd, *J* = 15.0, 8.5 Hz, 1H, CH₂-indole), 2.29 ppm (s, 3H, phenyl-CH₃).



4.3. Experimental procedure chapter 2.3 indolizinoindolones scaffold

4.3.1. General procedure for cyclocondensation reactions

To a solution of a particular aminoalcohol (0.660mmol, 1 equivalent) in toluene (5ml) was added the appropriate oxocarboxylic acid (0.730mmol). The mixture was heated at reflux for 10-24h under *dean-stark* apparatus, until total consumption of the starting aminoalcohol. The solvent was evaporated and the residue was dissolved in ethyl acetate. The organic phase was washed with saturated aqueous solutions of NaHCO₃ and NaCl, dried with anhydrous magnesium sulfate, filtered and evaporated. The crude was absorbed on silica and purified by flash chromatography using ethyl ethyl acetate /*n*-hexane as eluent.



Scheme 4.3. (*S*)-tryptophanol-derived bicyclic lactams cyclocondensation reaction procedure.

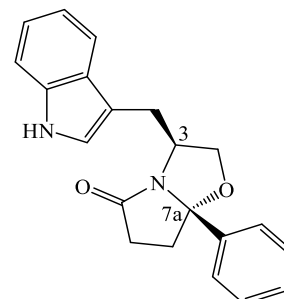
34: for the preparation see pg. 60.

38: for the preparation see pg. 60.

38': for the preparation see pg. 61.

(3*S*, 7*aS*)-3-((1*H*-indol-3-yl)methyl)-7*a*-phenyltetrahydropyrrolo[2,1-*b*]oxazol-5(6*H*)-one, 47*a*:

Following the general procedure, to a solution of (*S*)-tryptophanol **9** (0.155 g, 0.816 mmol) in toluene (7.5 mL) was added benzylpropionic acid (0.175 g, 0.980 mmol). Reaction time: 16 hours. Eluent for flash chromatography: ethyl acetate/ *n*-hexane, 1:1. The product was obtained as a white amorphous solid (0.196 g, 72.3%); pf 153-156 °C; [α]₂₀^D = +40.7° (c = 0.21, CH₂Cl₂); ¹H NMR (300 MHz, CDCl₃) δ 8.00 (s, 1H, *NH*),

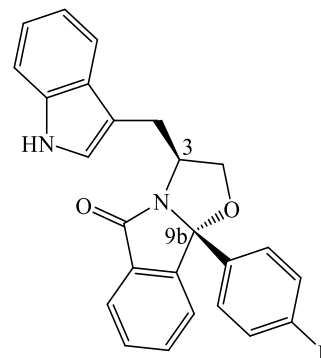


7.53 – 7.48 (m, 2H, *ArH*), 7.40 (tdd, *J* = 6.7, 5.8, 2.7 Hz, 4H, *ArH*), 7.33 (d, *J* = 8.1 Hz, 1H, *ArH*), 4.58 (dq, *J* = 9.3, 6.8 Hz, 1H, *H*-3), 4.16 (dd, *J* = 8.7, 7.5 Hz, 1H, *H*-2), 3.61 (dd, *J* = 8.8, 6.9 Hz, 1H, *H*-2),

3.08 (dd, $J = 14.7, 6.2$ Hz, 1H, CH_2 -indole), 2.92 – 2.77 (m, 1H, $H-6$), 2.63 (dd, $J = 10.0, 3.4$ Hz, 1H, CH_2 -indole), 2.57 – 2.41 (m, 2H, $H-6$ and $H-7$), 2.28 – 2.19 ppm (m, 1H, $H-7$); as previously described in literature [77].

(3*R*,9*bS*)-3-((1*H*-indol-3-yl)methyl)-9*b*-(4-fluorophenyl)-2,3-dihydrooxazolo[2,3-*a*]isoindol-

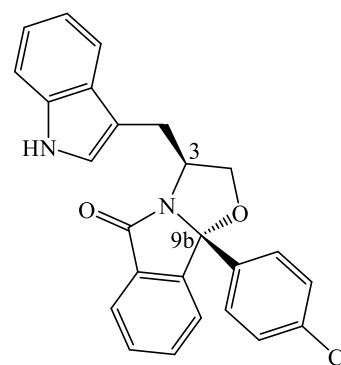
5(9*bH*)-one 47b: Following the general procedure, to a solution of (*S*)-tryptophanol **9** (0.172 g, 0.905 mmol) in toluene (5 mL) was added 2-(4-fluorobenzoyl)benzoic acid (0.412 g, 1.09 mmol). Reaction time: 23 hours. Eluent for flash chromatography: ethyl acetate/ *n*-hexane, 1:1. The product was obtained as a white solid (0.207 g, 65.9%); mp: 203–207 °C; 1H NMR (300 MHz, $CDCl_3$) δ 8.01 (s, 1H, NH), 7.83 – 7.76 (m, 1H, ArH), 7.63 – 7.54 (m, 2H, ArH), 7.54 – 7.45 (m, 3H, ArH), 7.38 – 7.30 (m, 1H, ArH), 7.21 (dt, $J = 4.4, 2.7$ Hz, 2H, ArH), 7.18 –



7.09 (m, 2H, ArH), 7.06 (ddd, $J = 9.8, 5.9, 2.6$ Hz, 2H, ArH), 4.72 (dq, $J = 8.8, 6.5$ Hz, 1H, $H-3$), 4.47 (dd, $J = 8.7, 7.5$ Hz, 1H, $H-2$), 3.98 (dd, $J = 8.8, 6.7$ Hz, 1H, $H-2$), 3.17 (ddd, $J = 14.8, 6.3, 0.9$ Hz, 1H, CH_2 -indole), 2.68 (dd, $J = 14.7, 9.0$ Hz, 1H, CH_2 -indole); ^{13}C NMR (75 MHz, $CDCl_3$) δ 174.69 ($C=O$), 164.72 (ArC), 147.19 (ArC), 136.26 (ArC), 134.89 (ArC), 133.52 (ArC), 131.06 (ArC), 130.34 (ArC), 127.88 (ArC), 127.77 (ArC), 127.58 (ArC), 124.56 (ArC), 123.47 (ArC), 122.30 (ArC), 122.24 (ArC), 119.64 (ArC), 118.85 (ArC), 116.00 (ArC), 115.71 (ArC), 111.84, 111.24 ($C-9b$), 76.40 ($C-2$), 55.88 ($C-3$). Anal. Calcd. ($C_{23}H_{19}FN_2O_2 \cdot 0.15H_2O$): C, 74.90%; H, 4.86%; N, 6.99%. Found C, 74.31%; H, 5.10%; N, 7.16%.

(3*S*,9*bR*)-3-((1*H*-indol-3-yl)methyl)-9*b*-(4-chlorophenyl)-2,3-dihydrooxazolo[2,3-*a*]isoindol-

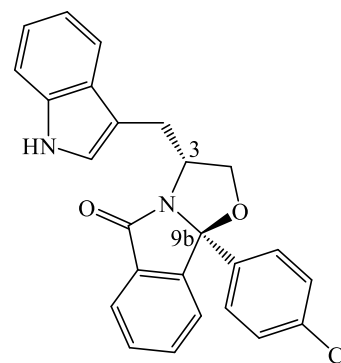
5(9*bH*)-one 47c: Following the general procedure, to a solution of (*S*)-tryptophanol **9** (0.113 g, 0.593 mmol) in toluene (5 mL). Reaction time: 16 hours. Eluent for flash chromatography: ethyl acetate/ *n*-hexane, 4:6. The product was obtained as a white solid (0.209 g, 85.0%). The 1H -NMR spectrum was found to be identical to the one of compound **47c'**.



(3*R*,9*bS*)-3-((1*H*-indol-3-yl)methyl)-9*b*-(4-chlorophenyl)-2,3-dihydrooxazolo[2,3-*a*]isoindol-

5(9*bH*)-one 47c': Following the general procedure, to a solution of (*R*)-tryptophanol **44** (0.0952 g, 0.500 mmol) in toluene (5 mL) was added 2-(4-chlorobenzoyl)benzoic acid (0.177 g, 0.681 mmol).

Reaction time: 15.5 hours. Eluent for flash chromatography: ethyl acetate/ *n*-hexane, 1:1. The product was obtained as a white crystalline solid (0.1452 g, 70%); mp: 84-86 °C; ¹H NMR (300 MHz, CDCl₃) δ 8.08 (s, 1H, *NH*), 7.84 – 7.77 (m, 1H, *ArH*), 7.56 – 7.51 (m, 3H, *ArH*), 7.51 – 7.46 (m, 2H, *ArH*), 7.38 – 7.30 (m, 3H, *ArH*), 7.23 – 7.16 (m,

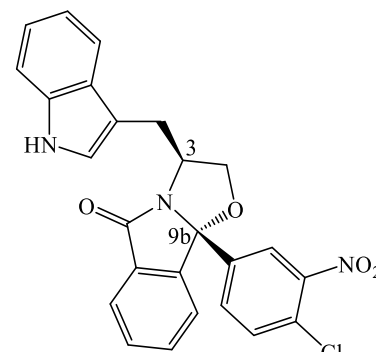


2H, *ArH*), 7.16 – 7.07 (m, 2H, *ArH*), 4.72 (dq, *J* = 8.7, 6.6 Hz, 1H, *H*-3), 4.47 (dd, *J* = 8.7, 7.5 Hz, 1H, *H*-2), 3.98 (dd, *J* = 8.8, 6.7 Hz, 1H, *H*-2), 3.22 – 3.10 (dd, *J* = 14.8, 5.7 Hz, 1H, *CH*₂-indole), 2.70 (dd, *J* = 14.8, 8.8 Hz, 1H, *CH*₂-indole); ¹³C NMR (75 MHz, CDCl₃) δ 174.70 (*C*=O), 146.92 (*ArC*), 137.67 (*ArC*), 136.23 (*ArC*), 134.71 (*ArC*), 133.55 (*ArC*), 131.01 (*ArC*), 130.41 (*ArC*), 129.08 (*ArC*), 127.49 (*ArC*), 127.35 (*ArC*), 124.54 (*ArC*), 123.46 (*ArC*), 122.31 (*ArC*), 122.21 (*ArC*), 119.55 (*ArC*), 118.79 (*ArC*), 111.57 (*ArC*), 111.27 (*ArC*), 100.66 (*C*-9*b*), 76.36 (*C*-2), 55.91 (*C*-3), 30.15 (*ArCH*₂); Anal. Calc. (C₂₅H₁₉ClN₂O₂•0.25CH₂Cl₂): C, 69.53%; H, 4.52%; N, 6.42%. Found C, 69.18%; H, 4.63%; N, 6.21%.

(3*S*,9*bR*)-3-((1*H*-indol-3-yl)methyl)-9*b*-(4-chloro-3-nitrophenyl)-2,3-dihydrooxazolo[2,3-*a*]isoindol-

5(9*bH*)-one 47d: Following the general procedure, to a solution of (*S*)-tryptophanol **9** (0.101 g, 0.526 mmol) in toluene (5 mL) was added 2-(4-chloro-3-nitrobenzoyl)benzoic acid (0.412 g, 1.35 mmol). Reaction

time: 19.5 hours. Eluent for flash chromatography: ethyl acetate/ *n*-hexane, 1:1. The product was obtained as a bright yellow solid (0.119 g, 49.1%); mp: 94-98 °C; ¹H NMR (300 MHz, CDCl₃) δ 7.99 (d, *J* = 2.1 Hz, 1H, *ArH*), 7.96 (s, 1H, *NH*), 7.85 – 7.80 (m, 1H, *ArH*), 7.52 (ddd, *J* = 7.8, 2.9, 1.9 Hz, 3H, *ArH*), 7.37 (dd, *J* = 8.4, 2.1 Hz, 1H, *ArH*),



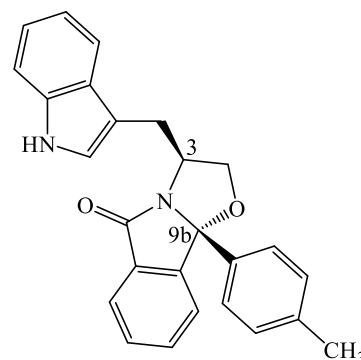
7.30 (t, *J* = 7.7 Hz, 2H, *ArH*), 7.22 – 7.02 (m, 4H, *ArH*), 4.72 (dt, *J* = 12.6, 7.4 Hz, 1H, *H*-3), 4.53 (dd, *J* = 8.8, 7.5 Hz, 1H, *H*-2), 4.09 (dd, *J* = 8.4, 6.6 Hz, 1H, *H*-2), 3.06 (dd, *J* = 14.9, 5.3 Hz, 1H, *CH*₂-indole), 2.89 (dd, *J* = 14.7, 8.0 Hz, 1H, *CH*₂-indole); ¹³C NMR (75 MHz, CDCl₃) δ 174.72 (*C*=O), 147.87 (*ArC*), 146.27 (*ArC*), 140.19 (*ArC*), 136.13 (*ArC*), 133.89 (*ArC*), 132.05 (*ArC*), 130.92 (*ArC*), 130.88 (*ArC*), 130.51 (*ArC*), 127.55 (*ArC*), 126.98 (*ArC*), 124.80 (*ArC*), 123.45 (*ArC*), 122.73 (*ArC*), 122.26 (*ArC*), 119.67 (*ArC*), 118.70 (*ArC*), 111.32 (*ArC*), 110.88 (*ArC*), 99.89 (*C*-9*b*), 75.98 (*C*-2), 56.62 (*C*-3), 29.36 (*ArCH*₂); Anal. Calc. (C₂₅H₁₈ClN₃O₄•0.5CH₂Cl₂): C, 60.96%; H, 3.82%; N, 8.37%. Found C, 61.32%; H, 3.89%; N, 8.09%.

(3*R*,9*bS*)-3-((1*H*-indol-3-yl)methyl)-9*b*-(*p*-tolyl)-2,3-dihydrooxazolo[2,3-*a*]isoindol-5(9*bH*)-one,

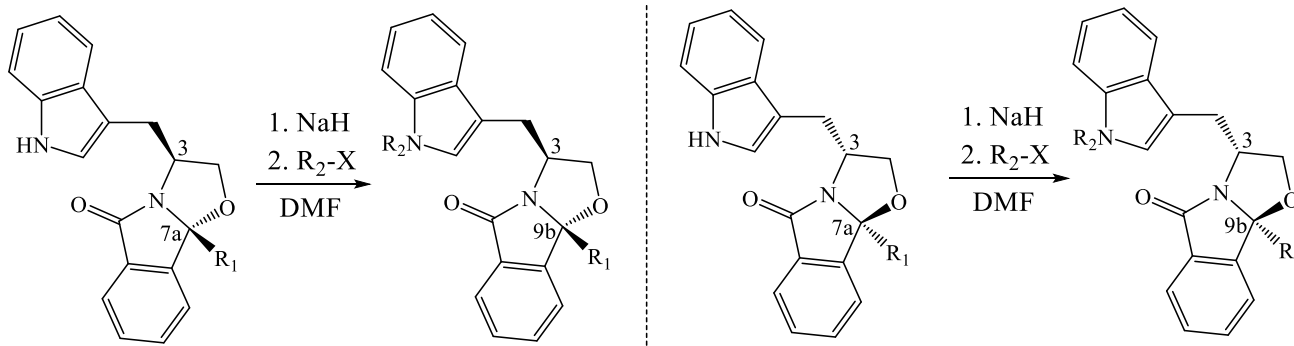
47e: Following the general procedure, to a solution of (*S*)-tryptophan **9** (0.177 g, 0.931 mmol) in toluene (7.5 mL) was added 2-(4-methylbenzoyl)benzoic acid (0.412 g, 1.09 mmol). Reaction time: 17 hours. Eluent for flash chromatography: ethyl acetate/ *n*-hexane, 6:4.

The product was obtained as a white solid (0.302 g, 82.1%); mp: 155-157 °C ¹H NMR (300 MHz, CDCl₃) δ 8.00 (s, 1H, *NH*), 7.81 – 7.77 (m, 1H, *ArH*), 7.52 (d, *J* = 8.1 Hz, 3H, *ArH*), 7.49 – 7.45 (m, 2H, *ArH*), 7.34 (d, *J* = 8.0 Hz, 1H, *ArH*), 7.25 – 7.22 (m, 1H, *ArH*), 7.20 (d, *J* = 7.8 Hz, 3H, *ArH*), 7.16 (d, *J* = 1.5 Hz, 1H, *ArH*), 7.14 – 7.07 (m, 1H, *ArH*), 4.70 (dq, *J* = 8.8, 6.6 Hz, 1H, *H*-3), 4.46 (dd, *J* = 8.7, 7.5 Hz, 1H, 3.99 (dd, *J* = 8.7, 6.7 Hz, 1H, *H*-2), 3.20 (dd, *J* = 14.7, 6.3 Hz, 1H, *CH*₂-indole),

2.67 (dd, *J* = 14.7, 8.9 Hz, 1H, *CH*₂-indole), 2.38 (s, 3H, *ArCH*₃); ¹³C NMR (75 MHz, CDCl₃) δ 174.62 (*C*=O), 147.29 (*ArC*), 138 (*ArC*), 136.12 (*ArC*), 135.78 (*ArC*), 133.27 (*ArC*), 131.05 (*ArC*), 130.02 (*ArC*), 129.50 (*ArC*), 127.45 (*ArC*), 125.73 (*ArC*), 124.32 (*ArC*), 123.38 (*ArC*), 122.09 (*ArC*), 119.43 (*ArC*), 118.82 (*ArC*), 111.99 (*ArC*), 111.08 (*ArC*), 101.01 (*C*9*b*), 76.36 (*CH*-2), 55.62 (*CH*-3), 30.20 (*CH*₂-indole), 21.24 (*ArCH*₃).



4.3.2. General procedure for *N*-methylation and *N*-ethylation



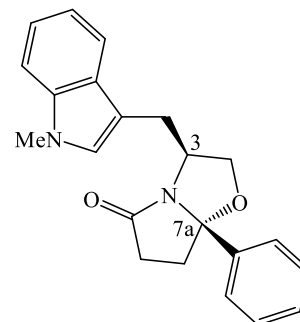
Scheme 4.4. (*S*) and (*R*)-tryptophan-derived bicyclic lactams protected on the indole moiety.

To a stirred solution of the appropriate (*S*)- or (*R*)- oxazoloisoindolinone derivative (0.320 mmol, 1 equivalent) in dry dimethylformamide, DMF (3 mL) under inert atmosphere of nitrogen and ice bath was added sodium hydride, NaH (2 equivalent, 95% anhydrous reagent). The mixture was allowed to stir for 30 minutes and then methyl iodide (2 equivalents) was added. The reaction was kept stirring at room temperature for 30 minutes. After this period, ethyl acetate was added to the crude of reaction and then extracted with room temperature deionized water. The organic phase was washed firstly with an aqueous saturated solution of sodium monohydrogen carbonate, NaHCO₃ and then with brine solution

(saturated aqueous solution of sodium chloride, NaCl); dried with sodium sulphate, NaSO₄ and in the end the solvent was evaporated. The crude was absorbed in silica, purified by flash chromatography using ethyl acetate/n-hexane as eluent mixture and recrystallized.

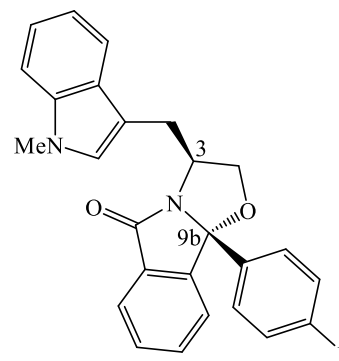
(3*S*,7*aS*)-3-((1-methyl-1*H*-indol-3-yl)methyl)-7*a*-phenyltetrahydropyrrolo[2,1-*b*]oxazol-5(6*H*)-one 48a:

Following the general procedure, starting from compound **47a** (0.0692 g, 0.208 mmol), sodium hydride, NaH 95%, (0.010 g, 0.416 mmol) and methyl iodide (0.026 mL, 0.416 mmol, $d = 2.28 \text{ g mL}^{-1}$) were added. Reaction time: 1.5 hours. Eluent for flash chromatography: 1:1, *n*-hexane/ ethyl acetate. Recrystallization with the same combination of solvents. The product was obtained as a white light solid (0.0605 g, 83.9%). ¹H NMR (300 MHz, CDCl₃) δ 7.52 – 7.48 (m, 2H, Ar*H*), 7.43 – 7.35 (m, 4H, Ar*H*), 7.25 (d, $J = 6.2 \text{ Hz}$, 2H, Ar*H*), 7.22 – 7.16 (m, 1H, Ar*H*), 7.06 (ddd, $J = 7.9, 6.7, 1.3 \text{ Hz}$, 1H, Ar*H*), 6.89 (s, 1H, CH-indole), 4.54 (ddd, $J = 13.1, 9.5, 7.0 \text{ Hz}$, 1H, *H*-3), 4.15 (dd, $J = 8.8, 7.5 \text{ Hz}$, 1H, *H*-2), 3.70 (s, 3H, NCH₃), 3.60 (dd, $J = 8.8, 6.9 \text{ Hz}$, 1H, *H*-2), 3.09 (dd, $J = 14.5, 5.8 \text{ Hz}$, 1H, CH₂-indole), 2.93 – 2.80 (m, 1H, *H*-6), 2.63 (dd, $J = 14.0, 9 \text{ Hz}$, 1H, CH₂-indole), 2.57 – 2.41 (m, 2H, *H*-6 and *H*-7), 2.28 – 2.19 ppm (m, 1H, *H*-7).



(3*S*,9*bR*)-9*b*-((4-fluorophenyl)-3-((1-methyl-1*H*-indol-3-yl)methyl)-2,3-dihydrooxazolo[2,3-*a*]isoindol-5(9*bH*)-one 48b:

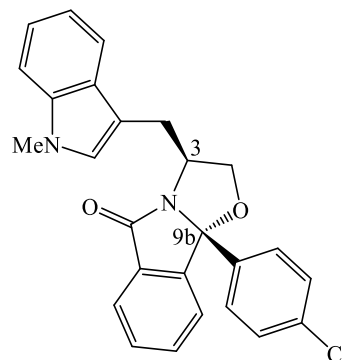
Following the general procedure, starting from compound **47b** (0.104g, 0.338 mmol), sodium hydride, NaH 95%, (0.0126 g, 0.523 mmol) and methyl iodide (0.033 mL, 0.523 mmol, $d = 2.28 \text{ g mL}^{-1}$) were added. Reaction time: 20 minutes. Eluent for flash chromatography 6:4, *n*-hexane/ ethyl acetate. Recrystallization with the same combination of solvents. The product appears as a white light solid (0.101 g, 93.9%); ¹H NMR (300 MHz, CDCl₃) δ 7.83 – 7.77 (m, 1H, Ar*H*), 7.59 – 7.52 (m, 2H, Ar*H*), 7.51 – 7.46 (m, 3H, Ar*H*), 7.24 (d, $J = 1.0 \text{ Hz}$, 1H, Ar*H*), 7.21 (dd, $J = 1.7, 0.9 \text{ Hz}$, 1H, Ar*H*), 7.19 (dd, $J = 3.4, 1.8 \text{ Hz}$, 1H, Ar*H*), 7.12 – 7.06 (m, 2H, Ar*H*), 7.03 (d, $J = 8.7 \text{ Hz}$, 2H, Ar*H*), 6.95 (s, 1H, CH-indole), 4.68 (ddd, $J = 13.1, 10.9, 6.3 \text{ Hz}$, 1H, *H*-3), 4.45 (dd, $J = 8.7, 7.5 \text{ Hz}$, 1H, *H*-2), 3.98 (dd, $J = 8.8, 6.8 \text{ Hz}$, 1H, *H*-2), 3.72 (s, 3H, NCH₃), 3.17 (dd, $J = 14.5, 5.9 \text{ Hz}$, 1H, CH₂-indole), 2.67 (dd, $J = 14.6, 9.2 \text{ Hz}$, 1H, CH₂-indole).



(3*S*,9*bR*)-9*b*-((4-chlorophenyl)-3-((1-methyl-1*H*-indol-3-yl)methyl)-2,3-dihydrooxazolo[2,3-*a*]isoindol-5(9*bH*)-one, 48c:

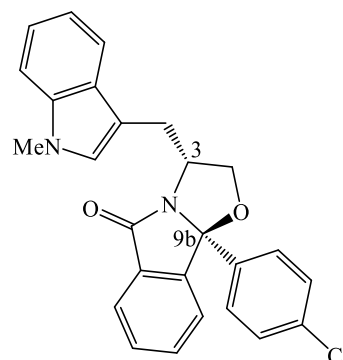
Following the general procedure, starting from compound **47c** (0.140g,

0.338 mmol), sodium hydride, NaH, 95% anhydrous reagent (0.0162 g, 0.676 mmol) and methyl iodide (0.042 mL, 0.677 mmol, $d = 2.28 \text{ g mL}^{-1}$) were added. Reaction time: 30 minutes. Eluent for flash chromatography 7:3, n-hexane/ ethyl acetate Recrystallization with the same mixture of solvents. The product was obtained as a white cry--stalline light solid (0.127 g, 87.6%). The $^1\text{H-NMR}$ spectrum was found to be similar to the one for **48c'**.



(3R,9bS)-9b-((4-chlorophenyl)-3-((1-methyl-1H-indol-3-yl)methyl)-2,3-dihydrooxazolo[2,3-a]isoindol-5(9bH)-one 48c': Following the general procedure,

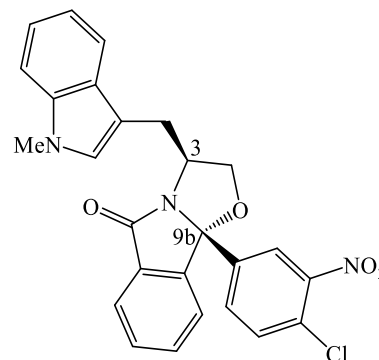
starting from compound **47c'** (0.129 g, 0.310 mmol), sodium hydride, NaH 95%, (0.0149 g, 0.621 mmol) and methyl iodide (0.0193 mL, 0.310 mmol, $d = 2.28 \text{ g mL}^{-1}$) were added. Reaction time: 30 minutes. Eluent for flash chromatography: 7:3, n-hexane/ ethyl acetate and recrystallization using the same combination of solvents a white crystalline light solid (0.117 g, 87.5%); mp: 70-73 °C; $^1\text{HNMR}$ (300 MHz, CDCl_3) δ 7.80 – 7.76 (m, 1H, ArH), 7.49 – 7.43 (m, 4H, ArH), 7.31 – 7.26 (m, 2H, ArH), 7.23 (dd, $J = 1.8, 1.0 \text{ Hz}$, 2H, ArH), 7.20 (dd, $J = 6.6, 1.1 \text{ Hz}$, 1H, ArH), 7.17 – 7.12 (m, 1H, ArH), 7.07 (ddd, $J = 8.0, 6.6, 1.4 \text{ Hz}$, 1H, ArH), 6.90 (s, 1H, CH-indole), 4.70 – 4.60 (m, 1H, H-3), 4.43 (dd, $J = 8.7, 7.5 \text{ Hz}$, 1H, H-2), 3.96 (dd, $J = 8.8, 6.8 \text{ Hz}$, 1H, H-2), 3.68 (s, 3H, NCH_3), 3.13 (dd, $J = 14.7, 5.7 \text{ Hz}$, 1H, CH_2 -indole), 2.68 (dd, $J = 14.7, 8.9 \text{ Hz}$, 1H, CH_2 -indole); $^{13}\text{C NMR}$ (75 MHz, CDCl_3) δ 174.60 (C=O), 146.89 (ArC), 137.62 (ArC), 136.87 (ArC), 134.50 (ArC), 133.39 (ArC), 130.99 (ArC), 130.28 (ArC), 128.90 (ArC), 127.93 (ArC), 127.24 (ArC), 126.98 (CH-indole), 124.47 (ArC), 123.34 (ArC), 121.70 (ArC), 118.97 (ArC), 118.89 (ArC), 109.87 (ArC), 109.16 (ArC), 100.56 (C-9b), 76.16 (CH-2), 56.00 (CH-3), 44.52, 32.64 (NCH_3), 29.82 (CH_2 -indole).



(3S,9bR)-9b-((4-chloro-3-nitrophenyl)-3-((1-methyl-1H-indol-3-yl)methyl)-2,3-dihydrooxazolo[2,3-a]isoindol-5(9bH)-one 48d: Following the general procedure, starting from

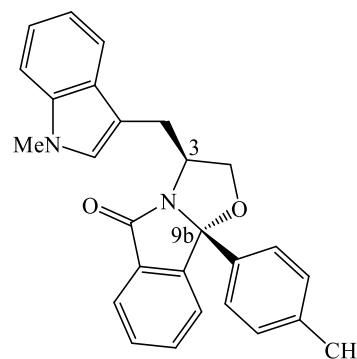
compound **47d** (0.0762 g, 0.166 mmol), sodium hydride, NaH, 95% anhydrous reagent (0.0080 g, 0.332 mmol) and methyl iodide (0.042 mL, 0.663 mmol, $d = 2.28 \text{ g mL}^{-1}$) were added. Reaction time: 1 hour. Eluent for flash chromatography 7:3, n-hexane/ ethyl acetate and recrystallization with the same mixture of solvents a light crystalline yellow solid (0.0548 g, 69.8%). $^1\text{H NMR}$ (300 MHz, CDCl_3) δ 8.01 (dd, $J = 10.7, 2.0 \text{ Hz}$, 1H, ArH), 7.83 (dd, $J = 5.0, 3.8 \text{ Hz}$, 1H, ArH), 7.55-7.48 (m, 3H, ArH), 7.37 (dd, $J =$

$J = 8.4, 2.1$ Hz, 1H, ArH), 7.30 (t, $J = 5.2$ Hz, 1H, ArH), 7.24 – 7.16 (m, 2H, ArH), 7.16 – 7.03 (m, 3H, ArH), 6.84 (s, 1H, CH-indole), 4.70 (td, $J = 15.1, 7.2$ Hz, 1H, H-3), 4.53 (dd, $J = 8.8, 7.5$ Hz, 1H, H-2), 4.10 (dd, $J = 14.0, 7.9$ Hz, 1H, H-2), 3.67 (s, 3H, NCH₃), 3.06 (ddd, $J = 14.9, 7.8$ Hz, 1H, CH₂-indole), 2.88 (dd, $J = 14.8, 8.0$ Hz, 1H, CH₂-indole).



3*R*,9*bS*)-3-((1-methyl-1*H*-indol-3-yl)methyl)-9*b*-(*p*-tolyl)-2,3-dihydrooxazolo[2,3-*a*]isoindol-

5(9*bH*)-one 48e: Following the general procedure, starting from compound **47e** (0.150 g, 0.379 mmol), sodium hydride, NaH 95%, (0.0182 g, 0.759 mmol) and methyl iodide (0.047 mL, 0.759 mmol, $d = 2.28$ g mL⁻¹) were added. Reaction time: 30 minutes. Eluent for flash chromatography 6:4, *n*-hexane/ ethyl acetate and recrystallization with the same combination of solvents a white light solid (0.129 g, 83.5%); mp: 150 - 151 °C; ¹H NMR (300 MHz, CDCl₃) δ 7.82 – 7.77 (m, 1H, ArH), 7.51 (d, $J = 8.1$ Hz, 3H, ArH),

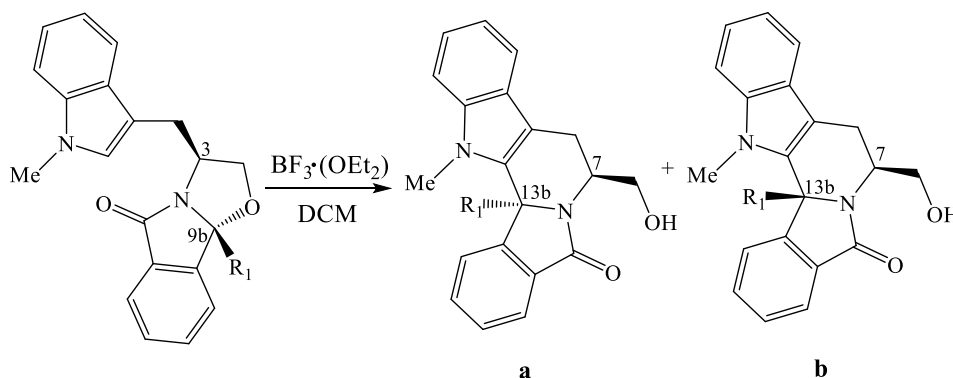


7.49 – 7.45 (m, 2H, ArH), 7.29 – 7.16 (m, 6H, ArH), 7.09 (ddd, $J = 8.0, 6.8, 1.3$ Hz, 1H, ArH), 6.97 (s, 1H, CH-indole), 4.67 (dq, $J = 9.2, 6.8$ Hz, 1H, H-3), 4.45 (dd, $J = 8.7, 7.5$ Hz, 1H, H-2), 3.99 (dd, $J = 8.7, 6.8$ Hz, 1H, H-2), 3.73 (s, 3H, NCH₃), 3.22 (dd, $J = 14.6, 6.0$ Hz, 1H, CH₂-indole), 2.66 (dd, $J = 14.7, 9.2$ Hz, 1H, CH₂-indole), 2.39 (s, 3H, ArCH₃); ¹³C NMR (75 MHz, CDCl₃) δ 174.62 (C=O), 147.34 (ArC), 138.45 (ArC), 136.88 (ArC), 135.82 (ArC), 133.24 (ArC), 131.09 (ArC), 129.99 (ArC), 129.46 (ArC), 127.90 (ArC), 126.91 (CH-indole), 125.73 (ArC), 124.31 (ArC), 123.37 (ArC), 121.63 (ArC), 118.94 (ArC), 118.87 (ArC), 110.28 (ArC), 109.13 (ArC), 100.99 (C-9*b*), 76.32 (CH-2), 55.78 (CH-3), 32.65 (NCH₃), 30.09 (CH₂-indole), 21.23 (ArCH₃).

4.3.3. General procedure for cyclization reactions

In inert atmosphere of Nitrogen and in stirring conditions the adequate oxazoloisoindolinone derivative (0.290 mmol, 1 equivalents) was added to a stoichiometric quantity of dry dichloromethane (5 mL each 0.14 mmol of compound to cyclize). The so formed solution is kept at room temperature and pure boron trifluoride diethyl etherate, 98+% (4 equivalents) is added to the mixture of reaction in order to afford the cyclized final product. The solvent of reaction was evaporated in rotavapor and the crude of reaction is dissolved in ethyl acetate. The organic phase was washed with brine solution (saturated aqueous solution of sodium chloride, NaCl); dried with sodium sulphate, Na₂SO₄ drying solid reagent, filtered

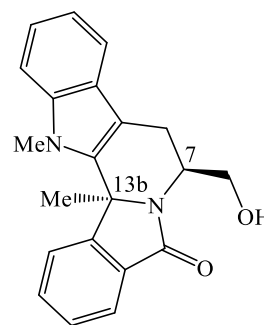
and in the end evaporated in rotavapor once again. The crude was absorbed in silica and purified by flash chromatography using ethyl acetate/ *n*-hexane as eluent mixture, followed by recrystallization.



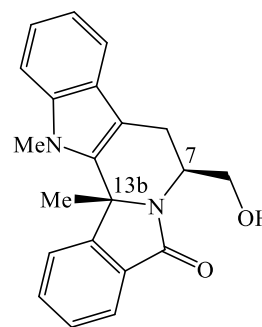
Scheme 4.5. (*S*)-tryptophan-derived bicyclic lactams and their cyclized products.

(7*S*,13*bS*)-7-(hydroxymethyl)-13,13*b*-dimethyl-7,8,13,13*b*-tetrahydro-5*H*-benzo[1,2indoli-zino[8,7-*b*]indol-5-one 50a) and (7*S*,13*bR*)-7-(hydroxymethyl)-13,13*b*-dimethyl-7,8,13,13*b*-tetrahydro-5*H*-benzo[1,2indoli-zino[8,7-*b*]indol-5-one 49b: Following the general procedure, to a solution of **38** (0.0962 g, 0.289 mmol) in pure dichloromethane (10 mL) was added $\text{BF}_3 \cdot \text{OEt}_2$ (145.40 μL , 1.16 mmol). Reaction time: 1 hour and 20 minutes. On the crude of reaction was performed the work up reported above and then, after drying it has been isolated compounds, purified by flash chromatography (ethyl acetate/ *n*-hexane, 1:1).

49a: Obtained as a white solid (0.037 g, 40%); mp: 224-228 °C; $[\alpha]_{\text{D}}^{20} = -83.2^\circ$ ($c=0.33$, MeOH); ^1H NMR (300 MHz, $\text{DMSO-}d_6$) δ 8.27 (d, $J = 7.8$ Hz, 1H, Ar*H*), 7.73 (t, $J = 7.6$ Hz, 1H, Ar*H*), 7.69 (d, $J = 7.7$ Hz, 1H, Ar*H*), 7.55 (td, $J = 7.6, 0.5$ Hz, 1H, Ar*H*), 7.43 (t, $J = 7.3$ Hz, 2H, Ar*H*), 7.18 – 7.12 (m, 1H, Ar*H*), 7.05 – 6.99 (m, 1H, Ar*H*), 5.18 (t, $J = 6.0$ Hz, 1H, OH), 4.39 – 4.24 (m, 2H, $\text{CH}_2\text{-OH}$), 4.02 (s, 3H, NCH_3), 3.81 (td, $J = 10.5, 5.1$ Hz, 1H, *H*-7), 2.99 – 2.83 (m, 2H, $\text{CH}_2\text{-indole}$), 2.02 (s, 3H, C13*b*- CH_3); ^{13}C NMR (75 MHz, $\text{DMSO-}d_6$) δ 168.5 (C=O), 148.1 (Cq), 138.8 (Cq), 137.7 (Cq), 134.4 (Cq), 132.4 (Cq), 129.4 (ArC), 129.0 (ArC), 128.1 (ArC), 125.5 (Cq), 125.5 (ArC), 123.4 (ArC), 122.4 (ArC), 119.5 (ArC), 118.7 (ArC), 111.3 (Cq), 109.9 (ArC), 71.8 (C-13*b*), 61.8 ($\text{CH}_2\text{-OH}$), 54.5 (CH-7), 33.6 (N-CH_3), 24.7 ppm ($\text{CH}_2\text{-indole}$), 21.15 ppm (C-13*b* CH_3).

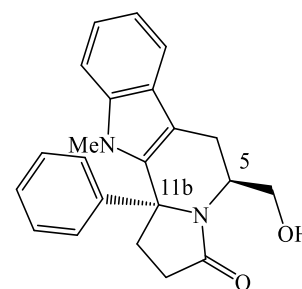


49b: Obtained as a white solid (0.026 g, 28%); mp: 254-258 °C; $[\alpha]_D^{20} = +155.5^\circ$ ($c = 0.27$, MeOH); $^1\text{H NMR}$ (300 MHz, DMSO- d_6) δ 8.24 (d, $J = 8.3$ Hz, 1H, ArH), 7.73 (t, $J = 7.8$ Hz, 2H, ArH), 7.55 (t, $J = 7.4$ Hz, 1H, ArH), 7.45 (t, $J = 7.6$ Hz, 2H, ArH), 7.17 (t, $J = 7.9$ Hz, 1H, ArH), 7.03 (t, $J = 7.5$ Hz, 1H, ArH), 5.05 (t, $J = 5.5$ Hz, 1H, OH), 4.97 (dd, $J = 14.3, 7.4$ Hz, 1H, CH₂-OH), 4.12 (s, 3H, NCH₃), 3.63 (dd, $J = 7.2, 5.8$ Hz, 2H, H-7 and CH₂-OH), 2.98 (d, $J = 15.8$ Hz, 1H, CH₂-indole), 2.78 (dd, $J = 15.7, 6.8$ Hz, 1H, CH₂-indole), 1.99 ppm (s, 3H, C13b-CH₃); $^{13}\text{C NMR}$ (75 MHz, DMSO- d_6) δ 168.1 (C=O), 149.0 (Cq), 140.7 (Cq), 137.8 (Cq), 132.9 (ArC), 131.8 (Cq), 131.1 (Cq), 129.3 (ArC), 128.6 (ArC), 126.1 (Cq), 125.3 (ArC), 123.5 (ArC), 122.6 (ArC), 118.7 (ArC), 110.0 (ArC), 108.4 (Cq), 68.9 (C-13b), 61.0 (CH₂-OH), 50.2 (CH-7), 34.4 (N-CH₃), 22.2 (CH₂-indole), 21.10 ppm (C-13bCH₃).



(5*S*,11*bR*)-5-(hydroxymethyl)-11-methyl-11*b*-phenyl-1,2,5,6,11,11*b*-hexahydro-3*H*-indolizino[8,7-*b*]indol-3-one 50a and (5*S*,11*bS*)-5-(hydroxymethyl)-11-methyl-11*b*-phenyl-1,2,5,6,11,11*b*-hexahydro-3*H*-indolizino[8,7-*b*]indol-3-one 50b: Following the general procedure, to a solution of **48a** (0.0605 g, 0.376 mmol) in pure dichloromethane (13.5 mL) was added BF₃·OEt₂ (189.11 μ L, 1.51 mmol). The reagents have been kept reacting for 2 hours and 15 minutes. On the crude of reaction was performed the work up reported above and then the compound was purified by flash chromatography in first attempt (ethyl acetate/n-hexane, 1:1) and then in second solution by preparative chromatography (ethyl acetate/n-hexane, 1:2).

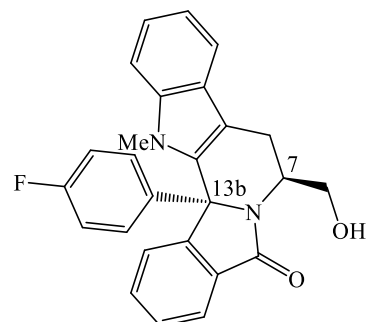
50a: Obtained as a white solid (0.084 g, 64.7%); mp: 261-263 °C; $[\alpha]_D^{20} = -37.1^\circ$ ($c = 0.49$, MeOH); $^1\text{H NMR}$ (300 MHz, DMSO- d_6) δ 7.49 (dd, $J = 10.5, 8.2$ Hz, 2H, ArH), 7.42 – 7.33 (m, 3H, ArH), 7.21 (d, $J = 7.2$ Hz, 1H, ArH), 7.16 (d, $J = 7.6$ Hz, 2H, ArH), 7.08 (t, $J = 7.4$ Hz, 1H, ArH), 4.86 (t, $J = 6.3$ Hz, 1H, OH), 3.96 (dt, $J = 11.5, 5.8$ Hz, 1H, H-5), 3.90 – 3.81 (m, 1H, CH₂-OH), 3.54 (s, 3H, NCH₃), 3.09 (dt, $J = 11.5, 6.0$ Hz, 1H, CH₂-OH), 2.99 (dd, $J = 12.8, 5.0$ Hz, 1H, CH₂-indole), 2.94 – 2.85 (m, 1H, CH₂-indole), 2.85 – 2.79 (m, 2H, CH₂), 2.79 – 2.67 (m, 1H, CH₂), 2.46 – 2.39 (m, 1H, CH₂).



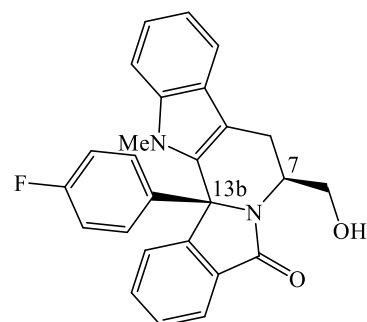
(7*S*,13*bS*)-13*b*-(4-fluorophenyl)-7-(hydroxymethyl)-13-methyl-7,8,13,13*b*-tetrahydro-5*H*-benzo[1,2]indolizino[8,7-*b*]indol-5-one 51a and (7*S*,13*bS*)-13*b*-(4-fluorophenyl)-7-(hydroxymethyl)-13-methyl-7,8,13,13*b*-tetrahydro-5*H*-benzo[1,2]indolizino[8,7-*b*]indol-5-one 51b: Following the general procedure, to a solution of **48b** (0.1012 g, 0.245 mmol) in pure dichloromethane (8.80 mL) was

added $\text{BF}_3 \cdot \text{OEt}_2$ (123.3 μL , 0.981 mmol). Reaction time: 15 minutes. Eluent for flash chromatography: ethyl acetate/*n*-hexane, 4:6.

51a: Obtained as a white solid (0.0517 g, 51.1 %); mp: 247-250 °C; $[\alpha]_D^{20} = -43.5^\circ$ ($c = 0.35$, MeOH); ^1H NMR (300 MHz, $\text{DMSO-}d_6$) δ 7.90 (d, $J = 7.8$ Hz, 1H), 7.79 (d, $J = 7.9$ Hz, 1H, ArH), 7.72 (td, $J = 7.5$, 1.3 Hz, 1H, ArH), 7.62 (td, $J = 7.3$, 0.5 Hz, 1H, ArH), 7.54 (d, $J = 7.7$ Hz, 1H, ArH), 7.45 (d, $J = 8.3$ Hz, 1H, ArH), 7.21 (t, $J = 8.6$ Hz, 3H, ArH), 7.09 (t, $J = 7.1$ Hz, 1H, ArH), 6.92 (dd, $J = 8.8$, 5.3 Hz, 2H, ArH), 4.97 (t, $J = 6.0$ Hz, 1H, OH), 4.26 (dt, $J = 12.4$, 6.3 Hz, 1H, $\text{CH}_2\text{-OH}$), 4.09 – 4.01 (m, 1H, $\text{CH}_2\text{-OH}$), 3.73 (s, 3H, NCH_3), 3.41 (m, 1H, H-7) 3.00 (qd, $J = 15.4$, 7.7 Hz, 2H, $\text{CH}_2\text{-indole}$); ^{13}C NMR (75 MHz, $\text{DMSO-}d_6$) δ 168.42 (C=O), 147.89 (Cq), 137.63 (Cq), 135.04 (Cq), 134.26 (Cq), 132.62 (ArC), 132.26 (ArC), 130.43 (Cq), 130.32 (ArC), 129.43 (ArC), 125.38 (ArC), 123.40 (ArC), 122.41 (ArC), 119.51 (ArC), 118.65 (ArC), 117.41 (ArC), 115.92 (ArC), 115.63 (ArC), 111.3 (Cq) 109.91 (ArC), 71.13 (C-13b), 61.70 ($\text{CH}_2\text{-OH}$), 54.43 (CH-7), 33.47 (N- CH_3), 24.57 ($\text{CH}_2\text{-indole}$).



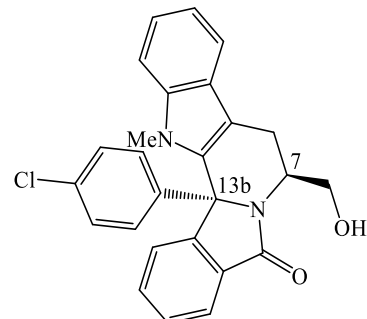
51b: Obtained as a white solid (0.0255 g, 25.2 %); mp: 259-261 °C; $[\alpha]_D^{20} = +41.7^\circ$ ($c = 0.35$, MeOH); ^1H NMR (300 MHz, $\text{DMSO-}d_6$) δ 7.85 (d, $J = 5.8$ Hz, 2H), 7.65 (dt, $J = 14.0$, 7.3 Hz, 2H, ArH), 7.53 (t, $J = 8.0$ Hz, 2H, ArH), 7.29 – 7.21 (m, 1H, ArH), 7.12 (dd, $J = 17.6$, 8.4 Hz, 3H, ArH), 6.92 – 6.82 (m, 2H, ArH), 4.88 (ddd, $J = 10.6$, 6.1, 4.5 Hz, 1H, H-7), 4.75 (dd, $J = 6.3$, 4.3 Hz, 1H, OH), 3.90 (s, 3H, NCH_3), 3.15 – 3.01 (m, 2H, $\text{CH}_2\text{-indole}$ and $\text{CH}_2\text{-OH}$), 2.92 (dd, $J = 15.1$, 6.9 Hz, 1H, $\text{CH}_2\text{-indole}$), 2.68 (ddd, $J = 12.9$, 7.3, 5.7 Hz, 1H, H-2); ^{13}C NMR (75 MHz, $\text{DMSO-}d_6$) δ 168.48 (C=O), 149.26 (Cq), 138.21 (Cq), 135.04 (Cq), 133.41 (ArC), 132.09 (Cq), 131.41 (Cq), 130.71 (Cq), 130.60 (ArC), 129.85 (ArC), 126.51 (ArC), 125.75 (ArC), 123.96 (ArC), 123.05 (ArC), 119.90 (ArC), 119.19 (ArC), 116.04 (ArC), 115.76 (ArC), 110.44 (ArC), 108.89 (Cq), 68.78 (C-13b), 61.45 ($\text{CH}_2\text{-OH}$), 50.59 (CH-7), 34.71 (N- CH_3), 22.57 ($\text{CH}_2\text{-indole}$).



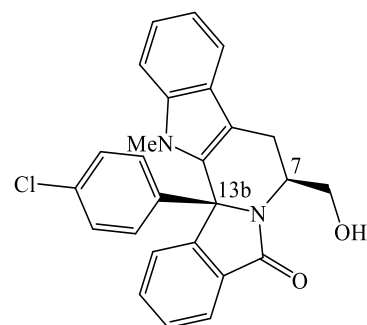
(7S,13bS)-13b-(4-chlorophenyl)-7-(hydroxymethyl)-13-methyl-7,8,13,13b-hexahydro-5H-benzo[1,2]indolizino[8,7-b]indol-5-one **52a** and **(7S,13bR)-13b-(4-chlorophenyl)-7-(hydroxymethyl)-13-methyl-7,8,13,13b-tetrahydro-5H-benzo[1,2]indolizino[8,7-b]indol-5-one**, **52b:** Following the general procedure, to a solution of **48c** (0.1102 g, 0.256 mmol) in pure

dichloromethane (12.2 mL) was added $\text{BF}_3 \cdot \text{OEt}_2$ (129 μL , 1.03 mmol). Reaction time: 15 minutes. Eluent for flash chromatography in first attempt (ethyl acetate/ *n*-hexane, 3:7).

52a: Obtained as a white solid (0.0654 g, 59.5 %); $[\alpha]_{\text{D}}^{20} = -58.5^\circ$ ($c = 0.41$, MeOH); $^1\text{H NMR}$ (300 MHz, $\text{DMSO-}d_6$) δ 7.92 (d, $J = 7.8$ Hz, 1H, ArH), 7.79 (d, $J = 7.6$ Hz, 1H, ArH), 7.72 (td, $J = 7.6$, 1.3 Hz, 1H, ArH), 7.63 (t, $J = 7.6$ Hz, 1H, ArH), 7.54 (d, $J = 7.5$ Hz, 1H, ArH), 7.45 (d, $J = 8.6$ Hz, 3H, ArH), 7.25 – 7.18 (m, 1H, ArH), 7.12 – 7.05 (m, 1H, ArH), 6.90 (d, $J = 8.6$ Hz, 2H, ArH), 4.96 (t, $J = 6.0$ Hz, 1H, OH), 4.30 – 4.20 (m, 1H, H-2), 4.11 – 4.00 (m, 1H, H-2), 3.73 (s, 3H, NCH_3), 3.22 (ddd, $J = 12.1$, 8.2, 2.6 Hz, 1H, H-7), 3.00 (qd, $J = 15.3$, 7.4 Hz, 2H, CH_2 -indole). As reported, the $^1\text{H-NMR}$ spectrum is found to be equal to the one of compound **52a**'.



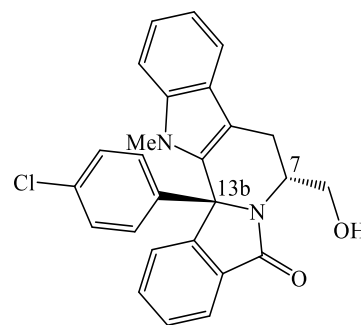
52b: Obtained as a white solid (0.0312 g, 28.4 %); $[\alpha]_{\text{D}}^{20} = +40.0^\circ$ ($c = 0.48$, MeOH); $^1\text{H NMR}$ (300 MHz, $\text{DMSO-}d_6$) δ 7.87 (d, $J = 4.2$ Hz, 1H, ArH), 7.86 – 7.83 (m, 1H, ArH), 7.69 (td, $J = 7.6$, 1.4 Hz, 1H, ArH), 7.65 – 7.59 (m, 1H, ArH), 7.53 (t, $J = 7.9$ Hz, 2H, ArH), 7.37 (d, $J = 8.8$ Hz, 2H, ArH), 7.28 – 7.21 (m, 1H, ArH), 7.13 – 7.06 (m, 1H, ArH), 6.86 (d, $J = 8.2$ Hz, 2H, ArH), 4.88 (ddd, $J = 10.6$, 6.1, 4.5 Hz, 1H, H-7), 4.76 (dd, $J = 6.3$, 4.3 Hz, 1H, OH), 3.89 (s, 3H, NCH_3), 3.14 – 3.01 (m, 2H, CH_2 -indole and H-2), 2.92 (dd, $J = 16.1$, 6.9 Hz, 1H, CH_2 -indole), 2.72 – 2.63 (m, 1H, CH_2 -OH); $^{13}\text{C NMR}$ (75 MHz, $\text{DMSO-}d_6$) δ 168.53 (C=O), 149.06 (Cq), 142.50 (Cq), 140.21 (Cq), 138.22 (ArC), 133.65 (Cq), 133.45 (ArC), 131.80 (Cq), 131.39 (Cq), 130.32 (ArC), 129.07 (ArC), 126.49 (Cq), 125.77 (ArC), 124.00 (ArC), 119.91 (ArC), 119.20 (ArC), 111.86 (ArC), 110.47 (ArC), 108.94 (Cq), 68.75 (C-13b), 61.45 (CH_2 -OH), 50.61 (CH-7), 34.72 (NCH_3), 22.55 (CH_2 -indole).



(7R,13bS)-13b-(4-chlorophenyl)-7-(hydroxymethyl)-13-methyl-7,8,13,13b-tetrahydro-5H-benzo[1,2]indolizino[8,7-b]indol-5-one 52a' and **(7R,13bR)-13b-(4-chlorophenyl)-7-(hydroxymethyl)-13-methyl-7,8,13,13b-tetrahydro-5H-benzo[1,2]indolizino[8,7-b]indol-5-one 52b'**: Following the general procedure, to a solution of **48c'** (0.0903 g, 0.211 mmol) in pure dichloromethane (9.20 mL) was added $\text{BF}_3 \cdot \text{OEt}_2$ (105.8 μL , 0.842 mmol). Reaction time: 15 minutes. Eluent for flash chromatography (ethyl acetate/*n*-hexane, 1:1).

52a': Obtained as a white solid (0.0433 g, 46.0%); mp: 246-248 °C; $[\alpha]_D^{20} = -52.1^\circ$ (c = 0.37, MeOH);

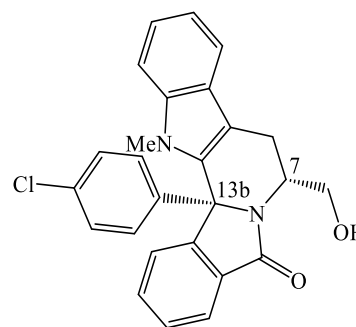
^1H NMR (300 MHz, DMSO- d_6) δ 7.91 (d, $J = 7.7$ Hz, 1H, ArH), 7.79 (d, $J = 7.4$ Hz, 1H, ArH), 7.72 (td, $J = 7.6, 1.3$ Hz, 1H, ArH), 7.62 (t, $J = 7.0$ Hz, 1H, ArH), 7.54 (d, $J = 7.7$ Hz, 1H, ArH), 7.45 (d, $J = 8.6$ Hz, 3H, ArH), 7.24 – 7.18 (m, 1H, ArH), 7.12 – 7.05 (m, 1H, ArH), 6.90 (d, $J = 8.6$ Hz, 2H, ArH), 4.96 (t, $J = 6.0$ Hz, 1H, OH), 4.26 (dt, $J = 12.6, 6.3$ Hz, 1H, H-2), 4.11 – 4.02 (m, 1H, H-2), 3.73 (s, 1H, NCH₃), 3.31 – 3.26 (m, 1H, H-7), 3.00 (qd, $J = 15.4,$



7.7 Hz, 2H, CH₂-indole); ^{13}C NMR (75 MHz, DMSO- d_6) δ 168.92 s(C=O), 148.16 (Cq), 138.33 (Cq), 138.12 (Cq), 134.46 (Cq), 134.18 (ArC), 133.13 (Cq), 132.75 (ArC), 130.49 (Cq), 129.97 (Cq), 129.42 (Cq), 125.92 (Cq), 125.86 (ArC), 123.90 (ArC), 122.92 (ArC), 119.99 (ArC), 119.13 (ArC), 111.87 (Cq), 110.41 (ArC), 71.58 (C-13b), 62.17 (CH₂-OH), 55.04 (CH-7), 33.96 (NCH₃), 25.02 (CH₂-indole).

52b': Obtained as a white solid (0.0395 g, 43.7%); mp: 282-285 °C; $[\alpha]_D^{20} = -37.5^\circ$ (c = 0.48, MeOH)

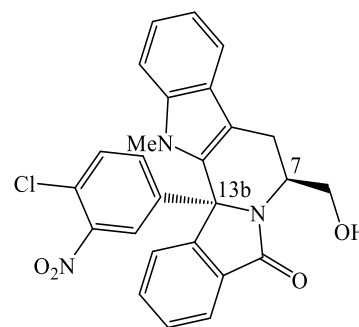
^1H NMR (300 MHz, DMSO- d_6) δ 7.89 – 7.83 (m, 2H, ArH), 7.69 (td, $J = 7.5, 1.5$ Hz, 1H, ArH), 7.62 (td, $J = 7.3, 0.8$ Hz, 1H, ArH), 7.53 (t, $J = 7.8$ Hz, 2H, ArH), 7.37 (d, $J = 8.9$ Hz, 2H, ArH), 7.25 (ddd, $J = 8.2, 7.1, 1.2$ Hz, 1H, ArH), 7.09 (dd, $J = 11.4, 4.3$ Hz, 1H, ArH), 6.86 (d, $J = 8.2$ Hz, 2H, ArH), 4.92 – 4.84 (m, 1H, H-7), 4.78 (dd, $J = 6.3, 4.4$ Hz, 1H, OH), 3.89 (s, 3H, NCH₃), 3.14 – 3.02 (m, 2H, CH₂-indole and CH₂-OH), 2.92 (dd, $J = 16.0, 6.9$ Hz, 1H, CH₂-indole), 2.71 – 2.63 (m, 1H, CH₂-OH). As reported, the ^1H -NMR spectrum is found to be equal to the one of compound **53b**.



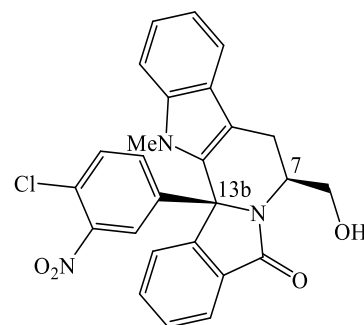
(7S,13bS)-13b-(4-chloro-3-nitrophenyl)-7-(hydroxymethyl)-13-methyl-7,8,13,13b-tetrahydro-5H-benzo[1,2]indolizino[8,7-b]indol-5-one 53a and (7S,13bR)-13b-(4-chloro-3-nitrophenyl)-7-(hydroxymethyl)-13-methyl-7,8,13,13b-tetrahydro-5H-benzo[1,2]indolizino[8,7-b]indol-5-one 53b:

Following the general procedure, to a solution of **48d** (0.0687 g, 0.145 mmol) in pure dichloromethane (6.10 mL) was added BF₃·OEt₂ (85.5 μL , 0.680 mmol). Reaction time: 1 hour and 20 minutes. Eluent for flash chromatography: ethyl acetate/ *n*-hexane, 4:6.

53a: Obtained as a yellow solid (0.0117 g, 17.0%); mp: 153-155 °C; $^1\text{H NMR}$ (300 MHz, $\text{DMSO-}d_6$) δ 7.97 (d, $J = 7.8$ Hz, 1H, ArH), 7.82 – 7.70 (m, 3H, ArH), 7.65 (td, $J = 7.4, 0.7$ Hz, 1H, ArH), 7.57 (d, $J = 2.3$ Hz, 1H, ArH), 7.55 (d, $J = 7.8$ Hz, 1H, ArH), 7.48 (d, $J = 8.3$ Hz, 1H, ArH), 7.26 – 7.18 (m, 2H, ArH), 7.12 – 7.06 (m, 1H, ArH), 4.91 (t, $J = 6.1$ Hz, 1H, OH), 4.23 – 4.13 (m, 2H, $\text{CH}_2\text{-OH}$), 3.76 (s, 3H, NCH_3), 2.98 (ddd, $J = 22.3, 16.8, 9.3$ Hz, 2H, $\text{CH}_2\text{-indole}$).



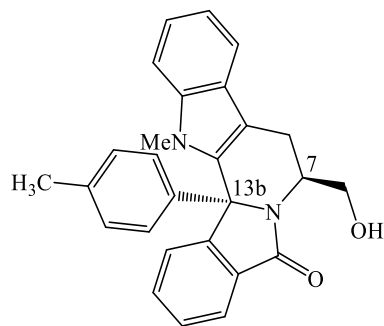
53b: Obtained as a yellow pale solid (0.0460 g, 67.0%); mp: 168-170 °C; $[\alpha]_D^{20} = + 53.7^\circ$ ($c = 0.41$, MeOH); recrystallized in dichloro- methane/ *n*-hexane; $^1\text{H NMR}$ (300 MHz, $\text{DMSO-}d_6$) δ 7.94 (d, $J = 7.6$ Hz, 1H, ArH), 7.87 (dd, $J = 7.3, 1.0$ Hz, 1H, ArH), 7.71 (td, $J = 7.5, 1.5$ Hz, 1H, ArH), 7.69 (d, $J = 8.5$ Hz, 1H, ArH), 7.64 (dd, $J = 7.4, 0.7$ Hz, 1H, ArH), 7.54 (dd, $J = 7.8, 3.4$ Hz, 3H, ArH), 7.26 (ddd, $J = 8.3, 7.1, 1.0$ Hz, 1H, ArH), 7.17 (d, $J = 8.8$ Hz, 1H, ArH), 7.11 (t, $J = 7.2$ Hz, 1H, ArH), 4.95 – 4.87 (m, 1H, H-7), 4.74 (dd, $J = 5.7, 4.6$ Hz, 1H, OH), 3.91 (s, 3H, NCH_3), 3.14 (td, $J = 9.9, 6.0$ Hz, 1H, $\text{CH}_2\text{-indole}$), 3.01 – 2.94 (m, 2H, $\text{CH}_2\text{-indole}$ and $\text{CH}_2\text{-OH}$), 2.80 (dt, $J = 10.3, 5.3$ Hz, 1H, $\text{CH}_2\text{-OH}$); $^{13}\text{C NMR}$ (75 MHz, $\text{DMSO-}d_6$) δ 168.30 (C=O), 147.83 (Cq), 147.44 (Cq), 141.89 (Cq), 137.91 (Cq), 133.26 (ArC), 133.15 (ArC), 131.89 (Cq), 130.83 (ArC), 130.35 (ArC), 129.79 (ArC), 125.91 (ArC), 125.32 (ArC), 125.18 (Cq), 124.98 (Cq), 123.73 (ArC), 122.80 (ArC), 119.52 (ArC), 118.83 (ArC), 110.17 (ArC), 108.99 (Cq), 67.71 (C-13b), 60.75 ($\text{CH}_2\text{-OH}$), 50.23 (CH-7), 34.20 (N- CH_3), 22.00 ($\text{CH}_2\text{-indole}$).



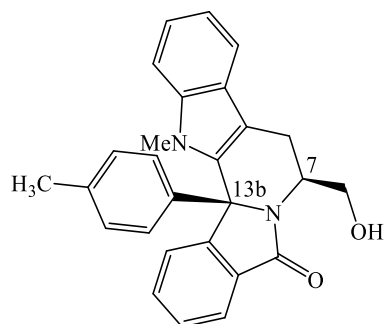
(7S,13bS)-7-(hydroxymethyl)-13-methyl-13b-(p-tolyl)-7,8,13,13b-tetrahydro-5H-benzo[1,2]indolizino[8,7-b]indol-5-one 54a and (7S,13bR)-7-(hydroxymethyl)-13-methyl-13b-(p-tolyl)-7,8,13,13b-tetrahydro-5H-benzo[1,2]indolizino[8,7-b]indol-5-one 54b: Following the general procedure, to a solution of **48e** (0.0964 g, 0.236 mmol) in pure dichloromethane (8.80 mL) was added $\text{BF}_3 \cdot \text{OEt}_2$ (119.0 μL , 0.944 mmol). Reaction time: 15 minutes. On the crude of reaction was performed Eluent for flash chromatography: ethyl acetate/*n*-hexane, 4:6.

54a: Obtained as a white solid (0.0771 g, 80.0 %); mp: 247-250 °C; $[\alpha]_D^{20} = - 82.0^\circ$ ($c = 0.50$, MeOH); $^1\text{H NMR}$ (300 MHz, $\text{DMSO-}d_6$) δ 7.87 (d, $J = 7.7$ Hz, 1H, ArH), 7.78 (d, $J = 7.3$ Hz, 1H, ArH), 7.70 (t, $J = 7.3$ Hz, 1H, ArH), 7.61 (t, $J = 7.3$ Hz, 1H, ArH), 7.53 (d, $J = 7.7$ Hz, 1H, ArH), 7.43 (d, $J = 8.1$ Hz, 1H, ArH), 7.20 (t, $J = 8.9$ Hz, 3H, ArH), 7.08 (t, $J = 7.4$ Hz, 1H, ArH), 6.76 (d, $J = 7.9$ Hz, 2H, ArH)

5.00 (t, $J = 5.8$ Hz, 1H, OH), 4.33 – 4.22 (m, 1H, CH₂-OH), 4.05 – 3.95 (m, 1H, CH₂-OH), 3.72 (s, 3H, NCH₃), 3.09 – 2.90 (m, 2H, CH₂-indole), 2.30 (s, 3H, *p*-CH₃); ¹³C NMR (75 MHz, DMSO-*d*₆) δ 168.89 (C=O), 148.62 (Cq), 138.92 (Cq), 138.08 (Cq), 136.24 (Cq), 135.06 (Cq), 132.98 (ArC), 132.82 (Cq), 129.93 (ArC), 129.75 (ArC), 128.43 (ArC), 125.98 (Cq), 125.86 (ArC), 123.80 (ArC), 122.77 (ArC), 119.91 (ArC), 119.06 (ArC), 111.64 (Cq), 110.33 (ArC), 72.05 (C-13b), 62.24 (CH₂-OH), 33.93 (N-CH₃), 25.12 (CH₂-indole), 21.13 (*p*-CH₃).

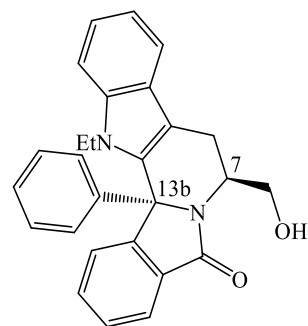


54b: Obtained as a white solid (0.0120 g, 12.5 %); mp: 259-261 °C; ¹H NMR (300 MHz, DMSO-*d*₆) δ 7.87 (d, $J = 4.2$ Hz, 1H, ArH), 7.86 – 7.83 (m, 1H, ArH), 7.69 (td, $J = 7.6, 1.4$ Hz, 1H, ArH), 7.65-7.59 (m, 1H, ArH), 7.53 (t, $J = 7.9$ Hz, 2H, ArH), 7.37 (d, $J = 8.8$ Hz, 2H, ArH), 7.28 – 7.21 (m, 1H, ArH), 7.13 – 7.06 (m, 1H, ArH), 6.86 (d, $J = 8.2$ Hz, 2H, ArH), 4.88 (ddd, $J = 10.6, 6.1, 4.5$ Hz, 1H, H-7), 4.76 (dd, $J = 6.3, 4.3$ Hz, 1H, OH), 3.89 (s, 3H, NCH₃), 3.14-3.01 (m, 2H, CH₂-indole and CH₂-OH), 2.92 (dd, $J = 16.1, 6.9$ Hz, 1H, CH₂-indole), 2.72 – 2.63 (m, 1H, CH₂-OH);



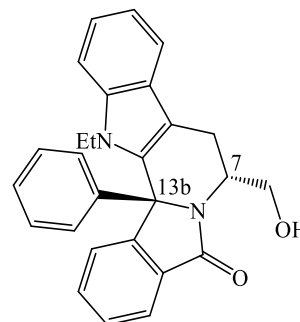
(7S,13bS)-13-ethyl-7-(hydroxymethyl)-13b-phenyl-7,8,13,13b-tetrahydro-5H-benzo[1,2]indolizino[8,7-b]indol-5-one 55a and (7S,13bR)-13-ethyl-7-(hydroxymethyl)-13b-phenyl-7,8,13,13b-tetrahydro-5H-benzo[1,2]indolizino[8,7-b]indol-5-one 55b: Following the general procedure, to a solution of **38b** (0.101 g, 0.248 mmol) in pure dichloromethane (9.00 mL) was added BF₃·OEt₂ (124.6 μ L, 0.992 mmol). Reaction time: 15 minutes. Eluent for flash chromatography: ethyl acetate/*n*-hexane, 4:6).

55a: Obtained as a white solid (0.0689 g, 68.0 %); mp: 273-275 °C; ¹H NMR (300 MHz, DMSO-*d*₆) δ 7.79 (dd, $J = 7.1, 6.0$ Hz, 2H), 7.75 – 7.69 (m, 1H), 7.63 (td, $J = 7.3, 1.0$ Hz, 1H), 7.54 (d, $J = 7.6$ Hz, 1H), 7.47 (d, $J = 8.2$ Hz, 1H), 7.42 – 7.35 (m, 3H), 7.24 – 7.17 (m, 1H), 7.11 – 7.05 (m, 1H), 6.89 – 6.85 (m, 2H), 4.98 (t, $J = 6.0$ Hz, 1H, OH), 4.25 (td, $J = 14.2, 7.4$ Hz, 3H, CH₂CH₃ and H-2), 4.07 – 3.97 (m, 1H, H-2), 3.28 – 3.24 (m, 1H, H-7), 3.02 (dd, $J = 13.9, 10.5$ Hz, 2H, CH₂-indole), 1.10 (t, $J = 6.9$ Hz, 3H, CH₂CH₃).



(7*R*,13*bR*)-13-ethyl-7-(hydroxymethyl)-13*b*-phenyl-7,8,13,13*b*-tetrahydro-5*H*-benzo[1,2]indolizino[8,7-*b*]indol-5-one 55*a*' and **(7*R*,13*bS*)-13-ethyl-7-(hydroxymethyl)-13*b*-phenyl-7,8,13,13*b*-tetrahydro-5*H*-benzo[1,2]indolizino[8,7-*b*]indol-5-one 55*b*'**: Following the general procedure, to a solution of **38*b*'** (0.0711 g, 0.174 mmol) in pure dichloromethane (6.20 mL) was added BF₃·OEt₂ (87.5 μL, 0.696 mmol). Reaction time: 15 minutes. Eluent for flash chromatography in first attempt (ethyl acetate/n-hexane, 4:6).

55*a*': Obtained as a white solid (0.0651 g, 64.3 %); ¹H NMR (300 MHz, DMSO-*d*₆) δ 7.83 – 7.68 (m, 1H, *ArH*), 7.63 (t, *J* = 6.8 Hz, 1H, *ArH*), 7.54 (d, *J* = 7.8 Hz, 1H, *ArH*), 7.47 (d, *J* = 8.3 Hz, 1H, *ArH*), 7.38 (dd, *J* = 8.3, 2.8 Hz, 1H, *ArH*), 7.24 – 7.17 (m, 1H, *ArH*), 7.08 (t, *J* = 7.6 Hz, 1H, *ArH*), 6.87 (dd, *J* = 7.4, 1.7 Hz, 1H, *ArH*), 4.98 (t, *J* = 5.9 Hz, 1H, *OH*), 4.25 (td, *J* = 14.2, 7.4 Hz, 3H, CH₂CH₃ and *H*-2), 4.05 – 3.97 (m, 1H, *H*-2), 3.28 – 3.24 (m, 1H, *H*-7) 3.05 – 2.94 (m, 2H, CH₂-indole), 1.10 (t, *J* = 6.9 Hz, 3H, CH₂CH₃).



4.4. Experimental procedure for the *in-vitro* yeast based screening assay of compounds 34, 34b, 34d, 34e, 38b and 38d

Plasmids: the yeast expression vector pLS76-(LEU2) encoding human mutant p53R280K under GAL1-10 inducible promoter (kindly provided by Dr. Gilberto Fronza; IST Istituto Nazionale per la Ricerca sul Cancro), was used.

Yeast transformation: the plasmids used for yeast transformation process were amplified in *Escherichia coli* DH5 α from Lucigen (Frilabo), and thereafter extracted using the GenEluteTM HP Plasmid Miniprep Kit (Sigma-Aldrich). After extraction, yeast strains were transformed using the LiAc/SS Carrier DNA/PEG method. In order to select transformed yeast, cells were routinely grown in selective minimal medium with 2% (w/w) glucose (Sigma-Aldrich), 0.7% (w/w) yeast nitrogen base without amino acids from Difco (Quilaban), and all the aminoacids required for yeast growth (50 μ g/mL), except leucine, and incubated at 30 °C, under continuous orbital shaking (200 rpm).

Yeast-based screening assay: for expression of human proteins, cells (routinely grown in minimal selective medium) were diluted to 0.05 OD₆₀₀ in induction selective medium containing 2% (w/w) galactose (Sigma-Aldrich), 1% (w/w) raffinose (Acros Organics), 0.7% (w/w) yeast nitrogen base without amino acids from Difco (Quilaban), and all the amino acids required for yeast growth (50 μ g/mL), as referred above. Cells transformed with empty vector were used as control. Yeast cells were incubated at 30 °C under continuous orbital shaking (200 rpm) in the presence of 1-30 μ M of compounds or 0.1% DMSO only, for approximately 48 h (time required by control yeast, incubated with DMSO only, to achieve 0.4 OD₆₀₀). Yeast growth was analyzed by counting the number of colony-forming units (CFU) after 2 days of incubation at 30°C on Sabouraud Dextrose Agar plates (Liofilchem).

4.5. Experimental procedure of the stability studies

4.5.1. Metabolic stability assay – Identification of Phase I metabolites by LC-ESI-MS upon microsomes incubation of compounds 34 and 34e

4.5.1.1. Materials

Pooled male rat liver microsomes and Vivid regeneration system were acquired from ThermoFischer Scientific (Spain). Pooled donor human liver microsomes were acquired from BD Biosciences (US). Nicotinamide-Adenine Dinucleotide Phosphate in its reduced form (NADPH) and Neviripine were acquired from Sigma-Aldrich (Germany). Neviripine was purchased from Cipla (Mumbai, India). 100

mM of Phosphate Buffer solution was prepared adding in 90 mL of deionized water 1.42g of Na₂HPO₄ and 1.56g of NaH₂PO₄·2H₂O. The pH was adjusted to 7.4 with a solution of NaOH(aq) 250 mM and the volume completed to 100 mL. All drugs, chemical and solvents were acquired from commercial suppliers at highest purity available.

4.5.1.2. Methods

To separate and identify the structures of compounds **34** and **34e** and its metabolites, an Ionization-Tandem Mass Spectrometry (LC-ESI-MS/MS) was used. LC-ESI-MS/MS analyses were performed with ion trap LCQ Fleet Mass Spectrometer (Thermo Scientific) fitted with an Ultimate 3000RS LC nano HPLC system (Thermo Scientific) was used. The HPLC system was equipped with a Luna C18(2) column (2.0 mm i.d. x 50 mm, 100 Å pore size) using a gradient elution of 0.1% formic acid in water (mobile phase A) and 0.1% formic acid in acetonitrile (mobile phase B) at a flow rate of 200 µL/min. Gradient condition were as follows: 5-70% mobile phase B for 30 min, 70-100% mobile phase B for 2 min, 100% mobile phase B for 8 min, 100-5% mobile phase B for 5 min and finally 5% mobile phase B for 7min. The column and the sampler were maintained at a constant temperature of 40 °C and 8 °C respectively. Mass spectra were obtained with the electrospray ionization source (ESI) in both negative and positive modes optimized with the following settings: sheath gas flow rate, 40 (arbitrary units); auxiliary gas flow rate, 10 (arbitrary units); spray voltage, 4.5 kV; capillary voltage, -18/16 V; tube lens voltage, -125/63 V; skimmer voltage, 28 V; vaporizer temperature: 185 °C; capillary temperature, 300 °C. Data were acquired using Xcalibur software (ThermoFischer Scientific). Internal calibration was performed for sodium formate/acetate clusters.

In rat microsomes: Thawed male rat pooled liver microsomes (20 mg protein/ mL), a solution of NADPH (16.7mg in 1 mL of 100 mM phosphate buffer 7.4) regenerating system, NRS regenerating system and 5 mM stock solution of compounds **34** and **34e** (100% DMSO) are prepared. To reach the final volume of 500 µL, for the drug incubation, the reaction mixture at the end contains 449 µL of 100 mM phosphate buffer pH 7.4, 20 µL of male rat microsomes (0.8 mg protein/ mL final concentration), 1 µL of 5 mM drug stock solution (10 µM of drug in 500 µL final concentration for the incubation) and 5 µL of Vivid regenerating system solution. After a period of pre-incubation of 5 minutes at 37 °C in an *Eppendorf*® *thermomixer C* water bath, 25 µL of NADPH solution is added to the so-composed system and the phase I reactions are let started. At different time points (0 minutes, 30 minutes, 60 minutes, 120 minutes, 180 minutes, 24 hours, 48 hours) 100 µL of reaction mixture is withdrawn and 100 µL of cold solution 2.5 µM of Reserpine in acetonitrile is added in order to stop any enzymatic activity. Then, the mixtures are centrifuged at 10000 rpm for 15 minutes at room temperature and the

supernatant is immediately recollected and saved in Eppendorfs, which they have been stored at -20 °C till further analysis. At each time point the compounds are analysed using LC-MS/MS. A rationalized identification of phase I metabolites is performed successfully. Neviripine is used as positive control.

In human microsomes: Thawed human pooled liver microsomes (20 mg protein/ mL), a solution of NADPH (16.7mg in 1 mL of 100 mM phosphate buffer 7.4) regenerating system, NRS regenerating system and 5 mM stock solution of compounds **34** and **34e** (100% DMSO) are prepared. To reach the final volume of 500 µL, for the drug incubation, the reaction mixture at the end contains 449 µL of 100 mM phosphate buffer pH 7.4, 20 µL of male rat microsomes (0.8 mg protein/ mL final concentration), 1 µL of 5 mM drug stock solution (10 µM of drug in 500 µL final concentration for the incubation) and 5 µL of Vivid regenerating system solution. After a period of pre-incubation of 5 minutes at 37 °C in an *Eppendorf*® *thermomixer C* water bath, 25 µL of NADPH solution is added to the so-composed system and the phase I reactions are let started. At different time points (0 minutes, 30 minutes, 60 minutes, 120 minutes, 180 minutes, 24 hours, 48 hours) 100 µL of reaction mixture is withdrawn and 100 µL of cold solution 2.5 µM of Reserpine in acetonitrile is added in order to stop any enzymatic activity. Then, the mixtures are centrifuged at 10000 rpm for 15 minutes at room temperature and the supernatant is immediately recollected and saved in Eppendorfs, which they have been stored at -20 °C till further analysis. At each time point the compounds are analysed using LC-ESI(+)-MS/MS. A rationalized identification of Phase I metabolites is performed successfully. Neviripine is used as positive control.

4.5.2. Determination of stability of compounds 34 and 34e in human plasma by LC-ESI-MS and HPLC/UV-Vis

4.5.2.1. Materials

Human plasma was acquired commercially. Phosphate buffer solution was prepared as in section **IV.4.1.1**. Procaine hydrochloride was acquired from Sigma-Aldrich (Germany). All drugs, chemical and solvents were acquired from commercial suppliers at highest purity available.

4.5.2.2. Methods

For the specifics of the LC-DAD see section **4.4.1.2**. HPLC analyses were conducted on an Ultimate 3000 Dionex system, consisting of an LPG-3400A quaternary gradient pump and a diode array spectrophotometric detector (Dionex Co., Sunnyvale, CA), and equipped with a Rheodyne model 8125

injector (Rheodyne, Rohnert Park, CA). HPLC analyses were performed with a Luna C18 (2) column (250 mm × 4.6 mm; 5 μm; Phenomenex, Torrance, CA), at a flow rate of 1 mL/min. A 30-min linear gradient from 5 to 95% acetonitrile in 0.1% aqueous formic acid, followed by a 2-min linear gradient to 100% acetonitrile and an 8-min isocratic elution with acetonitrile, was used in all instances. The UV absorbance was monitored at 269 nm.

LC-MS/MS analysis: Thawed human plasma is firstly centrifuged at 2000 rpm for 5 minutes and then diluted 1:1 with a 100 mM phosphate buffer 7.4. 5 mM stock solution of the compounds (100% DMSO) and are prepared. Procaine is used as reference drug for these studies and its 4 mM stock solution (100% DMSO) is prepared. 975 μL of phosphate buffer is placed in 37 °C *Eppendorf*® *thermomixer C* shaking water bath for 10 minutes and after this period of time 25 μL of procaine stock solution and 25 μL of test drug stock solutions are added. At different time points (0 minutes, 30 minutes, 60 minutes, 120 minutes, 180 minutes, 24 hours, 48 hours) 100 μL of reaction mixture is withdrawn and 300 μL of cold solution 2.5 μM of Reserpine in acetonitrile is added in order to stop any enzymatic activity. Then, the mixtures are centrifuged at 10000 rpm for 10 minutes at room temperature and the supernatant is immediately recollected and saved in Eppendorfs, which they have been stored at -20 °C till further analysis. At each time point the compounds are analysed using LC-MS/MS. A rationalized identification of phase I metabolites is performed successfully.

HPLC/UV-Vis analysis: Thawed human plasma is firstly centrifuged at 2000 rpm for 5 minutes and then diluted 1:1 with a 100 mM phosphate buffer 7.4. 5 mM stock solution of the compounds (100% DMSO) and are prepared. Procaine is used as reference drug for these studies and its 4 mM stock solution (100% DMSO) is prepared. 975 μL of phosphate buffer is placed in 37 °C *Eppendorf*® *thermomixer C* shaking water bath for 10 minutes and after this period of time 25 μL of procaine stock solution and 25 μL of test drug stock solutions are added. At different time points (0 minutes, 30 minutes, 60 minutes, 120 minutes, 180 minutes, 24 hours, 48 hours) 100 μL of reaction mixture is withdrawn and 300 μL of cold solution 10⁻¹ mM of Reserpine in acetonitrile is added in order to stop any plasma enzymatic activity. Then, the mixtures are centrifuged at 10000 rpm for 10 minutes at room temperature and the supernatant is immediately recollected and saved in Eppendorfs, which they have been stored at -20 °C till further analysis. At each time point the compounds are analysed using HPLC/UV-Vis methodology. A rationalized identification of Phase I metabolites is performed successfully.

4.5.3. Determination of stability of compounds 34 and 34e in phosphate buffer solution by LC-ESI-MS and HPLC/UV-Vis

A solution 100 mM of phosphate buffer pH 7.4 is prepared and after a period of 10 minutes where 975 μL of this buffer solution are placed in a 37 °C *Eppendorf*® *thermomixer C* shaking water bath, 25 μL of procaine stock solution and 25 μL of test drug stock solutions are added. At different time points (0 minutes, 30 minutes, 60 minutes, 120 minutes, 180 minutes, 24 hours, 48 hours) 100 μL of reaction mixture above described is withdrawn and 300 μL of cold solution 10⁻¹ mM of Reserpine in acetonitrile is added. The mixtures are centrifuged at 10000 rpm for 10 minutes at room temperature and the supernatant is immediately recollected and saved in Eppendorfs, which they have been stored at -20 °C till further analysis. At each time point the compounds are analysed using LC-MS/MS and HPLC/UV-Vis methodologies respectively to analyse the stability at neutral pH of each test compound along the time. Procaine is used as reference drug for this study.

5. References

- [1] D. K. Kondepudi and D. J. Durand, "Chiral Asymmetry in Spiral Galaxies?," *Chirality*, vol. 13, pp. 351-356, 2001.
- [2] K. G. Fahlsbusch, F. J. Hammerschmidt, J. Panten, W. Pickenhagen, D. Schatowski, K. Bauer, D. Garbe and H. Surbrg, "Flavors and Fragrance," in *Ullmann's Encyclopedia of Industrial Chemistry*, 2012, pp. 73-198.
- [3] A. D. McNaught and A. Wilkinson, "IUPAC Compendium of Chemical Terminology," 2014, pp. 499-1621.
- [4] E. L. Eliel and S. H. Wilen, *Stereochemistry of Organic Compounds*, Wiley, 1994.
- [5] Z. Shen, C. Lv and S. Zeng, "Significance and challenges of stereoselectivity assessing methods in drug metabolism," *Journal of Pharmaceutical Analysis*, vol. 6, pp. 1-10, 2016.
- [6] Z. G. Hajos and D. R. Parrish, "Asymmetric Synthesis of Bicyclic Intermediate of Natural Product Chemistry," *J. Org. Chem.*, vol. 39, pp. 1615-1621, 1974.
- [7] B. L. Feringa and R. A. van Delden, "Absolute Asymmetric Synthesis: The Origin, Control, and Amplification of Chirality," *Angew. Chem. Int. Ed.*, vol. 38, pp. 3418-3438, 1999.
- [8] A. Rouf and S. C. Taneja, "Synthesis of Single-enantiomer Bioactive Molecules: A Brief Overview," *Chirality*, vol. 26, pp. 63-78, 2014.
- [9] A. Ghanem and H. Y. Aboul-Enein, "Lipase-mediated Chiral Resolution of Racemates in Organic Solvents," *Tetrahedron: Asymmetry*, vol. 15, pp. 3331-3351, 2004.
- [10] R. Noyori, M. Tokumaga and M. Kitamura, "Stereoselective Organic Synthesis via Dynamic Kinetic Resolution," *Bull Chem. Soc. Jpn*, vol. 68, pp. 36-56, 1995.
- [11] F. Nahra and O. Riant, "Recruiting the Student to Fight Cancer: Total Synthesis of Goniotalamin," *J. Chem. Educ.*, vol. 92, pp. 179-182, 2015.
- [12] J. D. Morrison and H. D. Mosher, *Asymmetric Organic Reactions*, New Jersey: Prentice-Hall, 1971.
- [13] T. Oh and M. Reiley, "Reagent-controlled Asymmetric Diels-Alder Reaction. A review," *Organic Preparation and Procedures Int.*, vol. 26, pp. 129-158, 1994.
- [14] F. Glorius and Y. Ginis, "Chiral Auxiliaries- Principles and Recent Applications," *Synthesis*, vol. 12, pp. 1899-1930, 2006.
- [15] S.-M. Paek, M. Jeong, Y. M. Heo, Y. T. Han and H. Yun, "Recent Advances in Substrate-controlled Asymmetric Induction Derived from Chiral Pool α -Amino Acids for Natural Product Synthesis," *Molecules*, vol. 21, p. 951, 2016.

- [16] C. Najera and J. M. Sansano, "Catalytic Assymmetric Synthesis of α -Amino Acids," *Chem Rev.*, vol. 107, pp. 4584-4671, 2007.
- [17] L. Nguyen, H. He. and C. Pham-Huy, "Chiral Drugs: An overview," *Int. J. Boimed. Sci.*, vol. 2, no. 2, pp. 85-100, 2006.
- [18] L. Hartmut, J. N. Graeme and E. Bayer, "Rapid Gas Chromatographic Separation of Amino Acid Enantiomers with a Novel Chiral Stationary Phase," *J. of Chromatographic Science*, vol. 15, pp. 174-176, 1977.
- [19] G. Casiraghi and F. Zanardi, "Stereoselective Approaches to Bioactive Carbohydrates and Alkaloids- With a Focus on Recent Syntheses Drawing from Chiral Pool," *Chem. REv.*, vol. 95, pp. 1677-1716, 1995.
- [20] H.-U. Blaser, "The Chiral Pool as a Source of Enantioselective Catalysts and Auxiliaries," *Chem. Rev.*, vol. 92, pp. 835-852, 1992.
- [21] S. Halaema, S. P. Vavan , I. Ibnusaud, P. I. Polavarapu and H. B. Kagan, "Enantiomerically pure compounds related to chiral hydroxy acids derived from renewable resources," *RSC Adv.*, vol. 2, pp. 9257-9285, 2012.
- [22] K. Tatsuta, T. Ishiyama, S. Tajima, Y. Koguchi and H. Gunji, "The Total Synthesis of Oleandomycin," *Tetrahedron*, vol. 31, pp. 702-712, 1990.
- [23] M. Amat, M. M. M. Santos, O. Bassas, N. Llor, C. Escolano, A. Gomez-esque', E. Molins, S. M. Allin, V. McKee and J. Bosch, "Straightforward methodology for the enantioselective synthesis of benzo [a]- and indolo [2,3-a] quinolizidines," *J. Org. Chem.*, vol. 72, pp. 5193-5201, 2007.
- [24] K. M. Rentsch, "The importance of stereoselective determination of drugs in the clinical laboratory," *Journal of Biochemical and Biophysical Methods*, vol. 56, pp. 9843-9873, 2000.
- [25] M. D. Groaning and A. I. Meyers, "Chiral Non-Racemic Bicyclic Lactams. Auxiliary-Based Asymmetric Reactions," *Tetrahedron*, vol. 56, pp. 9843-9873, 2000.
- [26] D. Romo and A. I. Meyers, "Chiral Non-Racemic Bicyclic Lactams. Vehicles for Construction of Natural and Unnatural Products Containing Quaternary Carbon Centers," *Tetrahedron*, vol. 47, pp. 9503-9569, 1991.
- [27] P. Karrer and P. Portmann, "Reduction von L-tryptophan-methylester mit LiAlH_4 ," *Helvetica Chimica Acta.*, vol. 32, pp. 1034-35, 1949.
- [28] N. A. L. Pereira, A. Monteiro, M. Machdo, J. Gut, E. Molins, M. J. Perry, R. Moreira, P. J. Rosenthal, M. Prudêncio and M. M. M. Santos, "Enantiopure Indolizinoindolones with *in vitro* Activity against Blood-and Liver- Stage Malaria Parasites," *ChemMedChem*, vol. 10, pp. 2080-2089, 2015.

- [29] "World Cancer Report," 2014.
- [30] G. M. Cooper and R. E. Huasman, *The Cell: A Molecular Approach*, Sunderland: Boston University, 2006.
- [31] B. Vogelstein, D. Lane and A. J. Levine, "Surfing the p53 network," *Nature*, vol. 408, pp. 307-310, 2000.
- [32] C. P. Martins, I. Brown-Swigart and G. I. Evan, "Modelling the therapeutic efficacy of p53 restoration in tumors," *Cell*, vol. 127, pp. 1323-1334, 2006.
- [33] A. Ventura, D. G. Kirsch, M. E. McLaughlin, D. A. Tuveson, J. Grimm, L. Lintault, J. Newmann, E. E. Reczek, R. Weissleder and T. Jacks, "Restauration of p53 function leads to tumor regression in vivo," *Nature*, vol. 445, pp. 661-665, 2007.
- [34] W. Xue, L. Zender, C. Miething, R. A. Dickins, E. Hernando, V. Krizhanovsky, C. Cordon-Cardo and S. W. Lowe, "Senescence and tumor clearance is triggered by p53 restauration in murine liver carcicomas," *Nature*, vol. 445, pp. 656-660, 2007.
- [35] K. H. Vousden and C. Prives, "Blinded by the light: the growing complexity of p53," *Cell*, vol. 137, pp. 413-431, 2009.
- [36] G. Selinanova and K. G. Wiman, "Reactivation of mutant p53: molecular mechanisms and therapeutic potential," *Oncogene*, vol. 26, pp. 2243-2254, 2007.
- [37] P. George, "p53 How crucial is its role in cancer?," *International Journal of Current Pharmaceutical Research*, vol. 3, pp. 19-25, 2011.
- [38] V. J. Bykov, N. Issaeva, A. Shilov, M. Hultcrantz, E. Pugacheva, P. Chumakov, J. Bergman, K. G. Wiman and G. Selinanova, "Restoration of the tumor supressor function to mutant p53 by a low-molecular-wieght compound," *Nat. Med*, vol. 8, pp. 282-288, 2002.
- [39] S. N. Jones, A. E. Roe, L. A. Donehowwer and A. Bradley, "Rescue of embryonic lethality in Mdm2-deficient mice by absence of p53," *Nature*, vol. 378, pp. 206-208, 1995.
- [40] R. Montes de Oca Luna, D. S. Wagner and G. Lozano, "Rescue of early embryonic lethality in Mdm2-deficient mice by deletion of p53," *Nature*, vol. 378, pp. 203-206, 1995.
- [41] J. Parant, A. Chavez-Reyes, N. A. Little, W. R. Yan and A. G. Jochemsen, "Rescue of embryonic lethality in Mdm4-null mice by loss of Trp53 suggests a nonoverlapping pathway with MDM2 to regulate p53," *Nat. Genet.*, vol. 29, pp. 92-95, 2001.
- [42] Q. Li and G. Lozano, "Molecular pathways: targeting Mdm2 and Mdm4 in cancer therapy," *Clin. Cancer Res.*, vol. 19, pp. 34-41, 2013.

- [43] J. Momand, G. P. Zambetti, D. C. Olson, D. George and A. J. Levine, "The mdm-2 oncogene product forms a complex with p53 protein and inhibits p53-mediated transactivation," *Cell*, vol. 69, pp. 1237-1245, 1992.
- [44] M. A. Lohrum, D. B. Woods, R. L. Ludwig and E. Balint, "C-terminal ubiquitination of p53 contributes to nuclear export," *Mol. Cell. Biol.*, vol. 21, pp. 8521-8532, 2001.
- [45] M. H. Kubutat, S. N. Jones and K. H. Vousden, "Regulation of p53 stability by Mdm2," *Nature*, vol. 387, pp. 299-303, 1997.
- [46] Y. Haupt, R. Maya, A. Kazaz and M. Oren, "Mdm2 promotes the rapid degradation of p53," *Nature*, vol. 387, pp. 296-299, 1997.
- [47] R. Stad, N. A. Little, D. P. Xirodimas, R. Frenk, A. J. van der Eb, D. P. Lane, M. K. Savile and A. G. Jochemsens, "Mdmx stabilizes p53 and Mdm2 via two distinct mechanisms," *EMBO*, vol. 2, pp. 1029-1034, 2001.
- [48] M. Wade, Y. C. Li and G. M. Wahl, "MDM2, MDMX and p53 in oncogenesis and cancer therapy," *Nat. Rev. Cancer*, vol. 13, pp. 83-86, 2013.
- [49] K. Onel and C. Cordon-Cardo, "MDM2 and prognosis," *Mol. Cancer Res.*, vol. 2, pp. 1-8, 2004.
- [50] S. Gomes, M. Leão, L. Raimundo, H. Ramos, J. Soares and L. Saraiva, "p53 family interactions and yeast: together in anticancer therapy," *Drug Discovery Today*, vol. 4, pp. 616-624, 2016.
- [51] L. T. Vassilev, B. T. Vu, B. Graves, D. Carvajal, F. Podlaski, Z. Filipovic, N. Kong, U. Kammlott, C. Lukacs, C. Klein, N. Fotouhi and E. A. Liu, "In vivo activation of the p53 pathway by small-molecule antagonist of MDM2," *Science*, vol. 303, pp. 844-848, 2004.
- [52] Y. Zhao, Y. Shangai, W. Sun, L. Liu, D. McEachern, S. Shargary, D. Bernard, X. Li, T. Zhao, P. Zou, D. Sun and S. Wang, "A potent small-molecule inhibitor of the MDM2-p53 interaction (MI-888) achieved complete and durable tumor regression in mice," *J. Med. Chem.*, vol. 56, pp. 5553-5561, 2013.
- [53] M. Xia, D. Knezevic, C. Tovar, B. Huang, D. C. Heimbrosk and L. T. Vassilev, "Elevated MDM2 boosts the apoptotic activity of p53-MDM binding inhibitors by facilitating MDMX degradation," *Cell Cycle*, vol. 7, pp. 1604-1612.
- [54] M. Wade, E. T. Wong, M. Tang, J. M. Stommel and G. M. Wahl, "MdmX modulates the outcome of p53 activation in human tumor cells," *J. Biol. Chem.*, vol. 281, pp. 33030-33035, 2006.
- [55] B. Hu, D. M. Gilkes, B. Farooqi, S. M. Sebti and J. Chen, "MDMX overexpression prevents p53 activation by the MDM2 inhibitor Nutlin," *J. Biol. Chem.*, vol. 281, pp. 33030-33035, 2006.

- [56] D. Reed, Y. Shen, A. A. Shelat, L. A. Arnold, A. M. Ferreira, F. Zhu, N. Mills, D. C. Smithson, C. A. Regni, D. Bashford, S. A. Cicero, B. A. Schulman, A. G. Jochemsen, R. K. Guy and M. A. Dyer, "Identification and characterization of the first small molecule inhibitor of MDMX," *J. Biol. Chem.*, vol. 285, no. 14, pp. 10786-10796.
- [57] B. Graves, T. Thompson, M. Xia, C. Lukacs, D. Deo, P. Di Lello, D. Fry, g, C. Garvie, K. S. Huang, L. Gao, C. Tovar, A. Lovey, J. Wanner and L. T. Vassilev, "Activation of p53 pathway by -small molecule- induced MDM2 and MDMX dimerization," *Proc. Natl. Acad. Sci. USA*, vol. 109, pp. 11788-11793, 2012.
- [58] "World Health Organization (2015): fact sheet no. 94," 2015. [Online]. Available: <http://www.who.int/mediacentre/factsheets/fs094/en/>.
- [59] R. W. Snow, C. A. Guerra, A. M. Noor, H. Y. Myint and S. I. Hay, "The global distribution of clinical episodes of *Plasmodium falciparum* malaria," *Nature*, vol. 434, pp. 214-217, 2005.
- [60] A. M. Vaughan, A. S. Aly and S. H. Kappe, "Malaria parasite pre-erythrocytic stage infection: gliding and hiding," *Cell Host Microbe*, vol. 4, pp. 209-218, 2008.
- [61] S. C. Ayala, "Checklist, host index, and annotated bibliography of *Plasmodium* from reptiles," *J. Eukaryot. Microbiol.*, vol. 25, pp. 87-100, 1978.
- [62] A. G. Craig, G. E. Grau, C. Janse, J. W. Kazura, D. Milner, J. W. Barnwell, G. Turner and J. Langhorne, "The role of Animal Models for Research on Severe Malaria," *PLOS Pathogens*, vol. 8, pp. 1-10, 2012.
- [63] A. Kaushansky, A. S. Ye, L. S. Austin, A. S. Mikalajczak, A. M. Vaughan, N. Camargo, P. G. Metzger, A. N. Doulgass, G. MacBeath and S. H. I. Kappe, "Interrogation of infected hepatocyte signalling reveals that suppression of host p53 is critical for *Plasmodium* liver stage infection," *Cell Rep.*, vol. 3, pp. 630-637, 2013.
- [64] J. Wang, T. Zheng, X. Chen, X. Song, X. Meng, N. Bhatta, S. Pan, H. Jiang and L. Liu, "MDM2 antagonist can inhibit tumor growth in hepatocellular carcinoma with different types of p53 in vitro," *J. Gastroenterol Hepatol.*, vol. 26, pp. 371-377, 2011.
- [65] S. Biswal, U. Sahoo, S. Sethy, H. Kumary and M. Banerjee, "Indole: the molecule of diverse biological activities," *Asisan J. Pharm. Clin. Res.*, vol. 5, pp. 1-6, 2012.
- [66] N. Kaushik, P. Attri, N. Kumar, C. Kim, A. Verma and E. Choi, "Biomedical importance of indole," *Molecules*, vol. 18, pp. 6620-6662, 2013.
- [67] Y. Zhang, P. Yang, C. J. Chou, C. Liu, X. Wang and W. Xu, "Development of N-Hydroxycinnamide-based histone deacetylase inhibitors with indole-containing can group," *ACS Med. Chem. Lett.*, vol. 4, pp. 235-238, 2013.

- [68] M. K. Akkoc, M. Y. Yuksel, L. Durmaz and R. C. Atalay, "Design, synthesis and biological evaluation of indole-based 1.4 disubstituted piperazines as cytotoxic agents," *Turk. J. Chem.*, vol. 36, pp. 515-525, 2012.
- [69] P. Singh, M. Kaur and P. Verma, "Design, synthesis and anticancer activities of hybrids of indole and barbituric acids- Identification of highly promising leads," *Bioorg. Med. Chem. Lett.*, vol. 19, pp. 3054-3058, 2009.
- [70] J. Soares, L. Raimundo, N. A. L. Pereira, D. J. V. A. Santos, M. Pérez, G. Queiroz, M. Leão, M. M. Santos and L. Saraiva, "A tryptophanol-derived oxazolopiperidone lactam is cytotoxic against tumors via inhibition of p53 interaction with murine double minute proteins," *Pharmacol. Res.*, Vols. 95-96, pp. 42-52, 2015.
- [71] K. Kaur, M. Jain, T. Kaur and R. Jain, "Antimalarials from nature," *Bioorg. Med. Chem.*, vol. 17, pp. 3229-3256, 2009.
- [72] M. Rottman, C. McNamara, B. K. S. Yeung, M. C. S. Lee, B. Zou, B. Russel, P. Seitz, D. M. Plouffe, N. V. Dharia, T. H. Keller, D. A. Fidock, E. A. Winzeler and T. T. Diagana, "Spiroindolones, a potent compound class for the treatment of malaria," *Science*, vol. 329, pp. 1175-1180, 2010.
- [73] P. Horrocks, S. Fallon, L. Denman, O. Devine, L. J. Duffy, A. Harper, E. L. Meredith, S. Hasenkamp, A. Sidaway, D. Monnery, T. R. Phillips and S. M. Allin, "Synthesis and evaluation of a novel series of indoloisoquinolines as small molecule anti-malarial leads," *Bioorg. Med. Chem. Lett.*, vol. 22, pp. 1770-1773, 2012.
- [74] J. Soares, L. Raimundo, N. A. L. Pereira, A. Monteiro, S. Gomes, C. Bessa, C. Pereira, G. Queiroz, A. Bisio, J. Fernandes, C. Gomes, F. Reis, J. Gonçalves, A. Inga, M. M. M. Santos and L. Saraiva, "Reactivation of wild-type and mutant p53 by tryptophanol-derived oxazoloisoindolinone SLMP53-1, a novel anticancer small-molecule," *Oncotarget*, vol. 7, pp. 4326-4643, 2015.
- [75] J. Soares, L. Raimundo, N. A. L. Pereira, A. Monteiro, S. Gomes, C. Bessa, C. Pereira, G. Queiroz, A. Bisio, J. Fernandes, C. Gomes, F. Reis, A. Inga, M. M. M. Santos and L. Saraiva, "Reactivation of wild-type and mutant p53 by tryptophanol-derived oxazoloisoindolinone SLMP53-1, a novel anticancer small-molecule," *Oncotarget*, vol. 7, pp. 4326-4343, 2015.
- [76] A. Rouf and S. Taneja, "Synthesis of single-enantiomer bioactive molecules. A brief overview," *Chirality*, vol. 26, pp. 63-78, 2014.
- [77] N. A. L. Pereira, A. Monteiro, M. Machado, J. Gut, E. Molins, M. J. Perry, J. Dourado, R. Moreira, P. J. Rosenthal, M. Prudencio and M. M. M. Santos, "Enantiopure indolizinoindolones

- with in vitro activity against blood- and liver-stage malaria parasites,” *MedChemMed*, vol. 10, pp. 2080-2089, 2015.
- [78] L. Jia and X. Liu, “The conduct of drug metabolism studies considered good practise (II): in vitro experiments,” *Curr Drug Metab*, vol. 8, pp. 822-829, 2007.
- [79] L. Di, E. H. Kerns, Y. Hong and H. Chen, “Development and application of high throughput plasma stability assay fro drug discovery,” *Internation Journal of Pharmaceutics*, vol. 297, pp. 110-119, 2005.
- [80] V. Sharma , P. Kumar and D. Pathak, “Biological importance of the indole nucleus in recent years: a comprehensive review,” *Journal of Heterocyclic Chemistry*, vol. 47, pp. 491-502, 2010.
- [81] K. Kaur, M. Jain, T. Kaur and R. Jain , “Antimalarials from nature,” *Bioorg Med Chem*, vol. 17, pp. 3229-3256, 2009.
- [82] P. Horrocks, S. Fallon, L. Denman, O. Devine, L. J. Duffy, A. Harper, E. L. Meredith, S. Hasenkamp, A. Sidaway, D. Monnery, T. R. Phillips and S. M. Allin , “Synthesis and evaluation of a novel series of indoloisoquinolines as small molecule anti-malarials leads,” *Bioorg Med Chem Lett*, vol. 22, pp. 1770-1773, 2012.
- [83] M. Jida, O.-M. Soueidan, B. Deprez, G. Laconde and R. Deprez-Poulain, “Racemic and diastereoselective construction of indole alkaloids under solvent- and catalyst-free microwave assisted Pictet-Spengler condensation.,” *Green Chemistry*, vol. 14, pp. 909-911, 2012.
- [84] B. E. Maryanoff, H. -C. Zhang, J. H. Cohen, I. J. Turchi and C. A. Maryanoff, “Cyclization of N-acyliminium Ions,” *Chem. Rev.*, vol. 104, no. 3, pp. 1431-1628, 2004.
- [85] M. Amat, M. M. Santos, A. M. Gomez, D. Jokic, E. Molins and J. Bosch, “Enantioselective Spirocyclizations from Tryptophanol-Derived Oxazolopiperidone Lactams,” *Organic Letters*, vol. 9, no. 15, pp. 2907-2910, 2007.
- [86] P. Deslongchamps, Stereoelectronic effect in organic chemistry, Oxford: Baldwin, J. E., Ed.; Pergamon, 1983.
- [87] I. H. J. Ploemen, M. Prudencio , B. G. Douradinha, F. G. Ramesar, J. Fomager, G. J. van Gemert, A. J. F. Luty, C. C. Hermsen, R. W. Sauerwein, F. G. Baptista, M. M. Mota, A. P. Waters, I. Que, C. W. G. M. Lowik, S. M. Khan, C. J. Janse and B. M. D. Franke, “Visualisation and quantitative analysis of the rodent malaria liver stage by real time imaging,” *PLos One*, vol. 4, p. e7881, 2009.
- [88] M. Prudêncio, M. M. Mota and A. M. Mendes, “A toolbox to study liver stage malaria,” *Trends. Parasit*, vol. 27, pp. 565-574, 2011.
- [89] A. Rouf and S. Taneja, “Synthesis of single-enantiomer Bioactive Molecules: A Brief Overview,” *Chirality*, vol. 26, pp. 63-78, 2014.

- [90] o, K. Onel and C. Cordon-Cardo, "MDM2 and prognosis," *Mol Cancer Res*, vol. 2, pp. 1-8, 2004.
- [91] D. Reed, Y. Shen, A. A. Shelat, L. A. Arnold, A. M. Ferreira, F. Zhu, N. Mills, D. C. Smithson, r, r, C. A. Regni, D. Bashford, B. A. Schulman, A. G. Jochemsen and R. K. Guy, "Identification and characterization of the first small molecule inhibitor of MDMX," *J. Biol Chem.*, vol. 285, pp. 10786-10796, 2006.
- [92] R. W. Snow, C. A. Guerra, A. M. Noor, H. Y. Myint and S. I. Hay, "The global distribution of clinical episodes of *Plasmodium falciparum* malaria," *Nature*, vol. 434, pp. 214-217, 2005.
- [93] V. Sharma, P. Kumar and D. Pathak, "Biological importance of the indole nucleus in recent years: a comprehensive review," *Journal of Heterocyclic Chemistry*, vol. 47, pp. 491-502, 2010.
- [94] M. M. M. Santos, "Recent advances in the synthesis of biologically active spirooxindoles," *Tetrahedron*, vol. 70, pp. 9735-9757, 2014.
- [95] D. J. Ager, I. Prakash and D. R. Schaad, "1,2- Amino alcohols and their heterocyclic derivatives as chiral auxiliaries in asymmetric synthesis," *Chem. Rev.*, vol. 96, pp. 835-876, 1996.
- [96] G. Casnati, A. Dossena and A. Pochini, "Electrophilic substitution in indoles: direct attack at the 2-position of 3-alkylindoles," *Tetrahedron Letters*, vol. 52, pp. 5277-5280, 1972.
- [97] P. Kowalski, A. J. Bojarski and J. L. Mokrosz, "Structure and spectral properties of beta-carbolines. 8. Mechanism of the Pictet-Spengler cyclization. An MNDO approach," *Tetrahedron*, vol. 51, pp. 2737-2742, 1995.

6. Annex

6.1. Experimental Procedure for the *in-vitro* screening of indolizinoindoles 50-56a and 50-56b

Immunofluorescence and Live Imaging. Huh-7 cells, a human hepatoma cell line, were cultured in 1640 RPMI medium supplemented with 10% v/v fetal calf serum (FCS), 1% v/v non-essential amino acids, 1% v/v penicillin/streptomycin, 1% v/v glutamine and 10 mM HEPES, pH 7, and maintained at 37 °C with 5% CO₂. Inhibition of *P. berghei* liver stage infection was determined by measuring the luminescence of Huh-7 cell lysates 48 hours after infection with a firefly luciferase-expressing *P. berghei* line, PbGFP-Luccon, as previously described ([87], [88]). Briefly, cells (10×10^3 /well) were seeded in 96-well plates the day before drug treatment and infection. Tested compounds were prepared in the following way: 2.5 mM, 5 mM or 10 mM stock solutions were obtained by dissolving accurately weighed compounds in DMSO and dilutions subsequently made with medium to the desired concentration. Medium was replaced by fresh medium containing the appropriate concentration of each compound 1 hour prior to infection. Sporozoites (10,000 spz/well), freshly obtained through disruption of salivary glands of infected female *Anopheles stephensi* mosquitoes, were added to the wells 1 hour after compound addition. Sporozoite addition was followed by centrifugation at 1700 g for 5 min. Parasite load was determined 48 hours after infection by luminescence measurement using Biotium's Firefly Luciferase Assay Kit. The effect of the compounds on the viability of Huh-7 cells was assessed by the Alamar Blue assay (Invitrogen, UK), using the manufacturer's 40 protocol. Nonlinear regression analysis was employed to fit the normalized results of the dose-response curves, and EC₅₀ values were determined using GraphPad software.